IDENTIFICATION OF HOST AND BACTERIAL FACTORS THAT CONTRIBUTE TO LUNG LESION STRUCTURE DURING PNEUMONIC PLAGUE

Nikolas M. Stasulli

A dissertation submitted to the faculty at the University of North Carolina at Chapel Hill in partial fulfillment of the requirements for the degree of Doctor of Philosophy in the Department of Microbiology and Immunology in the School of Medicine.

Chapel Hill
2015

Approved by:

William E. Goldman

Peggy A. Cotter

Virginia L. Miller

Thomas H. Kawula

Anthony R. Richardson

ABSTRACT

Nikolas M. Stasulli: Identification of Host and Bacterial Factors that Contribute to Lung Lesion Structure During Pneumonic Plague
(Under the direction of William E. Goldman)

Yersinia pestis, the causative agent of plague, is a high-priority pathogen that continues to cause outbreaks worldwide. The ability of *Y. pestis* to be transmitted via respiratory droplets and its history of weaponization has led to its classification as a Tier 1 Select Agent most likely to be used as a biological weapon. The most deadly form of disease caused by *Y. pestis*, pneumonic plague, results from the deposition of bacteria into the lungs and has mortality rates approaching 100% in the absence of treatment within 24 hours of the onset of symptoms. The Goldman lab has previously characterized pneumonic plague progression as biphasic, presenting with two distinct disease phases. Rapid bacterial growth during an initial pre-inflammatory phase transitions into the second pro-inflammatory phase where disease symptoms present and lead to death of the host. Using *in vivo* analyses and focusing on relevant cell types during pneumonic plague infection host pathways can be identified that may be manipulated to extend the 24 hour window for treatment of pneumonic plague.

During pneumonic plague, the bacterium *Yersinia pestis* elicits the development of neutrophil-rich inflammatory lung lesions that continue to expand,

eventually consolidating entire lobes of the lung during infection. This lesion development and persistence is poorly understood. In this dissertation I examine spatially distinct regions of lung lesions using laser capture microdissection and RNAseq to identify transcriptional differences between lesion microenvironments. I provide evidence that cellular pathways involved in leukocyte migration and apoptosis are down-regulated in the center of lung lesions compared to the periphery. Probing for the bacterial factor(s) important for the alteration in neutrophil survival, I provide evidence that *Y. pestis* increases neutrophil survival through a mechanism that is dependent on the type III secretion system effector YopM. Additionally, I investigate the roles of reactive oxygen and nitrogen species that are typically used as neutrophil defense mechanisms, and provide evidence that these molecules are important for controlling early establishment of *Y. pestis* in the lungs. This research explores the complexity of spatially distinct host-microbe interactions *in vivo* and emphasizes the importance of cell-relevant assays in understanding *Y. pestis* virulence.

I dedicate this dissertation to Dr. Rebecca Roberts at Ursinus College who gave me my first opportunity in academic research and inspired me through both her teaching and her mentoring.

ACKNOWLEDGEMENTS

I want to thank Dr. Bill Goldman for his mentorship throughout my graduate career. He has taught me how to be thorough and take calculated risks as a researcher. His mentorship has gone well past the bench and he has shown me that balancing work and life makes for a fulfilling career. I want to thank him for encouraging my scientific creativity and supporting my research ideas even when those ideas seemed crazy… like proposing to dissect out regions of lung lesions 200 microns apart and convincing him there would be transcriptional differences between the regions.

I want to thank my dissertation committee, Drs. Peggy Cotter, Virginia Miller, Tom Kawula, and Tony Richardson, for their time and scientific input during my committee meetings that helped shape the direction of this work. I also want to thank the Miller laboratory, especially Dr. Eric Weening. His leadership in the BSL 3 laboratory has been invaluable to keeping everything running smoothly. I want to thank Dr. Joel Parker for his assistance in analyzing the RNAseq datasets and Dr. Stephanie Montgomery for interpreting lung pathology of mice. I want to thank Bob Bagnell, Alicia Brandt, and Nicole Maponga for helping me learn new techniques and providing me with samples for my research. Dixie Flannery also deserves all my gratitude for her help in the Microbiology and Immunology Department. The graduate

students would be lost without her and I am very grateful for all her work that kept me on track throughout my graduate career.

My graduate school experience would not have been the same without the members of the Goldman lab. Their sometimes abrasive and sophomoric antics have brought a lot of humor to many discouraging days when experiments just would not work. I especially want to thank Dr. Roger Pechous for mentoring me throughout my time in the lab and training me to work in the unique BSL 3 setting that *Y. pestis* warrants… also of all of the debauchery and "deep thoughts" that kept me focused. I want to thank Kara Eichelberger for being a superb mentee as I finish up my time in the lab. It has been great to share all the secrets of *Yersinia* that I have acquired over the years and I wish her the best of luck in graduate school. I also want to thank Vicky Sepulveda for keeping me grounded and giving me sage advice over the years… and for putting up with all the Colombian jokes and not actually ever setting me on fire.

My friends and family deserve a special level of thanks for their support over the years. I want to especially thank my parents, Mike and Karen, and my brother, Tim, for all their love and support as I've been on this journey. Thank you Mom and Dad for always being there with encouraging words while sharing in my excitements and my disappointments. Thank you for always reminding me where I come from and for making so many sacrifices for me to become the man I am today. I can never thank you enough for all the experiences you afforded me over the years. I hope that someday I will be the same kind of parent. Lastly, I want to thank Louise for all the

love and support she has provided as we shared this graduate school experience together. You are one of the first people I met here at UNC and I am glad every day for having you in my life. Thank you for listening to my science complaints, for cooking delicious meals, for putting up with my quirks, and for constantly helping me grow and become a better person. I can't wait to continue spending our lives together after this chapter comes to a close.

TABLE OF CONTENTS

LIST OF TABLES

LIST OF FIGURES

LIST OF ABBREVIATIONS

AEC – airway epithelial cell

BHI – brain/heart infusion

BM-PMN – bone marrow isolated neutrophil

BSL – biosafety level

BWC – Biological and Toxin Weapons Convention

CFU – colony-forming units

CO92 – Colorado 92 – fully virulent strain of *Y. pestis*

DEPC – diethylpyrocarbonate

DNA – deoxyribonucleic acid

FBS – fetal bovine serum

FFPE – formalin fixed paraffin embeded

H_2O_2 – hydrogen peroxide

HOCl – hypochlorous acid

IRB – Institutional Review Board

LCM – laser capture microdissection

MPO – myeloperoxidase

NADPH – nicotinamide adenine dinucleotide phosphate

NCBI – National Center for Biotechnology Information

NO – nitric oxide

NOS (e, i, n) – nitric oxide synthase (epithelial, inducible, neuronal)

O_2 – oxygen molecule

O_2^- – superoxide ion

O.C.T. – optimal cutting temperature

$ONOO^-$ – peroxynitrite

PBS – phosphate buffered saline

pgm$^-$ – a deletion of the pigmentation locus of *Yersinia pestis*

PHS – Public Health Service

RNA – ribonucleic acid

RNAseq – RNA deep sequencing

RNS – reactive nitrogen species

ROS – reactive oxygen species

RSK – ribosomal S6 kinase

RSNO – S-nitrosothiol

T3SS – type III secretion system

USDA – United States Department of Agriculture

WHO – World Health Organization

Yop – *Yersinia* outer protein

CHAPTER 1: INTRODUCTION

1.1 Overview

The causative agent of the disease known as “plague” was identified independently in August of 1894 by both Alexandre Yersin and Shibasaburo Kitasato. Yersin, however, is primarily credited with the official identification because of his more accurate and descriptive paper describing the gram-negative coccobacillus, which he named *Bacterium pestis*. He continued his research and by 1900 had used antiserum to cure a plague patient, and ultimately made the link between rats and plague outbreaks (Hirst, 1953; Zietz and Dunkelberg, 2004). The name of the bacterium identified by Yersin has changed several times since its discovery: first in 1900 to *Bacillus pestis*, then in 1923 to *Pasteurella pestis* (after Louis Pasteur, Yersin’s mentor), then finally in 1970 to *Yersinia pestis* (after its identifier) (Zietz and Dunkelberg, 2004).

Y. pestis is a high-priority pathogen that poses a severe threat to both human and animal health, and continues to cause modern day plague outbreaks worldwide (Inglesby et al., 2000; Stenseth et al., 2008). The ability of *Y. pestis* to be transmitted via respiratory droplets and its past weaponization has led to its classification as a Tier-1 select agent that must be handled under strict biosafety level 3 (BSL3) conditions. The natural re-emergence of plague as a global public health threat is

also of concern since the identification of the first antibiotic resistant strains of *Y. pestis* in 1995 (Galimand et al., 2006).

The most deadly form of plague disease known as primary pneumonic plague results from the inhalation of *Y. pestis*. The Goldman lab has previously characterized pneumonic plague in a murine model as a biphasic disease with an initial anti-inflammatory phase followed by rapid activation of the innate immune system (Lathem et al., 2005). If antibiotic treatment is not administered within 24 hours after the onset of symptoms, the disease approaches 100% mortality (Inglesby et al., 2000). While not the most common form of plague disease, pneumonic plague is of the highest concern when considering transmission and disease treatment. The rapid bacterial growth in the lung during the initial anti-inflammatory phase primes the patient to be infectious to others once disease symptoms emerge. Additionally, the rapid disease progression can lead to death before *Y. pestis* infection can be diagnosed and confirmed.

1.2 Manifestations of plague

The identification of small mammals as the reservoir of endemic plague infections was established in 1927. The natural transmission cycle of *Y. pestis* between small mammals and fleas was termed sylvatic plague (Zietz and Dunkelberg, 2004). As humans unintentionally enter this sylvatic cycle (or as *Y. pestis* is intentionally dispersed through nefarious means) there are three manifestations of disease that can result: bubonic, pneumonic, and septicemic plague.

1.2.1 Bubonic plague

Bubonic plague is the most common disease caused by *Y. pestis*. Bubonic plague can be caused by contamination of open wounds or direct inoculation through the bite of an infected flea (Riedel, 2005). After establishing in the dermis, *Y. pestis* infiltrates the cutaneous lymphatics and migrates to the nearest draining lymph node (Gonzalez et al., 2015; Riedel, 2005). After an incubation period of 2-6 days after inoculation, there is a sudden onset of flu-like symptoms followed by a swelling of the draining lymph nodes that forms the namesake “buboes” (Riedel, 2005). In the pre-antibiotic era the mortality rate of bubonic plague could reach as high as 70% during epidemics (Stenseth et al., 2008). Today, with early detection and treatment, mortality has dropped to as low as 5% (Inglesby et al., 2000). Even if a patient recovers form bubonic plague, buboes may remain for several weeks after symptoms have dissipated (Riedel, 2005).

1.2.2 Pneumonic plague

When *Y. pestis* colonizes the lower respiratory system either secondary or primary pneumonic plague will result. Secondary pneumonic plague occurs after bubonic or septicemic plague disseminates into the lung compartment, allowing it to be spread by aerosol from person-to-person. Primary pneumonic plague occurs after inhalation of *Y. pestis* directly into the lungs. This can occur by person-to-person transmission, through aerosolizing bacteria (i.e. butchering an infected animal), or

during the intentional release of an aerosol as a biological weapon (Inglesby et al., 2000). It is believed that person-to-person transmission via respiratory droplets occurs within approximately one meter of an infected individual (Kool, 2005). Further discussion of pneumonic plague epidemiology throughout modern times can be found in Section 1.3.3 of Chapter 1.

There is a short quiescent time of 1-3 days after inhalation of bacteria before flu-like symptoms emerge. Unfortunately, pneumonic plague must be treated within 24 hours after symptoms begin or mortality approaches 100% only three to four days after inhalation (Inglesby et al., 2000). Disease progression and symptoms are similar in the murine model of infection. Based on our animal model, the progression of pneumonic plague is biphasic: an initial anti-inflammatory phase precedes a pro-inflammatory phase of disease. In the first phase, bacteria are present in the lungs and freely replicate with little to no detectable immune responses. Disease symptoms, increased cytokine levels, and the infiltration of neutrophils into the airways signal entry into the pro-inflammatory phase of infection. Pneumonic plague can be characterized by the formation of lung lesions followed by destruction of surrounding alveolar architecture. Condensed pockets of *Y. pestis* surrounded by innate immune cells, primarily neutrophils, form these pulmonary lesions (Lathem et al., 2005). Death from pneumonic plague can be attributed to pneumonia due to alveolar destruction and the subsequent septicemia late in disease resulting from dissemination of bacteria from the lungs (Finegold et al., 1968).

1.2.3 Septicemic plague

If *Y. pestis* manages to infiltrate the bloodstream of the host the disease will manifest as septicemic plague. Primary septicemic plague from direct inoculation of *Y. pestis* into the blood stream is fairly rare. However, secondary septicemic plague often results during the late stages of bubonic and pneumonic plague. Once bacteria have disseminated from initially localized sites, septicemia can induce shock, blood clots leading to gangrenous extremities, multiple organ failure, and respiratory distress (Riedel, 2005).

1.3 History and epidemiology of plague

The disease caused by *Yersinia pestis* known as “plague” has been described for thousands of years. It is generally agreed upon by scholars that the oldest written mention of plague is recounted in the Bible (1 Samuel 5&6) referring to a time between 1320 – 1000 BC (Griffin, 2000; Ligon, 2006). This bacterium has also been responsible for 3 major pandemics throughout recorded history that were so devastating to the population that it completely altered the makeup of society.

1.3.1 The Justinian pandemic

The first major plague pandemic is now referred to as the “plague of Justinian”, after the presiding emperor of Rome. The pandemic may have started as early as 532 BC, but definitively took hold in 541/42 BC with outbreaks in Constantinople and Greece (Ligon, 2006; Zietz and Dunkelberg, 2004). It is believed

that ~40% of Constantinople's population died during this outbreak. After disease spread through trade routes, up to 100 million Europeans are believed to have succumbed to plague over the next 250 – 300 years as pockets of disease continually reemerged. This devastating death toll depleted trade occupations, the ability to form armies, and the ability to staff many of the religious monasteries throughout Europe and Western Asia (Ligon, 2006).

1.3.2 The Black Death

The second and most well known plague pandemic is commonly referred to as "The Black Death". The initial outbreak is thought to have started in China in the 1330's. The disease then spread west through trade routes and began establishing itself in Europe. From 1346 – 1352 the spread of *Y. pestis* resulted in the death of over 25 million people, over one-third of the world's population at the time. Another 20 million were believed to have died by the end of the century. This pandemic lasted through the 1720's, decimating large cities with resurgences throughout Europe (Ligon, 2006; Zietz and Dunkelberg, 2004).

With over one-third of the world's population deceased within 6 years, this pandemic had wide rippling effects throughout society. Commerce, trade, and government came to a near standstill, and the economy of Europe collapsed from the large and sudden loss of life. The population and economy only began to rebound in the late 1600's. Interestingly, in Western Europe, the sudden decrease in the peasant population caused increased competition for the remaining, now

valuable, laborers. This competition is believed to have started an early form of capitalism and led to the rise of a "middle class" that was not present prior to the pandemic. Culture throughout Europe also began to morph and took on a macabre tone, with the influence of death permeating artwork, literature, and music. Many people at the time became more religious, as evidenced by the canonization of new "plague saints" by the Catholic Church. Unfortunately, this new-found focus on religion also caused societal rifts as Christians, Muslims, and Jews all blamed each other for incurring "God's wrath" and causing the horrible disease (Ligon, 2006; Zietz and Dunkelberg, 2004).

1.3.3 The Modern pandemic: global spread, and tracking of pneumonic plague

The "modern pandemic" of plague is believe to have started in China around 1855 in the Yunnan province, and marked a critical point in the dissemination of plague into a global issue. By 1894 plague had reached Hong Kong and, with the growth of the trans-oceanic shipping industry, lead to global spread of *Y. pestis* (Caten and Kartman, 1968; Ligon, 2006; Zietz and Dunkelberg, 2004). Stowaway rats on shipping vessels would transport *Y. pestis*, and the flea vectors that transmit it, across oceans. The first reported incidence of plague in the Western Hemisphere came in Santos, Brazil in October of 1899 (Furman and Williams, 1973), and marked the beginning of three decades of large epidemics throughout the world. Between 1900-1930 every continent except Antarctica experienced outbreaks of plague

(Ligon, 2006). Even Australia, which has not had a case of plague since 1925, was struck with over 1,300 cases of plague in the first part of the 1900's (Garrett, 1991).

In the United States, this first quarter of the 20th century also saw several epidemics of plague in California. The first epidemic occurred from 1900-1904 in a Chinese immigrant-populated district of San Francisco. This was followed by a second outbreak in San Francisco in 1907. These two outbreaks included both bubonic and pneumonic plague cases, infecting over 280 people. A smaller epidemic occurred in 1919 in Oakland, CA, where a man developed secondary pneumonic plague and became the source of 13 primary pneumonic plague cases, 12 of whom died (Anderson, 1978; Caten and Kartman, 1968; Kool, 2005). This was also documented as the first instance of a primary pneumonic plague epidemic in the Western Hemisphere (Kellogg, 1920). The fourth US outbreak occurred in Los Angeles in late 1924, and was also caused by pneumonic plague, resulting in 39 documented cases with 33 deaths (Anderson, 1978; Kool, 2005). A fifth outbreak occurred around the Gulf Coast of the United States in 1924, causing over 70 cases of plague (Anderson, 1978).

While there was a spike of plague cases in the United States between 1900-1908 and again between 1918-1926, after the mid-1920's there were relatively few yearly cases of plague. However, unlike Australia that was seemingly able to eradicate plague disease after 1925 (Garrett, 1991), endemic sylvatic plague established itself in small-mammal populations in the U.S. west of the Mississippi River (Anderson, 1978; Caten and Kartman, 1968). According to compiled

information from the Centers for Disease Control and Prevention and other published sources, beginning in the mid-1960's through the 1970's and into the early 1980's, there was a resurgence of plague cases in the U.S. (Anderson, 1978). These cases were located throughout the Southwestern U.S., mainly New Mexico, Arizona, and California (Anderson, 1978; Kaufmann et al., 1980). Between 1900 and 2010, there were over 1,400 reported cases of plague in the contiguous U.S. and Hawaii (Kaufmann et al., 1980). Of these U.S. cases, as many as 20% have been due to pneumonic plague.

In addition to the two pneumonic plague outbreaks in California in the early 1900's, there have been several global instances of pneumonic plague outbreaks during the "modern plague" era. The largest of these epidemics took place in the Manchuria region in China. This region had large pneumonic plague epidemics in 1910-1911 and again in 1920-1921 that left ~60,000 and ~9,300 people dead, respectively (Wu et al., 1936). Interestingly, the larger of the two epidemics in 1910-1911 was caused by a dramatic increase in the price of marmot fur. Thousands of poor laborers flocked to this region of China to hunt marmots, whose population was unknowingly endemically infected with *Y. pestis*. The butchering and eating of these animals by hunters unwittingly aerosolized the bacteria and caused a major epidemic (Summers, 2012). China continues to have relatively large numbers of plague cases yearly. Between 1994-2003 there were 11 countries that reported more than 100 confirmed cases of plague (China being number 11). The country with the highest rate of plague during this time was Madagascar, with approximately

3% of cases being pneumonic plague. For this 10 year time period, that equates to over 350 cases of pneumonic plague (Butler, 2009). In the first full decade of the 21st century, however, the WHO reported that the Congo became the number one reporting country with over 10,500 cases of plague. This increase in cases also coincided with a large pneumonic plague outbreak in 2005-2006 in the Oriental Province that left over 130 people dead from pneumonic plague alone (Butler, 2013). There should continue to be a heightened awareness of outbreaks of pneumonic plague to ensure that larger epidemics do not continue to occur, especially with the identification of naturally antibiotic-resistant *Y. pestis* strains (Galimand et al., 2006).

1.4 Yersinia pestis as a biological weapon

The first known use of *Y. pestis* as a biological weapon dates back to 1346 during the war between the Tartar army and Genoese sailors at the port city of Caffa. The Tartars were losing many of their soldiers to plague, and out of desperation placed the corpses of people who had died of plague onto catapults and flung them over the city walls to infect enemy troops. Similar corpse-catapulting strategies were documented in 1422 by the Lithuanians and in 1710 by the Russians (Ligon, 2006; Riedel, 2004).

During World War II, the Japanese army established a research program (Unit 731) that secretly studied biological-warfare agents. This unit extensively studied *Yersinia pestis*, and infected fleas were released over the Chinese population several times in the early 1940's. "Bombs" were built and tested that were constructed of clay pots filled with *Y. pestis* carrying fleas encased in rice and paper.

It is believed that tens-of-thousands of people died from plague epidemics throughout China during the 1940's due to Unit 731's biological-weapon experiments. Unit 731's field tests of *Y. pestis* on the Chinese people were ceased after Japanese troops died of plague due to the unpredictability of the fleas and spread of disease (Ligon, 2006; Riedel, 2004; Williams and Wallace, 1989).

After WWII, biological weapons programs were slowly dismantled, starting with the United Kingdom shutting down its program in 1950. The United States followed suit in 1969, but only after developing at least seven type-classified microorganisms into biological weapons. The shut down of the US biological weapons program preceded the drafting of the Biological and Toxin Weapons Convention (BWC) in 1972. The BWC called for multilateral disarmament of all biological weapons. The Soviet Union, however, continued with their biological weapons program until 1992 despite signing the BWC (Ligon, 2006; Riedel, 2004).

In 1970 just prior to the drafting of the BWC, the WHO convened a group of experts to determine the casualties that would be expected from an aerosolized biological attack from several select agents. The WHO committee determined that, under their defined parameters, the release of 50 kg of aerosolized *Y. pestis* over an economically developed city of 5,000,000 people would result in the incapacitation of 150,000 and death of 36,000 people, assuming prompt action is taken following the attack. Out of all biological weapon agents surveyed by this committee, only *B. anthracis* would cause more casualties, most likely due to its ability to travel farther and stay viable for much longer than *Y. pestis*. Unlike Anthrax, however, *Y. pestis*

can be spread from person to person, and any extended delay in initiating treatment could cause casualty numbers to rise. A sylvatic reservoir of *Y. pestis* could also be established if small mammals become infected during an attack. Along with the presence of susceptible flea populations, this new rodent reservoir could lead to more long-term effects of recurring bubonic plague due to the establishment of a sylvatic cycle. This assessment of biological and chemical weapons has been updated as recently as 2004 (World Health Organization, 2004). Despite the unlikely use of *Y. pestis* as a biological weapon there has also been an assessment of antibiotic treatment courses recommended in the case of both contained or mass casualty outbreaks (Inglesby et al., 2000).

Modeling of well-documented pneumonic plague outbreaks in the 20th century has found that R_0=~1.3 (the ability of an infection to sustain itself in a population). An R_0<1 indicates that an infection cannot sustain it self in a population. An R_0>1 indicates that pneumonic plague has the potential to sustain itself and spread in a population if action is not taken to control the infection. However, an R_0 value so close to 1 signifies the need for close proximity to infect and a small window of transmission before symptoms begin. The disease could be stopped through isolation of infected individuals and antibiotic treatment for those who have come into contact with the infected (Gani and Leach, 2004).

1.5 Pulmonary immune defense and neutrophils

The respiratory tract is continuously in contact with a diverse repertoire of constantly changing environmental antigens. To continue functioning efficiently, the

lungs must maintain an immunological homeostasis, balancing between potentially harmful and non-harmful antigens. Recognition of antigens begins in the mucosal tissue of the conducting airways. The airway epithelial cells (AECs) are the first line of defense. The AECs act as a physical barrier, but also secret proteins and peptides into the lung mucosa to defend against invading pathogens (Holt et al., 2008). Secreted proteins and molecules such as lysozyme, peroxidase, lactoferrin, defensins, collections, ficolins, and complement factors can all directly act on invading microbes to promote killing and help ensure lung homeostasis (Tsai and Grayson, 2008). From the conducting airways, the bronchi of the lungs continue to branch and form the parenchymal lung, consisting of bronchioles and alveolar ducts, and terminates in alveolar sacs that are necessary for oxygen exchange (Holt et al., 2008). Besides the AECs there are various resident dendritic cells and macrophages that patrol and sample the mucosa and alveolar spaces to ensure proper homeostasis and recruit additional immune cells if necessary (Guilliams et al., 2013; Holt et al., 2008).

In addition to the resident immune cells, neutrophils are an important and necessary component of the innate immune system. Neutrophils are short-lived cells that are constantly being generated in the bone marrow, circulating in the blood stream, and then returning to the bone marrow for cellular turnover. During their circulation, neutrophils also monitor the lung environment for invading pathogens. During a bacterial infection neutrophils are rapidly called to the site of insult and can quickly activate a myriad of antimicrobial functions in an attempt to control invading

pathogens (Craig et al., 2009; Segal, 2005). This rapid antimicrobial response is facilitated by neutrophil priming that results from signals initiated by the innate immune system upon detection of a pathogen. This priming retains neutrophils in the lungs as they “survey” during normal circulation (Singh et al., 2012; Summers et al., 2010). Upon direct interaction with a secondary stimulus, such as invading microbes, there is enhancement of the respiratory burst, cytoskeletal rearrangements that retain neutrophils in the lung and facilitate phagocytosis, regulation of neutrophil surface antigens (Singh et al., 2012), and release of antimicrobial peptides/proteins from granules (Kobayashi et al., 2003). After mounting an antimicrobial response, neutrophils ordinarily undergo necrosis, apoptosis, or NETosis, all of which ultimately lead to macrophage infiltration. The newly infiltrated macrophages facilitate the clearance of dead or dying neutrophils as well as any remaining bacteria (Brinkmann et al., 2004; Kebir and Filep, 2013; Luo and Loison, 2008; Silva, 2011). This double priming, however, can lead to acute lung injury if the neutrophils are not efficiently released from the pulmonary compartment back into circulation, or appropriate neutrophil turnover and removal does not occur (Singh et al., 2012; Summers et al., 2010). There is also data to suggest that there is cross talk between neutrophils and various other cell types at sites of inflammation that can promote a continued innate immune response and even bridge the gap between innate and adaptive immunity (Mantovani et al., 2011).

1.6 Pathogenesis and innate immune response during pneumonic plague

Pathogenic microbes have evolved ways to evade the immune system of the hosts that they infect. The work presented in this dissertation is focused on the ability of bacteria to manipulate activated neutrophils (Urban et al., 2006), resulting in increased disease severity and mortality (Balamayooran et al., 2010). Pathogens have been shown to utilize various mechanisms to alter neutrophil function including inhibiting neutrophil chemotaxis (Bignold et al., 1991; de Haas et al., 2004; Van Dyke et al., 1982), preventing phagocytosis (Grosdent et al., 2002; Spinner et al., 2013; 2008; Visser et al., 1995), altering degranulation (Arnett et al., 2014; Bertram et al., 1986), and, importantly for this work, inhibiting neutrophil apoptosis (Choi et al., 2005; Erttmann et al., 2014; Ge and Rikihisa, 2006; Schwartz et al., 2013; 2012).

Despite the recruitment of neutrophils to control *Y. pestis* in the lungs, bacterial numbers continue to increase throughout the duration of infection (Lathem et al., 2005). The increase in bacterial burden coincides with continued neutrophil recruitment, accumulation in the lungs, and subsequent targeting of neutrophils by the *Y. pestis* type III secretion system (T3SS) (Marketon et al., 2005; Pechous et al., 2013). The massive neutrophilic infiltration during pneumonic plague results in the formation of histopathologically distinct lung lesions that arise during the later (pro-inflammatory) phase of disease. These lesions expand in the lungs as neutrophils continue to accumulate until death of the host, with no evidence of bacterial or neutrophil clearance (Lathem et al., 2005). The continued influx of neutrophils and their apparent prolonged survival is contrary to typical neutrophil function but has

also been observed in neutrophils of cystic fibrosis patients (Tirouvanziam et al., 2008). The continuous neutrophil influx during pneumonic plague results in alveolar destruction within lung lesions and culminates in a severe and deadly necrotizing pneumonia (Finegold et al., 1968).

Yersinia pestis is known to inhibit the host immune response via various virulence mechanisms (Ben-Gurion and Shafferman, 1981; Du et al., 2002; Jackson and Burrows, 1956; Lathem et al., 2007; Trosky et al., 2008). However, It has just recently been appreciated that the functions of specific T3SS effectors may vary depending on the cell type being targeted (Spinner et al., 2010). Neutrophils are the most prominent immune infiltrate during pneumonic plague, are selectively targeted by *Y. pestis*, and are necessary for development of lung lesions (Pechous et al., 2013). Early recruitment of neutrophils is also linked to decreased bacterial burden and increased survival of *Y. pestis* infected mice (Vagima et al., 2015).

In the *Yersinia pestis* field, pneumonic plague is fairly understudied as a separate disease from bubonic plague despite the dissimilar disease progression. Most research is done using bubonic plague models or in *in vitro* assays. These results are usually inferred, but not directly tested, to be relevant during pneumonic plague. Relatively few laboratories use fully virulent *Y. pestis* to specifically study the effects of virulence factors on pneumonic plague (Cantwell et al., 2010; Lathem et al., 2007; van Lier et al., 2014). Most other groups working on pneumonic plague use attenuated strains missing either the pigmentation locus or the pCD1 plasmid (Fetherston et al., 2010; Galvan et al., 2010; Lee-Lewis and Anderson, 2009). This

dissertation and other studies from the Goldman lab continue to show the necessity of using fully virulent *Y. pestis* and *in vivo* infections by presenting data that could not be elucidated in less pathogenic models (Lathem et al., 2005; Pechous et al., 2013; 2015; Price, 2011).

1.7 Significance

Endemic maintenance of *Yersinia pestis* in sylvatic cycles continues to cause spikes of plague disease around the world. Despite the signing of the BWC there is still fear of *Y. pestis* being used as a biological weapon during acts of terrorism. With the vague symptoms and rapid progression of pneumonic plague, it remains important to be vigilant and continue to characterize this disease, particularly focusing on more effective late-stage treatments. With the development of pneumonia being caused by the continued replication of *Y. pestis* and infiltration of neutrophils into the pleural cavity, it is important to move away from *in vitro* studies and to study the disease in a more relevant *in vivo* setting.

I hypothesized that spatially distinct transcriptional modulation of the important neutrophil population would be observable in *Y. pestis* lung lesions. This line of *in vivo* questioning, which could not be undertaken *in vitro*, specifically looked at the most relevant cell type important during pneumonic plague disease. In this body of work, fully virulent *Y. pestis* is employed along with the novel use of laser capture microdissection (LCM) and RNAseq technology to evaluate host transcription within the expanding neutrophil-rich lung lesions that arise during pneumonic plague. I hoped to identify novel cellular responses that are necessary *in*

vivo for disease progression, and to characterize both bacterial and host factors responsible for the distinctive pneumonic plague lung lesions that form late during infection. It is necessary to interrogate this inflammatory environment in the context of neutrophils to understand how interactions with *Y. pestis* determine pneumonic plague presentation and progression. By determining how interaction of *Y. pestis* and neutrophils induce responses uniquely within sites of infection, the scientific community will better understand the mechanisms by which neutrophils typically work in a broad range of diseases in which neutrophil infiltration becomes harmful to the host.

REFERENCES

Anderson, E.T. (1978). Plague in the continental United States, 1900-76. Public Health Rep *93*, 297–301.

Arnett, E., Vadia, S., Nackerman, C.C., Oghumu, S., Satoskar, A.R., McLeish, K.R., Uriarte, S.M., and Seveau, S. (2014). The pore-forming toxin listeriolysin O is degraded by neutrophil metalloproteinase-8 and fails to mediate *Listeria monocytogenes* intracellular survival in neutrophils. Journal of Immunology *192*, 234–244.

Balamayooran, G., Batra, S., Fessler, M.B., Happel, K.I., and Jeyaseelan, S. (2010). Mechanisms of neutrophil accumulation in the lungs against bacteria. American Journal of Respiratory Cell and Molecular Biology *43*, 5–16.

Ben-Gurion, R., and Shafferman, A. (1981). Essential virulence determinants of different *Yersinia* species are carried on a common plasmid. Plasmid *5*, 183–187.

Bertram, T.A., Canning, P.C., and Roth, J.A. (1986). Preferential inhibition of primary granule release from bovine neutrophils by a *Brucella abortus* extract. Infection and Immunity *52*, 285–292.

Bignold, L.P., Rogers, S.D., SIAW, T.M., and Bahnisch, J. (1991). Inhibition of chemotaxis of neutrophil leukocytes to interleukin-8 by endotoxins of various bacteria. Infection and Immunity *59*, 4255–4258.

Brinkmann, V., Reichard, U., Goosmann, C., Fauler, B., Uhlemann, Y., Weiss, D.S., Weinrauch, Y., and Zychlinsky, A. (2004). Neutrophil extracellular traps kill bacteria. Science *303*, 1532–1535.

Butler, T. (2009). Plague into the 21st century. Clinical Infectious Diseases *49*, 736–742.

Butler, T. (2013). Plague gives surprises in the first decade of the 21st century in the United States and worldwide. American Journal of Tropical Medicine and Hygiene *89*, 788–793.

Cantwell, A.M., Bubeck, S.S., and Dube, P.H. (2010). YopH inhibits early pro-inflammatory cytokine responses during plague pneumonia. BMC Immunology *11*, 29.

Caten, J.L., and Kartman, L. (1968). Human plague in the United States, 1900-1966. Jama *205*, 333–336.

Choi, K.-S., Park, J.T., and Dumler, J.S. (2005). *Anaplasma phagocytophilum* delay of neutrophil apoptosis through the p38 mitogen-activated protein kinase signal pathway. Infection and Immunity *73*, 8209–8218.

Craig, A., Mai, J., Cai, S., and Jeyaseelan, S. (2009). Neutrophil recruitment to the lungs during bacterial pneumonia. Infection and Immunity *77*, 568–575.

de Haas, C.J., Veldkamp, K.E., Peschel, A., Weerkamp, F., Van Wamel, W.J., Heezius, E.C., Poppelier, M.J., Van Kessel, K.P., and van Strijp, J.A. (2004). Chemotaxis inhibitory protein of *Staphylococcus aureus,* a bacterial antiinflammatory agent. The Journal of Experimental Medicine *199*, 687–695.

Du, Y., Rosqvist, R., and Forsberg, A. (2002). Role of fraction 1 antigen of *Yersinia pestis* in inhibition of phagocytosis. Infection and Immunity *70*, 1453–1460.

Erttmann, S.F., Gekara, N.O., and Fällman, M. (2014). Bacteria induce prolonged PMN survival via a phosphatidylcholine-specific phospholipase C- and protein kinase C-dependent mechanism. PLoS One *9*, 0087859.

Fetherston, J.D., Kirillina, O., Bobrov, A.G., Paulley, J.T., and Perry, R.D. (2010). The yersiniabactin transport system is critical for the pathogenesis of bubonic and pneumonic plague. Infection and Immunity *78*, 2045–2052.

Finegold, M.J., Petery, J.J., Berendt, R.F., and Adams, H.R. (1968). Studies on pathogenesis of plague - blood coagulation and tissue responses of *Macaca mulatta* following exposure to aerosols of *Pasteurella pestis*. The American Journal of Pathology *53*, 99.

Furman, B., and Williams, R.C. (1973). A profile of the United States Public Health Service, 1798-1948 (National Institutes of Health).

Galimand, M., Carniel, E., and Courvalin, P. (2006). Resistance of *Yersinia pestis* to antimicrobial agents. Antimicrobial Agents and Chemotherapy *50*, 3233–3236.

Galvan, E.M., Nair, M.K.M., Chen, H., Del Piero, F., and Schifferli, D.M. (2010). Biosafety level 2 model of pneumonic plague and protection studies with F1 and Psa. Infection and Immunity *78*, 3443–3453.

Gani, R., and Leach, S. (2004). Epidemiologic determinants for modeling pneumonic plague outbreaks. Emerg Infect Dis *10*, 608–614.

Garrett, E. (1991). Plague in Sydney: The anatomy of an epidemic. Population Studies: a Journal of Demography *45*, 159–160.

Ge, Y., and Rikihisa, Y. (2006). *Anaplasma phagocytophilum* delays spontaneous human neutrophil apoptosis by modulation of multiple apoptotic pathways. Cellular Microbiology *8*, 1406–1416.

Gonzalez, R.J., Lane, C.M., Wagner, N.J., Weening, E.H., and Miller, V.L. (2015). Dissemination of a highly virulent pathogen: tracking the early events that define infection. PLoS Pathogens *11*.

Griffin, J.P. (2000). Bubonic plague in biblical times. Journal of the Royal Society of Medicine *93*, 449.

Grosdent, N., Maridonneau-Parini, I., Sory, M.P., and Cornelis, G.R. (2002). Role of Yops and Adhesins in Resistance of *Yersinia enterocolitica* to Phagocytosis. Infection and Immunity *70*, 4165–4176.

Guilliams, M., Lambrecht, B.N., and Hammad, H. (2013). Division of labor between lung dendritic cells and macrophages in the defense against pulmonary infections. Mucosal Immunol *6*, 464–473.

Hirst, L.F. (1953). The Conquest of Plague (Oxford : Clarendon Press).

Holt, P.G., Strickland, D.H., Wikstrom, M.E., and Jahnsen, F.L. (2008). Regulation of immunological homeostasis in the respiratory tract. Nature Reviews Immunology *8*, 142–152.

Inglesby, T.V., Dennis, D.T., Henderson, D.A., Bartlett, J.G., Ascher, M.S., Eitzen, E., Fine, A.D., Friedlander, A.M., Hauer, J., Koerner, J.F., et al. (2000). Plague as a biological weapon - Medical and public health management. The Journal of the American Medical Association *283*, 2281–2290.

Jackson, S., and Burrows, T.W. (1956). The Pigmentation of *Pasteurella pestis* on a Defined Medium Containing Haemin. British Journal of Experimental Pathology *37*, 570–576.

Kaufmann, A.F., Boyce, J.M., and Martone, W.J. (1980). From the Center for Disease Control. Trends in human plague in the United States. J. Infect. Dis. *141*, 522–524.

Kebir, El, D.D., and Filep, J.G.J. (2013). Modulation of Neutrophil Apoptosis and the Resolution of Inflammation through β2 Integrins. Frontiers in Immunology *4*, 60.

Kellogg, W.H. (1920). An epidemic of pneumonic plague. Am J Public Health (N Y) *10*, 599–605.

Kobayashi, S.D., Voyich, J.M., and DeLeo, F.R. (2003). Regulation of the neutrophil-mediated inflammatory response to infection. Microbes and Infection *5*, 1337–1344.

Kool, J.L. (2005). Risk of person-to-person transmission of pneumonic plague. Clinical Infectious Diseases *40*, 1166–1172.

Lathem, W.W., Price, P.A., Miller, V.L., and Goldman, W.E. (2007). A plasminogen-activating protease specifically controls the development of primary pneumonic plague. Science *315*, 509–513.

Lathem, W.W., Crosby, S.D., Miller, V.L., and Goldman, W.E. (2005). Progression of primary pneumonic plague: A mouse model of infection, pathology, and bacterial transcriptional activity. Proceedings of the National Academy of Sciences *102*, 17786–17791.

Lee-Lewis, H., and Anderson, D.M. (2009). Absence of inflammation and pneumonia during infection with nonpigmented *Yersinia pestis* reveals a new role for the pgm locus in pathogenesis. Infection and Immunity *78*, 220–230.

Ligon, B.L. (2006). Plague: a review of its history and potential as a biological weapon. Seminars in Pediatric Infectious Diseases.

Luo, H.R., and Loison, F. (2008). Constitutive neutrophil apoptosis: mechanisms and regulation. American Journal of Hematology *83*, 288–295.

Mantovani, A., Cassatella, M.A., Costantini, C., and Jaillon, S. (2011). Neutrophils in the activation and regulation of innate and adaptive immunity. Nature Reviews Immunology *11*, 519–531.

Marketon, M.M., DePaolo, R.W., DeBord, K.L., Jabri, B., and Schneewind, O. (2005). Plague bacteria target immune cells during infection. Science *309*, 1739–1741.

Pechous, R.D., Broberg, C.A., Stasulli, N.M., Miller, V.L., and Goldman, W.E. (2015). *In vivo* transcriptional profiling of *Yersinia pestis* reveals a novel bacterial mediator of pulmonary inflammation. mBio *6*, e02302–e02314.

Pechous, R.D., Sivaraman, V., Price, P.A., Stasulli, N.M., and Goldman, W.E. (2013). Early host cell targets of *Yersinia pestis* during primary pneumonic plague. PLoS Pathogens *9*, e1003679.

Price, P.A. (2011). Dominant suppression of early innate immune mechanisms by *Yersinia pestis*. All Theses and Dissertations (ETDs).

Riedel, S. (2004). Biological warfare and bioterrorism: a historical review. Proceedings (Baylor University. Medical Center) *17*, 400–406.

Riedel, S. (2005). Plague: from natural disease to bioterrorism. Proceedings (Baylor University. Medical Center) *18*, 116–124.

Schwartz, J.T., Bandyopadhyay, S., Kobayashi, S.D., McCracken, J., Whitney, A.R., DeLeo, F.R., and Allen, L.-A.H. (2013). *Francisella tularensis* alters human neutrophil gene expression: insights into the molecular basis of delayed neutrophil apoptosis. Journal of Innate Immunity *5*, 124–136.

Schwartz, J.T., Barker, J.H., Kaufman, J., Fayram, D.C., McCracken, J.M., and Allen, L.-A.H. (2012). *Francisella tularensis* inhibits the intrinsic and extrinsic pathways to delay constitutive apoptosis and prolong human neutrophil lifespan. Journal of Immunology (Baltimore, Md. : 1950) *188*, 3351–3363.

Segal, A.W. (2005). How neutrophils kill microbes. Immunology *23*, 197–223.

Silva, M.T. (2011). Macrophage phagocytosis of neutrophils at inflammatory/infectious foci: a cooperative mechanism in the control of infection and infectious inflammation. Journal of Leukocyte Biology *89*, 675–683.

Singh, N.R.P., Johnson, A., Peters, A.M., Babar, J., Chilvers, E.R., and Summers, C. (2012). Acute lung injury results from failure of neutrophil de-priming: a new hypothesis. European Journal of Clinical Investigation *42*, 1342–1349.

Spinner, J.L., Carmody, A.B., Jarrett, C.O., and Hinnebusch, B.J. (2013). Role of *Yersinia pestis* toxin complex family proteins in resistance to phagocytosis by polymorphonuclear leukocytes. Infection and Immunity *1*, 4041–4052.

Spinner, J.L., Cundiff, J.A., and Kobayashi, S.D. (2008). *Yersinia pestis* type III secretion system-dependent inhibition of human polymorphonuclear leukocyte function. Infection and Immunity *76*, 3754–3760.

Spinner, J.L., Seo, K.S., O'Loughlin, J.L., Cundiff, J.A., Minnich, S.A., Bohach, G.A., and Kobayashi, S.D. (2010). Neutrophils are resistant to *Yersinia* YopJ/P-induced apoptosis and are protected from ROS-mediated cell death by the type III secretion system. PLoS One *5*, e9279–e9279.

Stenseth, N.C., Atshabar, B.B., Begon, M., Belmain, S.R., Bertherat, E., Carniel, E., Gage, K.L., Leirs, H., and Rahalison, L. (2008). Plague: past, present, and future. PLoS Medicine *5*, e3–e3.

Summers, C., Rankin, S.M., Condliffe, A.M., Singh, N., Peters, A.M., and Chilvers, E.R. (2010). Neutrophil kinetics in health and disease. Trends Immunol *31*, 318–324.

Summers, W.C. (2012). The Great Manchurian Plague of 1910-1911 (Yale University Press).

Tirouvanziam, R., Gernez, Y., Conrad, C.K., Moss, R.B., Schrijver, I., Dunn, C.E., Davies, Z.A., Herzenberg, L.A., and Herzenberg, L.A. (2008). Profound functional and signaling changes in viable inflammatory neutrophils homing to cystic fibrosis airways. Proceedings of the National Academy of Sciences of the USA *105*, 4335–4339.

Trosky, J.E., Liverman, A.D.B., and Orth, K. (2008). *Yersinia* outer proteins: Yops. Cellular Microbiology *10*, 557–565.

Tsai, K.S., and Grayson, M.H. (2008). Pulmonary defense mechanisms against pneumonia and sepsis. Current Opinion in Pulmonary Medicine *14*, 260–265.

Urban, C.F., Lourido, S., and Zychlinsky, A. (2006). How do microbes evade neutrophil killing? Cellular Microbiology *8*, 1687–1696.

Vagima, Y., Zauberman, A., Levy, Y., Gur, D., Tidhar, A., Aftalion, M., Shafferman, A., and Mamroud, E. (2015). Circumventing *Y. pestis* virulence by early recruitment of neutrophils to the lungs during pneumonic plague. PLoS Pathogens *11*, e1004893.

Van Dyke, T.E., Bartholomew, E., Genco, R.J., Slots, J., and Levine, M.J. (1982). Inhibition of neutrophil chemotaxis by soluble bacterial products. Journal of Periodontology *53*, 502–508.

van Lier, C.J., Sha, J., Kirtley, M.L., Cao, A., Tiner, B.L., Erova, T.E., Cong, Y., Kozlova, E.V., Popov, V.L., Baze, W.B., et al. (2014). Deletion of braun lipoprotein and plasminogen-activating protease-encoding genes attenuates *Yersinia pestis* in mouse models of bubonic and pneumonic plague. Infection and Immunity *82*, 2485.

Visser, L.G., Annema, A., and van Furth, R. (1995). Role of Yops in inhibition of phagocytosis and killing of opsonized *Yersinia enterocolitica* by human granulocytes. Infection and Immunity *63*, 2570–2575.

Williams, P., and Wallace, D. (1989). Unit 731 (New York : Free Press).

World Health Organization (2004). Public health response to biological and chemical weapons: WHO guidance.

Wu, L.-T., Chun, J.W.H., Pollitzer, R., and Wu, C.Y. (1936). Plague. A Manual for Medical and Public Health Workers (Shanghai Station: National Quarantine Service).

Zietz, B.P., and Dunkelberg, H. (2004). The history of the plague and the research on the causative agent Yersinia pestis. Int J Hyg Environ Health *207*, 165–178.

CHAPTER 2: CHARACTERIZATION OF THE LUNG LESION MICROENVIRONTMENT BY LASER CAPTURE MICRODISSECTION AND RNAseq ANALYSIS*

2.1 Overview

This chapter describes the use of fully virulent *Y. pestis*, laser capture microdissection (LCM), and RNAseq technology to evaluate host transcription within the expanding neutrophil-rich lung lesions that arise during the pro-inflammatory disease phase of pneumonic plague. This work provides evidence that lung lesions begin as small foci that expand outward throughout infection, and that *Y. pestis* inhibits apoptosis of neutrophils in the center of lung lesions compared with those found around the lesion periphery. This work is the first application of LCM to evaluate the effects of a bacterial pathogen on a microenvironment within its host during infection. This novel use of LCM allowed us to identify spatially distinct transcriptional changes *in vivo* within sites of tissue injury that cannot be characterized *in vitro*. This work evaluates how interactions with *Y. pestis* induce unique transcriptional responses in neutrophils within spatially distinct sites of

* This data has been published in: Stasulli NM, Eichelberger KR, Price PA, Pechous RD, Montgomery SA, Parker JS, Goldman WE. 2015. Spatially distinct neutrophil responses within the inflammatory lesions of pneumonic plague. mBio 6(5):e01530-15. doi:10.1128/mBio.01530-15.

infection. Research of this nature will better help expound on mechanisms by which neutrophils typically work in a broad range of diseases where neutrophil infiltration becomes harmful to the host.

2.2 Introduction

Large dataset analyses have become invaluable for new and innovative research in the bacterial pathogenesis field. Several studies have investigated the regulation of the *Yersinia* transcriptome by both microarrays (Du et al., 2009; Han et al., 2007; Liu et al., 2009; Pechous et al., 2015; Sebbane et al., 2006; Zhou et al., 2006) and deep sequencing (Koo et al., 2011; Schiano et al., 2014; Yan et al., 2013) under varying environmental conditions *in vitro* and during disease *in vivo*. Very few studies, on the other hand, have focused on the transcriptional changes of the host during *Y. pestis* infection. One microarray study by Liu et al. evaluated both bacterial and host transcription in multiple organs by qRT-PCR and microarray analysis after pulmonary challenge with Y. pestis. This host analysis focused on transcriptional changes in cytokines (Liu et al., 2009). A less high-throughput study using Northern blot analysis also observed transcriptional changes in human neutrophils after interaction with *Y. pestis* (Subrahmanyam et al.).

Despite previous research on interactions between neutrophils and *Y. pestis in vivo* (Laws et al., 2010; Lukaszewski et al., 2005; Marketon et al., 2005; Pechous et al., 2013; Shannon et al., 2013), there is little information to explain the architecture and rapid expansion of neutrophil-rich lesions that are the pathological hallmark of pneumonic plague. Previous research has indicated that *Y. pseudotuberculosis* regulates its genes spatially within infected tissue (Davis et al., 2015). Combined with the information that bacterial pathogens can alter neutrophil gene expression (Schwartz et al., 2013; Subrahmanyam et al.), the research in this chapter investigates the possibility that spatially distinct transcriptional modulation of

neutrophils is observable in lung lesions that develop during pneumonic plague.

Laser capture microdissection (LCM) was first described in 1996 (Emmert-Buck et al., 1996), and is a technique that can be used to investigate spatial gene regulation in tissue samples. The work in this dissertation was performed using a UV laser Zeiss P.A.L.M. microscope. With this system, lung tissue slices are adhered onto a slide containing a polyethylene napthalate membrane for use with the UV laser. The laser is focused and cuts around the desired section of tissue. The defocused laser is then pulsed in the center of the cut membrane where it is catapulted off of the slide and into an RNA preserving resin in the top of an Eppendorf tube, where the RNA can be isolated for downstream applications (Espina et al., 2007; Schütze et al., 2007). This technique is sophisticated enough to allow for DNA, RNA, and protein extraction at the single-cell level (Suarez-Quian et al., 1999). Its use in the field of microbial pathogenesis, however, has rarely been exploited and has mainly been limited to plant pathogens (Balestrini et al., 2007; Berruti et al., 2013; Klink et al., 2005; Klink and Matthews, 2008; Klink et al., 2007) or *in vitro* studies (Schulte et al., 2011).

2.3 Methods

All reagents were obtained form Sigma-Aldrich™ unless otherwise noted.

2.3.1 Ethics statement

The use of live vertebrate animals was performed in accordance with the Public Health Service (PHS) policy on Humane Care and Use of Laboratory Animals,

the Amended Animal Welfare Act of 1985, and the regulations of the United States Department of Agriculture (USDA). All animal studies were approved by the University of North Carolina at Chapel Hill Office of Animal Care and Use, protocols #12-028.0 and #15-022.0.

2.3.2 Bacterial strains and culture conditions

The fully virulent *Yersinia pestis* strain CO92 was obtained from the U.S. Army, Ft. Detrick, MD. *Y. pestis* was grown on brain-heart infusion (BHI) agar (Difco Laboratories) at 26°C for two days. For infections, liquid cultures of *Y. pestis* CO92 were grown in BHI broth for 6–12 h at 26°C. The cultures were then diluted to an OD_{620} of 0.05–0.1 in BHI supplemented with 2.5 mM $CaCl_2$ and grown 12–16h at 37°C with constant shaking.

2.3.3 Animals and infections

Six- to eight-week old female C57BL/6J mice were obtained from Jackson Laboratories. Mice were provided with food and water ad libitum and maintained at 25°C and 15% humidity with alternating 12 h periods of light and dark. For animal infections, groups of three to ten mice were lightly anesthetized with ketamine/xylazine and inoculated intranasally with a lethal dose of 10^4 colony-forming units (CFUs) suspended in 20µL PBS. Actual CFUs inoculated was determined by plating serial dilutions of the inoculum on BHI.

2.3.4 Tissue preparation, Laser Capture Microdissection, and RNA isolation

All solutions are either RNase free or have been treated with diethylpyrocarbonate (DEPC). Lungs were inflated via tracheal cannulation with RNAlater® (Ambion®) and incubated for 30 min. Lungs were then fully inflated with 4% fresh paraformaldehyde and incubated for 2 h for fixation and removal from the BSL 3 laboratory. Lungs were placed in phosphate buffer (pH 7.4) with 30% Sucrose and 20% O.C.T. compound (Tissue-Tek®) for 3 h with intermittent inverting. Lungs were removed, covered in O.C.T. for 10 min, frozen on dry ice, and stored at -80°C.

Lungs were sectioned into 20-µm slices using a Leica®-1850 cryostat and adhered to 1.0 mm PEN-MembraneSlides (Zeiss™). To remove O.C.T. media from sections, slides were dipped in 100% ethanol and allowed to dry, incubated in DEPC-treated water for 3-5 min, then dipped into increasing concentrations of ethanol (70%, 95%, 100%) and allowed to fully dry.

For LCM, slides were then loaded onto a Zeiss PALM LCM microscope and a 4X objective was used to observe lung lesions. Opaque AdhesiveCap Eppendorf tubes were loaded and positioned directly over the slides. The desired sections of each lung lesion were traced, cut by a laser, and laser pulse-catapulted into the resin preservative in the top of the AdhesiveCap tubes. The tubes containing isolated lesion pieces were stored at -80°C prior to RNA isolation. Total RNA was isolated from the LCM-extracted lesion pieces using an RNeasy FFPE kit (Qiagen™) as per the manufacturers instructions with the exception of a 3 h incubation at 56°C after the addition of proteinase K.

For bone marrow neutrophil isolation, femurs of C57BL/6J mice were collected and flushed with cold PBS to extract marrow. Marrow cells were disaggregated by repetitive passes through an 18 gauge needle. Bone marrow neutrophils (BM-PMNs) were then isolated using a MACS Neutrophil isolation kit (Miltenyi Biotec) per the manufacturer's instructions. The final volume of BM-PMNs was resuspended in TRIzol® Reagent (Ambion®) and total RNA was isolated per the manufacturer's instructions.

2.3.5 RNAseq library prep and analysis

Total RNA was sent for library preparation and sequencing at the High Throughput Sequencing Facility at The University of North Carolina at Chapel Hill. Briefly, a Qubit™ RNA Assay Kit for use with a Qubit® Fluorometer was used to quantify the total RNA concentration of each sample. Both eukaryotic and prokaryotic ribosomal-RNA was then removed from the samples using an Epidemiology Ribo-Zero™ Magnetic Gold Kit (Epicentre®). Complementary DNA was generated using a SMARTer® Universal Low Input RNA Kit (Clontech®) followed by RNAseq library sequencing template preparation using a Low Input Library Prep Kit (Clontech®). The library was prepared and run on a MiSeq® sequencer (Illumina®) to test the quality of the library. After library verification, samples were diluted and barcoded for paired end amplification and clustered (TruSeq® SBS Kit v2 (200cycles) and TruSeq® PE Cluster Kit v2 (Illumina®)) using a cBot™ (Illumina®) for running on a HiSeq® 2000 system (Illumina®). Quality

control steps throughout the RNAseq library preparation were performed using a DNA 12K Analysis Kit (Experion®) or a LabChipGX HT DNA LabChip® Kit (Caliper™). All MiSeq and HiSeq kits used the v2 chemistry.

Purity filtered reads were aligned to the *Mus musculus* reference genome (mm9) using MapSplice (Davis et al., 2015; Wang et al., 2010). The alignment profile was summarized by Picard Tools (Broad Institute) v1.64. Aligned reads were sorted and indexed using SAMtools (Li et al., 2009; Schwartz et al., 2013; Subrahmanyam et al.), translated to transcriptome coordinates, and filtered for indels, large inserts, and zero mapping quality using UBU v1.0. Transcript abundance estimates for each sample were performed using an Expectation-Maximization algorithm implemented in RSEM (Li and Dewey, 2011) based on the UCSC knownGene definitions. Raw counts were normalized to the upper quartile (Bullard et al., 2010). Log transformed normalized gene expression estimates were assessed for differential expression using Student's t-test, and these results were filtered to highlight genes achieving $p < 0.05$ in both comparisons (BM-PMN and lung lesions). Cluster analysis was performed to assess the patterns of differential expression (hierarchical clustering based on complete linkage and a Pearson correlation) for several defined gene sets testing for differential activity between the conditions. The gene set test performed a Wilcoxon rank-sum test of the log fold change estimates between genes in a set and those in the entire transcriptome where there were greater than three gene reads. Gene set results were visualized using density plots in R (version 3.1.1). Raw RNAseq data is available on the NCBI repository, series record GSE70819.

2.4 Results

2.4.1 Characterizing host gene regulation in spatially defined regions of pneumonic plague lung lesions

Pulmonary infection of mice with *Y. pestis* results in the formation of distinct inflammatory lesions in the lung during the pro-inflammatory phase of disease. The lesions consist primarily of *Y. pestis* bacteria and densely packed pockets of neutrophils, and these inflamed sites expand throughout the duration of infection, ultimately covering entire lobes of the lung (Lathem et al., 2005). At 48 hours post-inoculation (hpi) with *Y. pestis* strain CO92, we observed that a typical H&E-stained lung section contained up to 5 distinct foci of inflammation per lobe. These sites were as large as 3 mm in diameter, with inflammation occupying 5-10% of the total examined tissue plane (Figure 2.1A). The inflammatory infiltrate displayed very little cellular necrosis and was composed predominantly of neutrophils, with fewer dispersed macrophages. Interspersed amid inflammatory infiltrate were abundant extracellular organisms and variable amounts of fibrin, hemorrhage, edema, and cellular debris. The majority of large and small bronchi remained unaffected, even those located immediately adjacent to inflammatory foci. Occasional dense aggregates of extracellular bacteria formed small colonies, particularly at the periphery of lesions (Figure 2.1C). These observations suggested that I could learn more quantitative information from these lesions by spatially dissecting them to analyze unique microenvironments.

To further characterize these inflammatory lung lesions, I focused on analyzing transcriptional responses in neutrophils to understand the lack of turnover and clearance of this key cell type. The T3SS of *Y. pestis* has potent anti-inflammatory effects on targeted mammalian cells (Aepfelbacher et al., 2007). As a result of their direct contact with *Y. pestis*, we predicted that those neutrophils found within the initiating focus of the lung lesions, the lesion "center," would have a different transcriptional profile than those found in the lesion periphery, where I assumed the most recent wave of migrating neutrophils would be found. To test this, I devised an approach to identify transcriptionally regulated host pathways in neutrophils found within these spatially distinct regions. Briefly, I infected mice with 10^4 CFU of *Y. pestis* CO92, a fully virulent strain previously isolated from a pneumonic plague patient. At 48 hpi I treated lungs with an RNA preservative, then used LCM on fixed and frozen sections to collect tissue from the center and periphery of the lesions (Figure 2.1D, E).

Total RNA was isolated from these captured microenvironments, RNAseq libraries were prepared, and samples were sequenced to define host transcriptional responses. Additionally, I harvested total RNA from MACS-isolated neutrophils residing in the bone marrow (BM-PMNs) of *Y. pestis*-infected (and mock-infected) mice at 48 hpi for comparison. Using Student's t-test, 976 genes were identified that were differentially expressed between the periphery and center of the lung lesions ($p\text{-value} < 0.05$). This analysis was simultaneously performed on the infected- and mock-infected-mouse BM-PMN samples. This comparison identified 3,198 genes

that were differentially expressed in BM-PMNs from infected mice compared to mock-infected mice. Importantly, transcriptionally altered BM-PMN genes represent neutrophil-specific responses to *Y. pestis* infection at 48 hpi, and are a heterologous tissue match to the lung lesion samples collected at the same time point during infection. Matching genes in the lesion periphery/center comparison to those genes found in the BM-PMN comparison allowed me to narrow the lung lesion gene set to those genes regulated specifically in neutrophils rather than other cell types in the lung. The initial list of 976 genes was reduced to 224 genes that were differentially expressed in both the BM-PMN and lung lesion comparisons, with a significant enrichment value of $p = 0.02$ (Figure 2.2, Table 2.1). This confirms that there are transcriptional alterations in neutrophil genes between the lesion periphery and center, and establishes that *Y. pestis* causes a sustained change in neutrophil transcription at distinct locations in lung lesions. Interestingly, when the four conditions (infected BM-PMN, mock-infected BM-PMN, lesion periphery, lesion center) were clustered across samples, the differential expression patterns of the 224 genes showed that (*i*) the BM-PMN from mock-infected mice and lesion center conditions clustered together, and (*ii*) the BM-PMN from *Y. pestis*-infected mice and lesion periphery conditions clustered together (Figure 2.2). This suggests that the neutrophils in the lesion center had a transcriptional pattern more similar to "unstimulated" bone marrow neutrophils, despite residing in a highly inflammatory microenvironment in the infected lungs.

2.4.2 Gene set analysis implications for lesion development and neutrophil fate.

Using the Ingenuity® Pathway Analysis (IPA®) program (QIAGEN Redwood City) and the Molecular Signatures Database (Subramanian et al., 2005), we compiled various gene sets (Table 2.2) to analyze pathways for differential gene expression patterns between the lesion periphery and center. Density curves were generated based on the ratio of RNA expression estimates between the lesion periphery and lesion center (when there were more than three reads in both conditions). A Wilcoxon rank-sum test was performed comparing the log ratio distribution from the individual gene sets to the entire transcriptome, with the goal of identifying bias in specific gene sets.

Based on the log ratio of lesion periphery compared to the center, there was a statistically significant shift for genes in “leukocyte migration” pathways compared to the entire transcriptome (Figure 2.3B). This shift indicates relatively lower expression in the center of lesions; i.e., the lesion centers show an overall down-regulation of genes in this list. In contrast, “general cell migration” genes showed no shift in the lesion periphery/center ratio compared to the entire transcriptome (Figure 2.3A, Table 2.2). These transcriptional comparisons in the “leukocyte migration” pathways suggest that newly infiltrating neutrophils are localized at the periphery of the expanding lesions, while the neutrophils at the center were likely recruited much earlier. The histopathological evidence in the lungs also supports this scenario. Centrally within inflammatory foci, neutrophils are densely packed, completely filling

alveolar spaces and leading to loss of the alveolar septa. Peripherally there are fewer, loosely packed neutrophils with some remaining clear air space.

We additionally evaluated whether neutrophil apoptosis/survival was being altered in the center of lung lesions, since this could explain continued neutrophil accumulation due to a lack of turnover in the lung. A set of genes representing various apoptosis pathways was compiled (Table 2.2) and showed a statistically significant shift in the lesion periphery/center ratio compared to the entire transcriptome, indicating a down regulation of genes in the apoptosis pathways in the lesion center (Figure 2.3C). Overlaying individual apoptotic genes from the density curve analysis with a p-value < 0.5 onto the IPA® "Apoptosis Signaling" pathway (QIAGEN) showed that small transcriptional changes throughout this pathway could result in decreased apoptosis in cells at the center of lung lesions (Figure 2.1).

2.5 Discussion

The work presented in this chapter describes a novel approach to examining bacterial pathogenesis, using LCM to dissect unique spatial phenotypes of tissue damage during infection *in vivo* that cannot be studied *in vitro*. I hypothesized that *Y. pestis* directly alters the ability of neutrophils to progress through their cellular life cycle, leading to a failure of clearance from the lungs. This lack of clearance likely leads to development of the continually expanding inflammatory lesions, causing significant pulmonary damage. In the work presented here, I show that RNAseq analysis after LCM is a viable technique to study host/pathogen interactions during

infection. Further, I can glean information about disease progression by spatially dissecting regions of inflammation and damage *in vivo* that could not be obtained through *in vitro* studies alone. In the future it will be beneficial to be able to perform dual RNAseq to obtain both the host and bacterial transcriptome simultaneously.

The formation of lung lesions during pneumonic plague is well documented in several animal models (Adamovicz and Worsham, 2006; Agar et al., 2009; Anderson et al., 2009; Fellows et al., 2012; Koster et al., 2010; Lathem et al., 2005; Layton et al., 2011; Van Andel et al., 2008). In this study, I present the first analysis of how these lung lesions develop and persist during pneumonic plague. Further, I probe the transcriptomes of host cells in the periphery and center of these lesions in an effort to better understand this complex microenvironment. The resulting data indicated that within the lung lesions, there are spatially defined differences in gene expression. Due to the high concentration of *Y. pestis* targeted neutrophils within the lesions (Marketon et al., 2005; Pechous et al., 2013), I was most interested in dissecting out neutrophil-specific transcriptional responses. When performing LCM, non-neutrophil RNA would also be isolated and complicate the neutrophil-specific analysis I was seeking. To abrogate this, I isolated BM-PMNs from mock-infected and *Y. pestis*-infected mice at 48 hpi to generate a list of genes I could identify as neutrophil-regulated responses to *Y. pestis* infection. By this time during infection, *Y. pestis* has disseminated into the bloodstream (Lathem et al., 2005) and can even be detected in the bone marrow (Vagima et al., 2012). I anticipated that any BM-PMN genes responsive to *Y. pestis* infection might also be identified in neutrophils in the

lesion comparison. Analyzing the lesion periphery and lesion center gave me an unbiased list of differentially expressed genes between these two regions in any cell type present. Matching differentially expressed genes from the lesion periphery/center comparison to the same genes in the BM-PMN comparison resulted in a set of 224 genes we identified as likely neutrophil-specific transcriptional responses to *Y. pestis* infection. Using the BM-PMN list gave me confidence that the 224 genes identified in both comparisons are indicating a significant alteration in neutrophil gene expression between the lesion periphery and center, as opposed to contaminating monocytic infiltrate or lung epithelium.

In addition to analyzing differential expression between regions of lung lesions, I wanted to test the hypothesis that lesions develop from small initiating foci and continue expanding outward throughout the course of infection. Alternatively, neutrophils could be infiltrating randomly into the lesion space. To examine this, the RNAseq data was analyzed based on defined lists of genes involved in general cell migration and leukocyte-specific migration compared to the entire transcriptome. The density distribution of the ratios of genes in each list was analyzed comparing the lesion periphery to the lesion center. This distribution was then compared to the same distribution from the entire transcriptome. This statistical comparison helped evaluate if transcription of genes in each of the lists were being skewed compared to the entire transcriptome. I observed a statistically significant shift in the log ratio in the leukocyte migration gene set, indicating decreased transcription in the center of lung lesions; in contrast, no shift was observed for genes involved in general cell

migration. This implies that neutrophils in the center of lesions were recruited earlier during infection, and these cells subsequently decreased transcription of genes such as cytokine and cell-cell adhesion receptors that are necessary for chemotaxis and lung infiltration (Table 2.2).

I also postulated that the lesions continue to expand over time as a result of *Y. pestis*-mediated alteration of neutrophil apoptosis and survival. The apoptotic pathways gene list was analyzed as described above. A significant shift in the log ratio distribution of the apoptosis gene set suggested that these pathways were down-regulated in the center of lesions compared to the periphery. Analyzing the RNAseq data at the pathway level allowed me to statistically evaluate how small changes in expression of pathway-related genes may manifest into greater changes downstream in the pathway, since individual genes in pathways did not always show discrete statistically significant differences ($p < 0.05$) between areas of the lesion. For example, caspases-8 and 9 both had non-significant p-values (< 0.5); Looking closer at where these caspases intersect in apoptosis signaling pathways, it can be observed how a transcriptional decrease in caspase-8 can prevent the activation of BID to tBID, ultimately preventing the release of proteins allowing for downstream caspase activation. Both caspases-8 and 9 are important for direct cleavage of caspase-3, the converging point of both the extrinsic and intrinsic apoptosis pathways (McCracken and Allen, 2014). The decrease in transcription of both of these initiator caspases is an additional downstream hindrance to apoptosis (Figure 2.4).

In summary, I introduced a unique application of LCM technology to directly examine the spatially distinct microenvironments resulting from host-pathogen interactions during primary pneumonic plague. As a result, I was able to identify pathways that are regulated by the interaction of *Y. pestis* with neutrophils in lung lesions during pneumonic plague. The directionality of these transcriptional changes suggest that neutrophils build from small foci in the lungs, and the neutrophils that first interact with *Y. pestis* in the center of these lesions are hindered in initiating apoptosis. Further defining and characterizing mediators of the dramatic pulmonary inflammation that occurs during pneumonic plague will help in understanding the lethality of this disease and may contribute to our understanding of severe pulmonary infection with other respiratory pathogens.

2.6 Figures and Tables

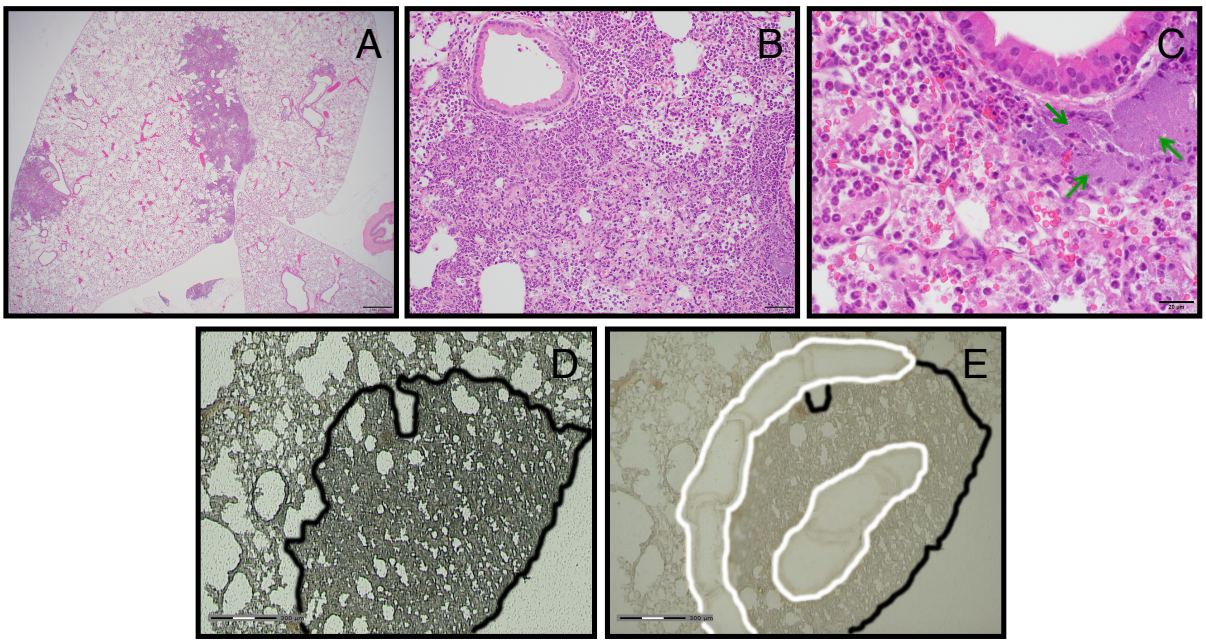

Figure 2.1: Lung lesion histology and laser capture microdissection of lesions

Representative H&E stained sections of a *Y. pestis*-infected lung at 48 hpi, shown at different magnifications (**A**-**C**, scale bar equals 500, 50, and 20u µm respectively). (**C**) The green arrows indicate dense aggregates of *Y. pestis*. Representative images of a lung section (**D**) before and (**E**) after laser capture microdissection (scale bar equals 300 µm). The lung lesion (outlined in black) was identified and the periphery and center of the lesions were spatially defined (outlined in white). Laser cutting and pulse catapulting into a preservative resin selectively removed white-outlined lesion sections.

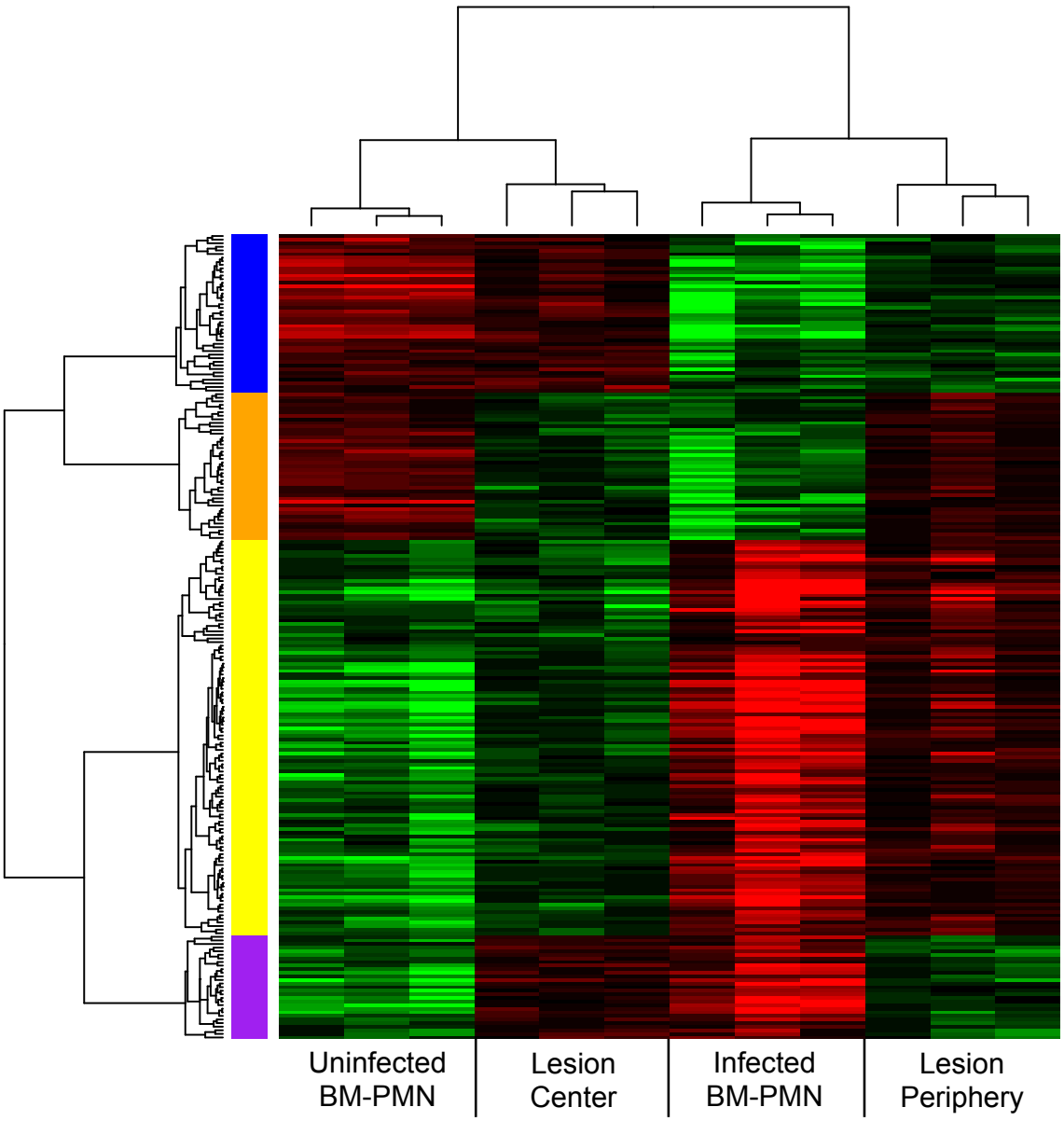

Figure 2.2: Clustered genes showing differential transcription

A heatmap showing 224 genes differentially expressed in two comparisons (BM-PMNs from mock-infected v. infected mice and lesion periphery v. center). The red and green colors represent an increase or decrease, respectively, relative to the median value of each of the two initial comparisons. The X-axis clustering shows that all triplicates clustered together and that mock-infected BM-PMN and lesion

center samples clustered more closely, as did infected BM-PMN and lesion periphery samples. Each gene shows significant differences ($p < 0.05$ in Student's t-test) in each of the two initial comparisons. The blue, orange, yellow, and purple colored bars represent the four possible outcomes of gene regulation comparisons (e.g., blue bar shows genes that were decreased in BM-PMNs from infected compared to mock-infected mice and increased in the lesion center compared to the periphery).

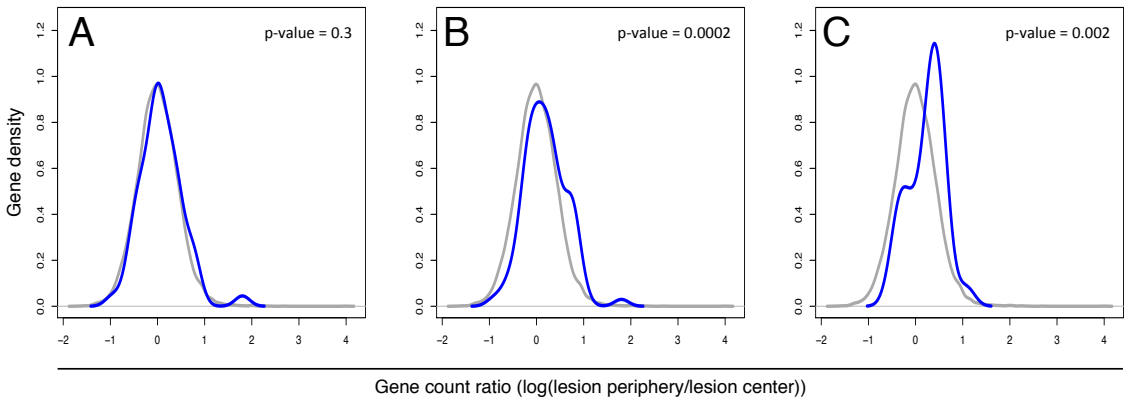

Figure 2.3: Density curves of defined gene sets compared to the entire transcriptome

Gene sets were compiled to represent A) general cell migration, B) leukocyte migration, and C) apoptosis pathways. Using the log ratio of RNAseq reads in lesion periphery compared to lesion center, log ratios of each of these compiled gene sets (blue lines) were contrasted against the entire transcriptome (grey lines) using a Wilcoxon rank-sum test. The Y-axis values are arbitrary units as calculated by Gaussian kernel density estimates. Only genes with > 3 reads from the RNAseq analysis were graphed.

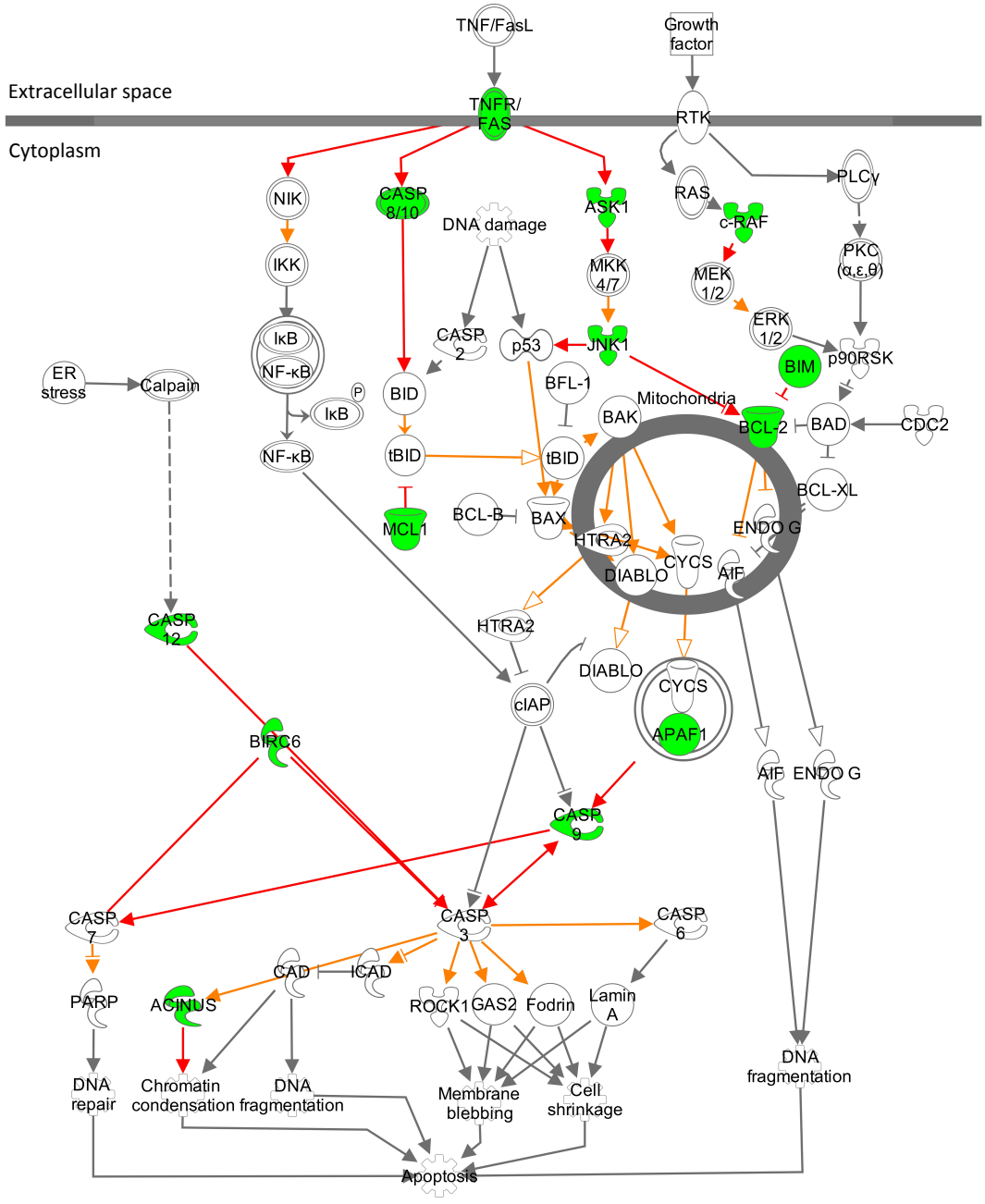

Figure 2.4: Ingenuity® Pathway Analysis "Apoptosis Signaling" pathway overlaid with relevant genes from density curve analysis

Genes from the "Apoptosis Signaling" pathway from IPA® were included in the "Apoptosis genes" list used in the density curve analysis. The density curve analysis identified the "Apoptosis genes" list as being transcriptionally decreased in the

center of lesions so individual genes with $p < 0.5$ were overlaid onto the IPA® "Apoptosis Signaling" pathway (green) to visually represent small transcriptional changes throughout the pathway in the center of lesions. Red lines represent direct interactions that would be affected by decreased transcription of identified genes in cells. Orange lines represent secondary affects of the identified genes being down-regulated in cells.

Table 2.1: List of 224 differentially regulated in both the infected versus uninfected BM-PMN and lesion periphery versus center comparisons

Gene names	Entrez numbers	p-value (infected/uninfected BM-PMN)	p-value (lesion periphery/center)	Pattern of differential expression
1700020L24Rik	66330	1.785E-03	3.813E-02	blue
2210018M11Rik	233545	2.390E-03	4.503E-02	yellow
2310021P13Rik	268721	1.884E-03	3.917E-02	blue
2410016O06Rik	71952	2.340E-05	1.943E-03	blue
2610101N10Rik	67958	2.148E-03	4.178E-02	yellow
4933427D14Rik	74477	8.521E-05	4.736E-03	purple
9030624J02Rik	71517	3.365E-04	1.289E-02	orange
A730017L22Rik	613258	8.267E-04	2.235E-02	yellow
A830007P12Rik	227612	1.342E-04	6.709E-03	blue
A930001N09Rik	77128	1.181E-04	6.266E-03	orange
Abi2	329165	5.410E-04	1.674E-02	yellow
Acd	497652	1.457E-04	7.469E-03	purple
Adam9	11502	3.363E-04	1.278E-02	yellow
Aftph	216549	2.212E-03	4.287E-02	orange
Agrn	11603	1.651E-03	3.675E-02	blue
Ahi1	52906	4.990E-05	3.264E-03	yellow
Ankrd33b	67434	2.271E-03	4.341E-02	blue
Ankrd44	329154	1.774E-03	3.806E-02	orange
Anxa4	11746	2.192E-03	4.258E-02	yellow
Arhgap23	58996	2.015E-03	4.055E-02	blue
Arl4a	11861	1.610E-04	7.882E-03	yellow
Arrb1	109689	2.618E-03	4.751E-02	orange
Arrdc3	105171	1.206E-03	2.863E-02	orange
Atl3	109168	2.172E-04	9.122E-03	yellow
Atp2c1	235574	4.490E-05	3.082E-03	orange
Atp5o	28080	2.394E-03	4.508E-02	yellow
BC005537	79555	3.890E-04	1.354E-02	orange
BC016423	105203	1.190E-04	6.309E-03	yellow
Beta-s	100503605	1.571E-03	3.535E-02	yellow
Bmpr1a	12166	2.208E-04	9.151E-03	orange
Bpnt1	23827	5.592E-04	1.717E-02	yellow
Brix1	67832	3.344E-06	4.679E-04	yellow
Btbd19	78611	5.192E-04	1.603E-02	blue
C1ra	50909	1.083E-03	2.650E-02	yellow
Camsap1	227634	7.791E-04	2.172E-02	purple
Canx	12330	1.442E-03	3.324E-02	yellow
Cd101	630146	2.684E-03	4.791E-02	blue
Cd47	16423	2.823E-03	4.935E-02	orange
Cdc37l1	67072	3.366E-05	2.394E-03	orange
Cdipt	52858	1.810E-03	3.837E-02	purple

Ceacam1	26365	1.634E-03	3.623E-02	yellow
Cenpf	108000	2.396E-03	4.514E-02	purple
Cep350	74081	4.066E-04	1.387E-02	orange
Cfh	12628	2.824E-04	1.152E-02	yellow
Chd9	109151	9.402E-05	5.200E-03	yellow
Cir1	66935	2.450E-03	4.566E-02	yellow
Cln3	12752	6.450E-07	3.500E-05	blue
Clock	12753	1.731E-03	3.785E-02	yellow
Clta	12757	6.241E-05	3.622E-03	blue
Crlf3	54394	2.848E-03	4.942E-02	blue
Csrp2bp	228714	5.572E-04	1.713E-02	purple
Ctcf	13018	1.609E-04	7.860E-03	yellow
Ctla2a	13024	3.487E-04	1.297E-02	purple
Cwc27	67285	8.800E-05	5.039E-03	yellow
Dbi	13167	5.053E-04	1.593E-02	yellow
Ddx17	67040	1.248E-03	2.958E-02	orange
Ddx46	212880	1.074E-03	2.643E-02	yellow
Dhx15	13204	1.771E-03	3.803E-02	yellow
Dlg1	13383	1.551E-05	1.377E-03	orange
Dock4	238130	1.785E-03	3.819E-02	yellow
Ebna1bp2	69072	3.270E-05	2.229E-03	purple
Eif1a	13664	1.037E-03	2.609E-02	yellow
Eif3i	54709	5.940E-04	1.817E-02	yellow
Elp2	58523	2.920E-04	1.180E-02	purple
Eltd1	170757	1.341E-03	3.110E-02	yellow
Esco1	77805	1.697E-04	7.903E-03	yellow
F630043A04Rik	219114	1.566E-03	3.526E-02	yellow
Fam102a	98952	1.886E-03	3.923E-02	blue
Fam193b	212483	6.371E-04	1.892E-02	blue
Fam40a	229707	2.790E-04	1.145E-02	blue
Fen1	14156	5.300E-04	1.651E-02	purple
Fkrp	243853	8.457E-04	2.276E-02	blue
Fmr1	14265	4.797E-04	1.562E-02	yellow
Fubp1	51886	1.234E-03	2.944E-02	yellow
Fundc2	67391	1.828E-06	3.273E-04	yellow
Gatad2b	229542	1.288E-03	3.001E-02	blue
Gclc	14629	3.705E-05	2.631E-03	yellow
Ghdc	80860	2.727E-04	1.110E-02	blue
Ghitm	66092	4.152E-04	1.412E-02	yellow
Gnb1	14688	2.041E-03	4.077E-02	orange
Gnpnat1	54342	5.198E-04	1.605E-02	yellow
Golim4	73124	8.254E-04	2.217E-02	orange
Golm1	105348	9.266E-05	5.169E-03	yellow
Gpr65	14744	5.077E-04	1.593E-02	yellow
Gpx3	14778	1.257E-04	6.321E-03	yellow
H2-T24	15042	1.869E-03	3.906E-02	orange

Hdlbp	110611	1.695E-03	3.753E-02	yellow
Hmg20a	66867	2.798E-04	1.150E-02	orange
Il15ra	16169	2.239E-04	9.260E-03	yellow
Il28ra	242700	2.156E-03	4.202E-02	orange
Il6st	16195	1.909E-04	8.574E-03	yellow
Impa1	55980	3.539E-05	2.513E-03	yellow
Itprip	414801	2.792E-03	4.904E-02	blue
Kalrn	545156	2.950E-04	1.197E-02	purple
Kcnk6	52150	2.365E-03	4.481E-02	purple
Kif1b	16561	1.276E-03	2.989E-02	orange
Klhl25	207952	8.177E-04	2.207E-02	blue
Las1l	76130	4.798E-05	3.210E-03	yellow
Lmnb1	16906	2.632E-03	4.759E-02	blue
Lpar6	67168	4.162E-04	1.417E-02	yellow
Lrp6	16974	1.936E-03	3.994E-02	yellow
Lrrc61	243371	6.254E-05	3.634E-03	blue
Ly6e	17069	1.917E-03	3.985E-02	yellow
M6pr	17113	4.919E-04	1.567E-02	yellow
Maz	17188	1.468E-03	3.373E-02	orange
Mrps25	64658	7.352E-04	2.069E-02	yellow
Mtap4	17758	1.368E-03	3.200E-02	orange
Mtpn	14489	1.020E-04	5.410E-03	yellow
Mylip	218203	1.128E-03	2.698E-02	orange
Mysm1	320713	2.689E-03	4.828E-02	yellow
Naip6	17952	2.473E-04	1.022E-02	purple
Nat10	98956	5.594E-04	1.751E-02	purple
Nat8l	269642	1.498E-04	7.494E-03	blue
Ndst2	17423	1.064E-04	5.747E-03	purple
Nek7	59125	2.560E-03	4.696E-02	yellow
Ngly1	59007	1.790E-03	3.825E-02	orange
Nipal3	74552	2.578E-03	4.713E-02	blue
Nol11	68979	2.463E-03	4.574E-02	purple
Nol8	70930	2.834E-03	4.937E-02	yellow
Nolc1	70769	1.704E-03	3.768E-02	purple
Npat	244879	3.345E-04	1.267E-02	yellow
Nt5e	23959	6.090E-05	3.585E-03	orange
Nup88	19069	9.513E-04	2.431E-02	yellow
Ogdh	18293	1.139E-04	6.009E-03	yellow
Orm1	18405	8.525E-04	2.302E-02	yellow
Pcnxl3	104401	9.165E-05	5.139E-03	blue
Pde5a	242202	5.994E-04	1.823E-02	yellow
Pdia6	71853	1.859E-03	3.881E-02	yellow
Pecam1	18613	1.219E-03	2.920E-02	yellow
Phc3	241915	1.428E-04	7.247E-03	yellow
Phf20l1	239510	1.113E-03	2.677E-02	orange
Piga	18700	6.141E-05	3.598E-03	yellow

Pigy	66459	4.350E-04	1.497E-02	yellow
Plec	18810	1.644E-03	3.661E-02	blue
Pmm2	54128	2.884E-03	4.979E-02	yellow
Polr3e	26939	1.820E-03	3.841E-02	purple
Ppan	235036	1.584E-03	3.551E-02	purple
Pphln1	223828	5.886E-04	1.813E-02	yellow
Prpf39	328110	3.325E-04	1.256E-02	yellow
Prpf40a	56194	3.789E-04	1.320E-02	yellow
Prr12	233210	2.271E-05	1.894E-03	blue
Psd3	234353	8.944E-04	2.379E-02	yellow
Pskh1	244631	5.221E-04	1.613E-02	purple
Ptpn4	19258	4.970E-04	1.574E-02	yellow
Qrich1	69232	6.860E-04	1.987E-02	yellow
Ralgapa2	241694	2.762E-04	1.133E-02	orange
Rap1gds1	229877	2.586E-03	4.734E-02	orange
Rbm33	381626	1.304E-03	3.015E-02	orange
Rbmxl1	19656	2.387E-04	9.591E-03	yellow
Rbpj	19664	1.376E-04	6.919E-03	yellow
Rif1	51869	2.219E-03	4.302E-02	yellow
Rin2	74030	1.648E-03	3.664E-02	orange
Rlim	19820	4.269E-04	1.471E-02	yellow
Rnf144b	218215	1.444E-04	7.281E-03	yellow
Rnf145	74315	1.145E-04	6.080E-03	blue
Rnft1	76892	5.695E-04	1.785E-02	yellow
Rpap1	68925	1.643E-03	3.648E-02	purple
Rpl36al	66483	1.841E-03	3.873E-02	yellow
Rps15a	267019	6.438E-04	1.916E-02	orange
Rrm2b	382985	3.912E-04	1.375E-02	yellow
Rtf1	76246	1.117E-03	2.689E-02	orange
Scaf1	233208	8.171E-05	4.572E-03	blue
Scly	50880	1.031E-03	2.593E-02	purple
Sec22c	215474	8.462E-04	2.279E-02	blue
Sec63	140740	4.979E-04	1.576E-02	yellow
Senp1	223870	1.393E-03	3.250E-02	yellow
Serbp1	66870	7.059E-04	2.012E-02	yellow
Sf3a1	67465	1.305E-03	3.016E-02	yellow
Sipa1l2	244668	1.016E-04	5.384E-03	blue
Slc10a3	214601	1.627E-03	3.609E-02	purple
Slc12a6	107723	1.127E-03	2.692E-02	orange
Slc31a1	20529	9.491E-04	2.423E-02	yellow
Slc38a10	72055	2.215E-04	9.159E-03	blue
Slc43a3	58207	1.613E-03	3.594E-02	yellow
Slc44a1	100434	1.165E-03	2.744E-02	orange
Slfn3	20557	4.833E-06	6.037E-04	yellow
Slfn9	237886	2.525E-03	4.653E-02	yellow
Slmap	83997	2.683E-04	1.087E-02	orange

Smcr7	237781	2.532E-04	1.039E-02	blue
Smek1	68734	2.066E-05	1.865E-03	orange
Snapc3	77634	1.707E-03	3.774E-02	yellow
Snrpd1	20641	1.607E-03	3.590E-02	yellow
Sptlc2	20773	1.205E-03	2.851E-02	orange
Stt3a	16430	2.715E-03	4.842E-02	yellow
Stx2	13852	6.584E-04	1.935E-02	blue
Sub1	20024	1.393E-03	3.246E-02	yellow
Sugt1	67955	2.735E-04	1.126E-02	yellow
Syncrip	56403	2.175E-03	4.235E-02	yellow
Sytl1	269589	5.621E-04	1.752E-02	blue
Tbp	21374	2.555E-04	1.057E-02	yellow
Timp3	21859	1.904E-03	3.947E-02	yellow
Tmem167	66074	7.523E-04	2.083E-02	yellow
Tmem229b	268567	2.096E-04	8.968E-03	purple
Tmem67	329795	1.155E-04	6.114E-03	yellow
Tmem8	60455	8.552E-04	2.312E-02	blue
Tpcn1	252972	3.229E-04	1.227E-02	blue
Tra2b	20462	2.422E-03	4.552E-02	yellow
Trerf1	224829	1.483E-03	3.409E-02	purple
Triobp	110253	1.482E-03	3.403E-02	blue
Trove2	20822	1.740E-03	3.788E-02	yellow
Ttk	22137	9.224E-05	5.162E-03	purple
Tubgcp6	328580	1.411E-04	7.009E-03	blue
Ube2j1	56228	9.973E-04	2.499E-02	yellow
Ube3a	22215	1.244E-03	2.954E-02	orange
Ubn1	170644	1.102E-03	2.654E-02	blue
Usp20	74270	2.059E-03	4.101E-02	purple
Utrn	22288	2.157E-03	4.211E-02	orange
Vcam1	22329	1.360E-03	3.141E-02	orange
Vwf	22371	1.093E-03	2.653E-02	yellow
Wdfy4	545030	2.603E-04	1.065E-02	blue
Yipf6	77929	1.027E-05	9.813E-04	yellow
Zbtb20	56490	1.257E-03	2.970E-02	orange
Zc3h12d	237256	2.045E-03	4.078E-02	blue
Zcchc4	78796	9.434E-04	2.416E-02	yellow
Zeb1	21417	1.783E-03	3.808E-02	yellow
Zfp187	432731	2.101E-04	9.036E-03	yellow
Zfp192	93681	5.407E-05	3.348E-03	yellow
Zfp207	22680	1.306E-03	3.020E-02	yellow
Zfp280c	208968	2.246E-03	4.317E-02	yellow
Zfp516	329003	1.144E-03	2.729E-02	blue
Zfp526	210172	9.628E-04	2.449E-02	purple
Zfp64	22722	7.049E-07	6.244E-05	purple
Zfp710	209225	8.023E-04	2.187E-02	blue
Zfp955b	100043468	4.244E-04	1.446E-02	yellow

Table 2.2: Gene composition of lists used for density curve analysis

General cell migration						Molecular Signatures Database *			
ABI2	BCAR1	CLIC4	GDNF	ITGB2	NF2	PARP9	SAA1	SPHK1	TRIP6
ABI3	BMP10	CNTN4	GLI2	KAL1	NRD1	PF4	SCG2	SPON2	UBB
ACVRL1	CALCA	CX3CL1	GTPBP4	KRT2	NRP1	PLG	SEMA3B	SYK	UNC5C
AIMP1	CCDC88A	CXCR2	HMGCR	LAMB1	NRP2	PPAP2A	SEMA4F	TBX5	VCL
ALOX15B	CD24	DOCK2	IL10	LAMC1	NRTN	PPAP2B	SFTPD	TDGF1	VEGFC
AMOT	CD2AP	DPYSL5	IL12A	MDGA1	NRXN1	PRSS3	SHH	TGFB2	WNT1
ANG	CD34	EGFR	IL12B	MIA3	NRXN3	PTEN	SHROOM2	THBS4	
ANGPTL3	CDH13	ENPEP	IL8	MYH9	OPHN1	RTN4	SIAH1	THY1	
ARAP3	CDK5R1	FEZ1	ITGB1	NEXN	OTX2	S100A2	SLIT1	TNFSF12	
AZU1	CKLF	FEZ2	ITGB1BP1	NF1	PARD6B	S100P	SLIT2	TNN	
Leukocyte migration						Molecular Signatures Database **			
ACTB	CKLF	CLDN3	CXCL12	GNAI3	LOC646821	MYL5	PIK3CD	PXN	SFTPD
ACTG1	CLDN1	CLDN4	CXCL2	ICAM1	MAPK11	MYL7	PIK3CG	RAC1	SIPA1
ACTN1	CLDN10	CLDN5	CXCR1	IL10	MAPK12	MYL9	PIK3R1	RAC2	SYK
ACTN2	CLDN11	CLDN6	CXCR2	IL8	MAPK13	MYLPF	PIK3R2	RAP1A	TGFB2
ACTN3	CLDN14	CLDN7	CXCR2	ITGA4	MAPK14	NCF1	PIK3R3	RAP1B	THY1
ACTN4	CLDN15	CLDN8	CXCR4	ITGAL	MIA3	NCF2	PIK3R5	RAPGEF3	TXK
AIMP1	CLDN16	CLDN9	CYBA	ITGAM	MLLT4	NCF4	PLCG1	RAPGEF4	VASP
ARHGAP35	CLDN17	CTNNA1	CYBB	ITGB1	MMP2	NOX1	PLCG2	RASSF5	VAV1
ARHGAP5	CLDN18	CTNNA2	DOCK2	ITGB2	MMP9	NOX3	PRKCA	RHOA	VAV2
BCAR1	CLDN19	CTNNA3	ESAM	ITGB2	MSN	OCLN	PRKCB	RHOH	VAV3
CD34	CLDN2	CTNNB1	EZR	ITK	MYL10	PECAM1	PRKCG	ROCK1	VCAM1
CD99	CLDN20	CTNND1	F11R	JAM2	MYL12A	PF4	PTK2	ROCK2	VCL
CDC42	CLDN22	CX3CL1	GNAI1	JAM3	MYL12B	PIK3CA	PTK2B	SAA1	
CDH5	CLDN23	CXCL1	GNAI2	LOC100418883	MYL2	PIK3CB	PTPN11	SCG2	
Apoptosis pathways						Ingenuity® Pathway Analysis ***			
ACIN1	BCL2	CASP10	CASP9	DIABLO	GAS2	Jnk	MCL1	PLC	SPTAN1
AIMF1	BCL2A1	CASP12	CDK1	ENDOG	GRB2	Jnkk	MYC	RAF1	TNF
Akt	BCL2L1	CASP2	CDKN2A	ERK1	GTRA2	LMNA	NFkB	Ras	TP53
APAF1	BCL2L10	CASP3	Ciap	ERK2	IGF1	MAP2K1	NIK	ROCK1	
BAD	BCL2L11	CASP6	CYCS	FADD	IGF1R	MAP2K2	PARP1	RPS6ka1	
BAK1	BID	CASP7	DFFA	FAS	IkB	MAP3K5	PI3K	SHC1	
BAX	BIRC6	CASP8	DFFB	FASLG	IKK	MAPK8	PKC	Sos	

* - Compiled from the Molecular Signatures Database (Subramanian et al., 2005) “KEGG Leukocyte Transendothelial Migration” (http://www.broadinstitute.org/gsea/msigdb/cards/KEGG_LEUKOCYTE_TRANSENDOTHELIAL_MIGRATION.html) and “Gene Ontology Leukocyte Migration” (http://www.broadinstitute.org/gsea/msigdb/cards/LEUKOCYTE_MIGRATION.html) pathways.

** - From the Molecular Signatures Database (Subramanian et al., 2005) from the “Gene Ontology Cell Migration” (http://www.broadinstitute.org/gsea/msigdb/cards/CELL_MIGRATION.html) pathway

*** - Compiled using Ingenuity® Pathway Analysis program from the “Apoptosis Signaling” and “Myc Mediated Apoptosis” pathways (QIAGEN Redwood City)

REFERENCES

Adamovicz, J.J., and Worsham, P.L. (2006). Biodefense research methodology and animal models. Taylor & Francis 107–135.

Aepfelbacher, M., Trasak, C., and Ruckdeschel, K. (2007). Effector functions of pathogenic *Yersinia* species. Thrombosis and Haemostasis *98*, 521–529.

Agar, S.L., Sha, J., Foltz, S.M., Erova, T.E., Walberg, K.G., Baze, W.B., Suarez, G., Peterson, J.W., and Chopra, A.K. (2009). Characterization of the rat pneumonic plague model: infection kinetics following aerosolization of *Yersinia pestis* CO92. Microbes and Infection *11*, 205–214.

Anderson, D.M., Ciletti, N.A., Lee-Lewis, H., Elli, D., Segal, J., DeBord, K.L., Overheim, K.A., Tretiakova, M., Brubaker, R.R., and Schneewind, O. (2009). Pneumonic plague pathogenesis and immunity in Brown Norway rats. The American Journal of Pathology *174*, 910–921.

Balestrini, R., Gómez-Ariza, J., Lanfranco, L., and Bonfante, P. (2007). Laser microdissection reveals that transcripts for five plant and one fungal phosphate transporter genes are contemporaneously present in arbusculated cells. Molecular Plant-Microbe Interactions *20*, 1055–1062.

Berruti, A., Borriello, R., Lumini, E., Scariot, V., Bianciotto, V., and Balestrini, R. (2013). Application of laser microdissection to identify the mycorrhizal fungi that establish arbuscules inside root cells. Frontiers in Plant Science *4*, 135–135.

Bullard, J.H., Purdom, E., Hansen, K.D., and Dudoit, S. (2010). Evaluation of statistical methods for normalization and differential expression in mRNA-Seq experiments. BMC Bioinformatics *11*, 94.

Davis, K.M., Mohammadi, S., and Isberg, R.R. (2015). Community behavior and spatial regulation within a bacterial microcolony in deep tissue sites serves to protect against host attack. Cell Host Microbe *17*, 21–31.

Du, Z., Tan, Y., Yang, H., Qiu, J., Qin, L., Wang, T., Liu, H., Bi, Y., Song, Y., Guo, Z., et al. (2009). Gene expression profiling of *Yersinia pestis* with deletion of *lcrG*, a known negative regulator for Yop secretion of type III secretion system. International Journal of Medical Microbiology *299*, 355–366.

Emmert-Buck, M.R., Bonner, R.F., Smith, P.D., Chuaqui, R.F., Zhuang, Z., Goldstein, S.R., Weiss, R.A., and Liotta, L.A. (1996). Laser capture microdissection. Science *274*, 998–1001.

Espina, V., Heiby, M., Pierobon, M., and Liotta, L.A. (2007). Laser capture microdissection technology. Expert Review of Molecular Diagnostics *7*, 647–657.

Fellows, P., Lin, W., Detrisac, C., Hu, S.-C., Rajendran, N., Gingras, B., Holland, L., Price, J., Bolanowski, M., and House, R.V. (2012). Establishment of a Swiss Webster mouse model of pneumonic plague to meet essential data elements under the animal rule. Clinical and Vaccine Immunology *19*, 468–476.

Han, Y., Qiu, J., Guo, Z., Gao, H., Song, Y., Zhou, D., and Yang, R. (2007). Comparative transcriptomics in *Yersinia pestis*: a global view of environmental modulation of gene expression. BMC Microbiology *7*, 96–96.

Klink, V.P., Alkharouf, N., MacDonald, M., and Matthews, B. (2005). Laser capture microdissection (LCM) and expression analyses of *Glycine max* (soybean) syncytium containing root regions formed by the plant pathogen *Heterodera glycines* (soybean cyst nematode). Plant Molecular Biology *59*, 965–979.

Klink, V.P., and Matthews, B.F. (2008). The use of laser capture microdissection to study the infection of *Glycine max* (soybean) by *Heterodera glycines* (soybean cyst nematode). Plant Signaling & Behavior *3*, 105–107.

Klink, V.P., Overall, C.C., Alkharouf, N.W., MacDonald, M.H., and Matthews, B.F. (2007). Laser capture microdissection (LCM) and comparative microarray expression analysis of syncytial cells isolated from incompatible and compatible soybean (*Glycine max*) roots infected by the soybean cyst nematode (*Heterodera glycines*). Planta *226*, 1389–1409.

Koo, J.T., Alleyne, T.M., Schiano, C.A., Jafari, N., and Lathem, W.W. (2011). Global discovery of small RNAs in *Yersinia pseudotuberculosis* identifies *Yersinia*-specific small, noncoding RNAs required for virulence. Proceedings of the National Academy of Sciences *108*, E709–E717.

Koster, F., Perlin, D.S., Park, S., Brasel, T., Gigliotti, A., Barr, E., Myers, L., Layton, R.C., Sherwood, R., and Lyons, C.R. (2010). Milestones in progression of primary pneumonic plague in cynomolgus macaques. Infection and Immunity *8*, 2946–2955.

Lathem, W.W., Crosby, S.D., Miller, V.L., and Goldman, W.E. (2005). Progression of primary pneumonic plague: A mouse model of infection, pathology, and bacterial transcriptional activity. Proceedings of the National Academy of Sciences *102*, 17786–17791.

Laws, T.R., Davey, M.S., Titball, R.W., and Lukaszewski, R. (2010). Neutrophils are important in early control of lung infection by *Yersinia pestis*. Microbes and Infection *12*, 331–335.

Layton, R.C., Brasel, T., Gigliotti, A., Barr, E., Storch, S., Myers, L., Hobbs, C., and Koster, F. (2011). Primary pneumonic plague in the African Green monkey as a model for treatment efficacy evaluation. J Med Primatol *40*, 6–17.

Li, B., and Dewey, C.N. (2011). RSEM: accurate transcript quantification from RNA-Seq data with or without a reference genome. BMC Bioinformatics *12*, –323.

Li, H., Handsaker, B., Wysoker, A., Fennell, T., Ruan, J., Homer, N., Marth, G., Abecasis, G., Durbin, R., and Durbin, R. (2009). The sequence alignment/map format and SAMtools. Bioinformatics *25*, 2078–2079.

Liu, H., Wang, H., Qiu, J., Wang, X., Guo, Z., Qiu, Y., Zhou, D., Han, Y., Du, Z., Li, C., et al. (2009). Transcriptional profiling of a mice plague model: insights into interaction between *Yersinia pestis* and its host. Journal of Basic Microbiology *49*, 92–99.

Lukaszewski, R.A., Kenny, D.J., Taylor, R., Rees, D.G.C., Hartley, M.G., and Oyston, P.C.F. (2005). Pathogenesis of *Yersinia pestis* infection in BALB/c mice: effects on host macrophages and neutrophils. Infection and Immunity *73*, 7142–7150.

Marketon, M.M., DePaolo, R.W., DeBord, K.L., Jabri, B., and Schneewind, O. (2005). Plague bacteria target immune cells during infection. Science *309*, 1739–1741.

McCracken, J.M., and Allen, L.-A.H. (2014). Regulation of human neutrophil apoptosis and lifespan in health and disease. Journal of Cell Death *7*, 15–23.

Pechous, R.D., Broberg, C.A., Stasulli, N.M., Miller, V.L., and Goldman, W.E. (2015). *In vivo* transcriptional profiling of *Yersinia pestis* reveals a novel bacterial mediator of pulmonary inflammation. mBio *6*, e02302–e02314.

Pechous, R.D., Sivaraman, V., Price, P.A., Stasulli, N.M., and Goldman, W.E. (2013). Early host cell targets of *Yersinia pestis* during primary pneumonic plague. PLoS Pathogens *9*, e1003679.

Schiano, C.A., Koo, J.T., Schipma, M.J., Caulfield, A.J., Jafari, N., and Lathem, W.W. (2014). Genome-wide analysis of small RNAs expressed by *Yersinia pestis* identifies a regulator of the Yop-Ysc type III secretion system. Journal of Bacteriology *196*, 1659–1670.

Schulte, L.N., Eulalio, A., Mollenkopf, H.-J., Reinhardt, R., and Vogel, J. (2011). Analysis of the host microRNA response to *Salmonella* uncovers the control of major cytokines by the let-7 family. EMBO Journal *30*, 1977–1989.

Schütze, K., Niyaz, Y., Stich, M., and Buchstaller, A. (2007). Noncontact laser microdissection and catapulting for pure sample capture. In Sciencedirect.com, (Methods in Cell Biology), pp. 647–673.

Schwartz, J.T., Bandyopadhyay, S., Kobayashi, S.D., McCracken, J., Whitney, A.R., DeLeo, F.R., and Allen, L.-A.H. (2013). *Francisella tularensis* alters human neutrophil gene expression: insights into the molecular basis of delayed neutrophil apoptosis. Journal of Innate Immunity *5*, 124–136.

Sebbane, F., Lemaitre, N., Sturdevant, D.E., Rebeil, R., Virtaneva, K., Porcella, S.F., and Hinnebusch, B.J. (2006). Adaptive response of *Yersinia pestis* to extracellular effectors of innate immunity during bubonic plague. Proceedings of the National Academy of Sciences *103*, 11766–11771.

Shannon, J.G., Hasenkrug, A.M., Dorward, D.W., Nair, V., Carmody, A.B., and Hinnebusch, B.J. (2013). *Yersinia pestis* subverts the dermal neutrophil response in a mouse model of bubonic plague. mBio *4*, –.

Suarez-Quian, C.A., Goldstein, S.R., Pohida, T., Smith, P.D., Peterson, J.I., Wellner, E., Ghany, M., and Bonner, R.F. (1999). Laser capture microdissection of single cells from complex tissues. Biotechniques *26*, 328–335.

Subrahmanyam, Y.V.B.K., Yamaga, S., Prashar, Y., Lee, H.H., Hoe, N.P., Kluger, Y., Gerstein, M., Goguen, J.D., Newburger, P.E., and Weissman, S.M. RNA expression patterns change dramatically in human neutrophils exposed to bacteria. Bloodjournal.Hematologylibrary.org.

Subramanian, A., Tamayo, P., Mootha, V.K., Mukherjee, S., Ebert, B.L., Gillette, M.A., Paulovich, A., Pomeroy, S.L., Golub, T.R., Lander, E.S., et al. (2005). Gene set enrichment analysis: a knowledge-based approach for interpreting genome-wide expression profiles. Proceedings of the National Academy of Sciences of the USA *102*, 15545–15550.

Vagima, Y., Levy, Y., Gur, D., Tidhar, A., Aftalion, M., Abramovich, H., Zahavy, E., Zauberman, A., Flashner, Y., Shafferman, A., et al. (2012). Early sensing of *Yersinia pestis* airway infection by bone marrow cells. Frontiers in Cellular and Infection Microbiology *2*.

Van Andel, R., Sherwood, R., Gennings, C., Lyons, C.R., Hutt, J., Gigliotti, A., and Barr, E. (2008). Clinical and pathologic features of cynomolgus macaques (*Macaca fascicularis*) infected with aerosolized *Yersinia pestis*. Comparative Medicine (Memphis) *58*, 68–75.

Wang, K., Singh, D., Zeng, Z., Coleman, S.J., Huang, Y., Savich, G.L., He, X., Mieczkowski, P., Grimm, S.A., Perou, C.M., et al. (2010). MapSplice: Accurate mapping of RNA-seq reads for splice junction discovery. Nucleic Acids Research *38*, 178.

Yan, Y., Su, S., Meng, X., Ji, X., Qu, Y., Liu, Z., Wang, X., Cui, Y., Deng, Z., Zhou, D., et al. (2013). Determination of sRNA expressions by RNA-seq in *Yersinia pestis* grown *in Vitro* and during infection. PLoS One *8*.

Zhou, D., Han, Y., Qiu, J., Qin, L., Guo, Z., Wang, X., Song, Y., Tan, Y., Du, Z., and Yang, R. (2006). Genome-wide transcriptional response of *Yersinia pestis* to stressful conditions simulating phagolysosomal environments. Microbes and Infection *8*, 2669–2678.

CHAPTER 3: INDUCTION OF NETUROPHIL SURVIVAL BY *Yersinia pestis* THROUGH THE TYPE III SECRETION SYSTEM EFFECTOR YopM[†]

3.1 Overview

This Chapter describes the ability of *Yersinia pestis* to prolong the survival of neutrophils, which may lead to more severe pneumonia due to the prolonged accumulation of neutrophils in the lower respiratory tract. Global transcriptional analysis in defined lesion microenvironments from Chapter 2 is used as a foundation for *in vitro* and *in vivo* characterization of neutrophils during a *Y. pestis* infection. These studies provide evidence that *Y. pestis* promotes neutrophil survival and inhibits apoptosis in a novel type III secretion system (T3SS) effector-dependent manner. By determining how *Y. pestis* alters neutrophil lifespan and induces unique transcriptional responses within sites of infection, we will better understand the mechanisms by which neutrophils typically work in a broad range of diseases in which neutrophil infiltration becomes harmful to the host.

[†] This data has been published in: Stasulli NM, Eichelberger KR, Price PA, Pechous RD, Montgomery SA, Parker JS, Goldman WE. 2015. Spatially distinct neutrophil responses within the inflammatory lesions of pneumonic plague. mBio 6(5):e01530-15. doi:10.1128/mBio.01530-15.

3.2 Introduction

While there are many genetic mutations and insertions that differentiate the three pathogenic species of *Yersinia* (*enterocolitica*, *pseudotuberculosis*, and *pestis*) there are several shared virulence plasmids and genomic islands that are vital for virulence (Perry and Fetherston, 1997; Wren, 2003). Three of these virulence determinants important during pneumonic plague are the pCD1 plasmid (Ben-Gurion and Shafferman, 1981), the genomic pigmentation locus (pgm) (Jackson and Burrows, 1956), and the *pla* gene encoded on the pPCP1 plasmid (Sodeinde et al., 1988).

The pCD1 plasmid (known as pYV in *Y. pseudotuberculosis* and *Y. enterocolitica*) is a common ancestral virulence factor for all three pathogenic *Yersinia* species (Wren, 2003). The acquisition of the pCD1 plasmid gave non-pathogenic environmental *yersiniae* the ability to transcribe genes for the functional needle complex of a T3SS, along with effector proteins that are injected by this apparatus (Cornelis et al., 1998). Despite the lack of an identified receptor for the *Y. pestis* T3SS, it appears to have an affinity for injecting innate immune cells during infection (Marketon et al., 2005; Pechous et al., 2013). Early during pneumonic plague, macrophages are the most frequently injected cell type. However, as neutrophils being to infiltrate the alveolar spaces they are preferentially injected by the *Y. pestis* T3SS (Pechous et al., 2013). While each Yop effector has unique functions and may act in different compartments of the cell, the global cell effects overlap to ultimately suppress innate immune anti-microbial functions. The effector YopE is a GTPase activating protein that leads to the inactivation of Rho and Rac

GTP binding proteins (Aepfelbacher et al., 2007). This results in the blocking of phagocytosis and inhibition of reactive oxygen species (ROS) production of several cell types including neutrophils (Ruckdeschel et al., 1996). The effector YopH is a tyrosine phosphatase that primarily dephosphorylates focal adhesion proteins. This effector, similar to YopE, results in decreased phagocytosis in various cell types and an inhibition of ROS generation in neutrophils (Aepfelbacher et al., 2007; Ruckdeschel et al., 1996). The effector YopJ/P is a serine/threonine acetyltransferase that has been shown to act on MAPK kinases and IκB kinase-β. This transferase activity has been shown to be important for dampening the immune response and promoting apoptosis of macrophages (Trosky et al., 2008). Interestingly, however, neutrophils are resistant to YopJ/P-induced apoptosis (Spinner et al., 2010). The effector YopM has no known enzymatic function. Rather, it has been shown to have protein-protein binding functions. While the global cellular effects of its scaffolding are not clear, it has been shown to be important for full virulence during bubonic plague (Trosky et al., 2008). The effector YopO (YpkA) has been shown to have multiple functions. YopO is a serine/threonine kinase that can auto-phosphorylate upon binding actin, disrupt the actin cytoskeleton, and has guanidine nucleotide dissociation inhibitor activity. While its function during plague pathogenesis is not fully understood, it has been shown to promote apoptosis in macrophages (Park et al., 2007), hinder phagocytosis, and it has been suggested that it may be the cause of the abnormal bleeding experienced during plague (Navarro et al., 2007; Trosky et al., 2008). The effector YopT is a cysteine protease

that targets Rho GTPases attached to an isoprenoid moiety. It has been shown to mildly inhibit phagocytosis and interfere with actin assembly in various cells including neutrophils (Aepfelbacher et al., 2007).

After acquiring the pCD1 virulence plasmid, two distinct species of *Yersinia* evolved, *Y. enterocolitica* and *Y. pseudotuberculosis*. One virulence factor that distinguishes these two species is the *pgm* locus that was acquired by *Y. pseudotuberculosis* (Wren, 2003). This locus contains two distinct gene islands: The first contains the genes necessary for the production and utilization of yersiniabactin, a small siderophore that sequesters host iron. The second island contains a somewhat random assortment of genes necessary for biofilm formation and flea transmission of *Y. pestis* to a mammalian host (Bearden et al., 1997; Buchrieser et al.; Hinnebusch et al., 1996). While regions of the *pgm* locus are necessary for full virulence in both bubonic and pneumonic plague (Fetherston et al., 2010; Hinnebusch et al., 1996), it is possible to complement a deletion of the *pgm* locus and restore pathogenesis during bubonic plague in an infected individual with elevated levels of iron (Quenee et al., 2012).

The final of these three virulence factors to be acquired was the *pla* gene via acquisition of the pPCP1 plasmid. The presence of *pla* is one of the factors that uniquely distinguishes *Y. pestis* from *Y. pseudotuberculosis* (Sodeinde et al., 1988; Wren, 2003). Pla is necessary for the development of both bubonic and pneumonic plague (Lathem et al., 2007; Perry and Fetherston, 1997). The *pla* gene encodes a protease that cleaves plasminogen into active plasmin that can degrade fibrin clots

(Perry and Fetherston, 1997). Pla is described as a promiscuous protease and can cleave many components of the plasminogen pathway, complement proteins, outer membrane proteins, and Fas ligand. There are also indications that it can act as an adhesin in addition to its proteolytic functions (Caulfield and Lathem, 2012; Caulfield et al., 2014; Perry and Fetherston, 1997; Sodeinde et al., 1988).

Deletion of any of these factors from the *Y. pestis* genome attenuates lung lesion development and ultimately virulence of *Y. pestis*. Both the *pgm*$^-$ and pCD1$^-$ strains of *Y. pestis* are attenuated to such a degree that they can be studied under BSL 2 conditions instead of the BSL 3 conditions required for fully virulent *Y. pestis*. While there have been many studies on these virulence factors, there is still more information to be assembled using disease-relevant cell types and *in vivo* infection models.

3.3 Methods

All reagents were obtained form Sigma-Aldrich™ unless otherwise noted.

3.3.1 Ethics statement

The use of live vertebrate animals was performed in accordance with the Public Health Service (PHS) policy on Humane Care and Use of Laboratory Animals, the Amended Animal Welfare Act of 1985, and the regulations of the United States Department of Agriculture (USDA). All animal studies were approved by the University of North Carolina at Chapel Hill Office of Animal Care and Use, protocols #12-028.0 and #15-022.0.

3.3.2 Bacterial strains and culture conditions

The fully virulent *Yersinia pestis* strain CO92 and the plasmid-cured strain (pCD1$^-$) were obtained from the U.S. Army, Ft. Detrick, MD. The presence or absence of pCD1 and the *pgm* locus was confirmed by PCR for each strain before use. The construction of *Y. pestis* strains Δ*pla* and Δ*yopH* has previously been described (Lathem et al., 2007; Price et al., 2012). Yop deletion strains (Δ*yopE, J, M, O, T*) were constructed using a lambda *red* recombination system as described previously (Price et al., 2012). The *yopM* gene was complemented back into its native site on the pCD1 plasmid using the pSR47S recombination method as previously described (Cathelyn et al., 2006; Walker and Miller, 2004).

Strains were grown on brain-heart infusion (BHI) agar (Difco Laboratories) at 26°C for two days. For infections, liquid cultures of *Y. pestis* CO92 were grown in BHI broth for 6–12 h at 26°C. The cultures were then diluted to an OD_{620} of 0.05–0.1 in BHI supplemented with 2.5 mM $CaCl_2$ and grown 12–16h at 37°C with constant shaking.

3.3.3 Animals and infections

Six- to eight-week old female C57BL/6J mice were obtained from Jackson Laboratories. Mice were provided with food and water ad libitum and maintained at 25°C and 15% humidity with alternating 12 h periods of light and dark. For animal infections, groups of three to ten mice were lightly anesthetized with

ketamine/xylazine and inoculated intranasally with a lethal dose of 10^4 colony-forming units (CFUs) suspended in 20µL PBS. Actual CFUs inoculated was determined by plating serial dilutions of the inoculum on BHI. Moribund animals were euthanized with an overdose of sodium pentobarbital. For determination of bacterial burden, lungs were removed at the indicated times and homogenized in PBS using a Dremel® Tissue Homogenizer. Serial dilutions of each organ homogenate were plated on BHI agar and reported as CFU/lung.

3.3.4 Isolation of primary human neutrophils and *in vitro* assays

Human blood samples were obtained anonymously from consenting donors through the UNC Center for AIDS Research Virology Core Laboratory by common venipuncture according to IRB protocols #96-0859 and #08-0328. Blood was mixed with equal parts of a 3% dextran in 0.9% saline solution at room temperature for erythrocyte sedimentation. The top serum layer was removed and centrifuged at 250 x g at 4°C for 10 min and the supernatant was removed. The pellet was resuspended in 0.9% saline and underlaid with Ficoll-Paque™ PLUS (GE Healthcare®). The gradient was centrifuged at 400 x g at 26°C for 40 min and both gradient layers were removed. To remove the remaining erythrocytes the pellet was resuspended in 0.2% saline for 1 min. An equal volume of 1.6% saline was added and the suspension was centrifuged at 250 x g at 4°C for 6 min. This erythrocyte wash was repeated and the final pellet was resuspended in cold PBS. Neutrophils were enumerated using a hemocytometer.

For *in vitro* assays 12-well cell culture plates (Costar®) were pre-incubated with fetal bovine serum for 1 h at 37°C. FBS was removed and the wells were washed three times with PBS. Wells were plated with ~10^6 freshly isolated neutrophils suspended in modified RPMI media (RPMI 1640 without phenol red and HEPES and with L-glutamine (Gibco™) was buffered to pH 7.2 with 0.25 mM HEPES) and each well was supplemented with 5% FBS (HyClone™), 2.0 mM L-glutamine (CellGro™), and 2.5 mM $CaCl_2$. The cells were then inoculated with various strains of *Y. pestis* or treated with chemical inhibitors for 24 h at 37°C with 5% CO_2. The chemical inhibitors BI-D1870 (Cayman Chemical Co.™) and Z-YVAD-FKM (BioVision™) were used at various concentrations to inhibit the kinase activity of RSK isoforms and inhibit the active site of caspase-1, respectively.

3.3.5 Harvesting and staining of neutrophils for flow cytometry

Neutrophils were resuspended in wells by repetitive pipetting, collected into Eppendorf tubes, and spun 2 min at 1000 x g. Cells were washed in 2% FBS in PBS (flow buffer) and pelleted by spinning 2 min at 1000 x g. Cells were resuspended in antibody staining solution (flow buffer plus desired conjugated antibodies at a 1:200 concentration: CD11b-phyoerythrin (Clone M1/70.15; Invitrogen), Ly6G-phycoerythrin-Cy7 (Clone 1A8; BD Bioscience) on ice for 30 min. Cells were then stained for the apoptotic marker phosphatidylserine using Annexin V-FITC and for cell death using Propidium Iodide (Annexin V Apoptosis Detection kit FITC, Affymetrix™) as per the manufacturers instructions. A Guava easyCyte™ 5HT flow

cytometer (EMD Millipore™) was used to detect cell staining in a 96-well plate format. Flow cytometry results were analyzed using InCyte Software (EMD Millipore™), analyzed in Microsoft Excel™ and graphs were generated using GraphPad Prism™.

3.3.6 Histopathology and TUNEL staining

Groups of three mice were inoculated intranasally as described above, and lungs were inflated with 10% neutral buffered formalin via tracheal cannulation, then removed and incubated in 10% formalin for a minimum of 24 h. Lungs were immersed in 70% EtOH, and embedded in paraffin. Five-µm lung sections were adhered to glass slides, stained with hematoxylin/eosin for examination, and a coverslip was added.

A TUNEL Apo-Green Detection kit (Biotool™) was used to detect damaged DNA indicative of apoptosis. Stained slides were mounted with SlowFade® Gold with DAPI (Invitrogen™) and coverslips were added prior to imaging with an Olympus BX60 fluorescence microscope and iVision software v. 4.0.0 (BioVision Technologies). All images were imported into Adobe Photoshop® to merge color channels. Input levels were then uniformly adjusted for images from the same staining experiment for publication purposes.

3.4 Results

Based on pathway analysis of the LCM/RNAseq data in Chapter 2 I wanted to verify that *Y. pestis* alters neutrophil death pathways leading to increased survival,

which may contribute to continued lesion expansion.

3.4.1 *Yersinia pestis* effects on human neutrophil survival *in vitro*.

I compared the survival of uninoculated primary human neutrophils to both *Y. pestis*- and non-pathogenic *Escherichia coli*-inoculated neutrophils *in vitro*. At 24 hours post infection (hpi) neutrophils were harvested for analysis of apoptotic and dying cells by flow cytometry. An aliquot of cells was also fixed at 0 hpi to retain the initial starting concentration of neutrophils in each assay. After 24 hpi, the population of remaining "healthy" ($AnnexinV^-$, PI^-) neutrophils ranged from 40-60% of the initial seeding population depending on the donor. Inoculation with non-pathogenic *E. coli* resulted in survival of only 20-30% of the initial population. In contrast, inoculation with *Y. pestis* resulted in 60-80% survival of the initial population (Figure 3.1A), a significant increase in surviving healthy neutrophils compared to uninoculated or *E. coli*-inoculated neutrophils.

3.4.2 Role of the type III secretion system in increased survival of human neutrophils

After determining that *Y. pestis* significantly increased the survival of neutrophils, I tested if this could be attributed to a known virulence determinant of *Y. pestis*. I inoculated human neutrophils *in vitro* with *Y. pestis* strains lacking the pigmentation locus (pgm^-), the plasminogen activator protease (*Δpla*), and the plasmid encoding the T3SS ($pCD1^-$). I observed that neutrophils inoculated with a

pgm$^-$ or *Δpla* mutant showed similar survival to those inoculated with wild type *Y. pestis*, while infection with a pCD1$^-$ mutant significantly decreased neutrophil survival (data not shown and Figure 3.1B), indicating that the phenotype is dependent on the T3SS. I next tested mutants of the six primary T3SS effectors (*ΔyopE, ΔyopH, ΔyopJ, ΔyopM, ΔyopO, ΔyopT*) in the neutrophil assay and observed that only infection with the *ΔyopM* mutant showed a significant decrease in neutrophil survival compared to inoculation with wild type *Y. pestis* (Figure 3.1C). I also observed that a *ΔyopM:yopM* complemented strain reproduced the phenotype of the wild type strain (Figure 3.1D), and validated my conclusion that YopM is important in modulating neutrophil survival.

3.4.3 A novel function for YopM in neutrophil survival

YopM is known to have two intracellular functions: (*i*) binding ribosomal S6 kinase (RSK) and protein kinase N1 (PKN) (McDonald et al., 2003), which induces prolonged activation of RSK (Hentschke et al., 2010); and (*ii*) inhibiting caspase-1 activity and inflammasome formation that leads to pyroptotic cell death (Chung et al., 2014; LaRock and Cookson, 2012). To determine which function of YopM might be responsible for enhancing neutrophil survival, I performed a neutrophil infection assay in the presence of inhibitors of these two functions. To test the effect of continued YopM-induced RSK activity on neutrophil survival, I used the RSK inhibitor BI-D1870. Addition of increasing doses of BI-D1870 to neutrophils inoculated with wild type *Y. pestis* showed no decrease in neutrophil survival (Figure 3.2A),

indicating that the prolonged kinase activity of RSK induced by YopM had no effect on neutrophil survival. I validated the functionality BI-D1870 by monitoring the phosphorylation of the S6 protein (Roux et al., 2007) at the highest tested dose of this RSK inhibitor. Even after 24 hours, neutrophils treated with BI-D1870 showed decreased phosphorylation of S6 (Figure 3.3). I next tested the effect of inhibiting caspase-1 during inoculation with a *ΔyopM* mutant, using the caspase-1 inhibitor Z-YVAD-FMK. In the presence of this inhibitor, neutrophil survival was not enhanced after inoculation with the *ΔyopM* mutant compared to uninoculated neutrophils. I did observe an overall increase in neutrophil survival in samples treated with Z-YVAD-FMK, though this was significantly lower than the survival seen during infection with wild type *Y. pestis*. This indicates that there is a certain amount of caspase-1-dependent neutrophil death, but this is not the mechanism through which YopM is acting (Figure 3.2B). These findings suggest a novel function of YopM specifically related to neutrophil survival that does not involve its known functions of RSK and PKN binding or caspase-1 inhibition.

3.4.4 Role of YopM in the inhibition of apoptosis in lung lesions

Since YopM is important for prolonging neutrophil survival *in vitro*, I tested if YopM is involved in sustaining neutrophil health within inflammatory lung lesions *in vivo*. Lungs of mice infected with wild type or *ΔyopM Y. pestis* were collected at 48 hpi and sectioned for hematoxylin & eosin staining. Neither the size nor number of inflammatory lesions was significantly altered in the *ΔyopM*-infected lungs compared

to wild type infection. The bacterial burden in the lungs was similar between the two infections, but there was a significant decrease in the bacterial burden in spleens of *ΔyopM*-infected mice (Figure 3.3A). This decreased spleen burden indicates a decreased ability of *Y. pestis* to disseminate from the lungs. While the overall pattern of pulmonary inflammation was similar between the two infections (Figure 3.3B,C), the centers of the largest inflammatory foci in the *ΔyopM* mutant displayed more prominent necrosis of the alveolar septa. I also observed a striking difference in lung lesion cellular appearance between wild type and *ΔyopM* mutant-infected mice (Figure 3.3D, E). In the *ΔyopM* mutant-infected tissues, increased numbers of neutrophils were degranulated and had faded nuclei. Additionally, amidst viable inflammatory cells there were individual amphophilic cell bodies (3-5 *μ*m in diameter, round to slightly misshapen) that lacked a discernible nucleus and often displayed faint stippling (Figure 3.3E blue arrows). Correspondingly, I observed increased DNA damage via fluorescent TUNEL staining in lung lesions of *ΔyopM* mutant-infected mice compared to wild type *Y. pestis*-infected mice (Figure 3.4). This TUNEL staining is indicative of apoptotic cell death and correlates with the presence of the amphophilic cell bodies. These *in vivo* observations confirm the importance of YopM-induced neutrophil survival *in vitro.* Furthermore, these results are consistent with the RNAseq analysis suggesting that the cells in the center of lesions have a decreased capacity to undergo apoptosis during wild type *Y. pestis* infection, leading to the distinctive lung lesions seen in pneumonic plague.

3.5 Discussion

In this chapter I sought to confirm that apoptosis is inhibited during *Y. pestis* infection *in vitro* and *in vivo*, and also identify the bacterial factor(s) that are responsible for this phenotype. I therefore inoculated primary human neutrophils with fully virulent *Y. pestis*, as well as a repertoire of mutant strains lacking key virulence-related genes for a more detailed analysis. Prior to inoculation, *Y. pestis* was grown at 37°C and was not pre-opsonized to most closely mimic conditions during pneumonic plague disease (Lathem et al., 2005). It has previously been observed that the pCD1 virulence plasmid of *Y. pestis* is necessary to inhibit neutrophil production of reactive oxygen species and decrease neutrophil apoptosis (Spinner et al., 2010). Though I initially began evaluating apoptosis and death of neutrophils I found that, despite an obvious loss of viable neutrophils, AnnexinV staining was not consistently different by 24 hpi. While neutrophils express phosphatidylserine as a marker of apoptosis, they continue to progress through apoptosis and are no longer detectable by flow cytometry at later time points. Thus, examining a singular time point only visualizes cells that are currently apoptotic and fails to capture those that have already gone through apoptosis. I therefore changed my readout to detect surviving "healthy neutrophils" by subtracting the apoptotic neutrophils ($AnnexinV^+$), dead neutrophils (PI^+), and neutrophils that became undetectable by flow cytometry due to turnover (subtracting neutrophils at 24 hpi from total starting neutrophils) from the starting number of neutrophils. I have shown with this assay that *Y. pestis* leads to increased survival of primary human neutrophils, and that the T3SS effector YopM is necessary for this phenotype. This is the first direct evidence that a single *Y.*

pestis gene is able to extend the survival of neutrophils.

After testing for the known YopM functions of RSK activation and caspase-1 inhibition, I was unable to confirm that either of these functions had any effect on neutrophil survival *in vitro*. I hypothesize that, similar to YopJ/P (Spinner et al., 2010), YopM has a function in neutrophils that differs from what is observed in macrophages. YopM was initially shown to bind α-thrombin (Leung et al., 1990) and subsequently α_1-antitrypsin (Heusipp et al., 2006), though neither of these binding functions contribute to *Y. pestis* virulence (Leung et al., 1990). YopM was later shown to bind p90 ribosomal S6 kinase (RSK) and protein kinase N1 (PKN) isoforms (McDonald et al., 2003). The C-terminal end of YopM binds phosphorylated RSK (McCoy et al., 2010), inhibiting dephosphorylation and prolonging its kinase activity (Hentschke et al., 2010). YopM binding to RSK and PKN also facilitates activated RSK to phosphorylate PKN and activate its kinase activity (McDonald et al., 2003). The RSK and PKN binding domains of YopM are required for IL-10 production during a *Y. pseudotuberculosis* intravenous infection (McPhee et al., 2010) and the deletion of these domains result in attenuation of virulence (McPhee et al., 2012). More recently it has been shown that YopM can also bind both active caspase-1 (LaRock and Cookson, 2012) and IQGAP1 (Chung et al., 2014), depending on the isoform of YopM being tested. Both of these binding activities lead to an inhibition of inflammasome assembly and impede pyroptosis in macrophages. Other studies have shown the effects of YopM on bubonic plague and systemic infection through cytokine analysis and organ-specific cell composition of lesions (Kerschen et al.,

2004; Ye et al., 2014; 2009; 2011), but this is the first study to suggest a function of YopM during pneumonic plague as well as its ability to promote neutrophil survival.

The influence of YopM on apoptosis of neutrophils has been previously studied in systemic infection by a *pgm*$^-$ strain of *Y. pestis,* and appears to be organ-specific (Ye et al., 2014). My work focuses on neutrophils and pathology in the lung during infection with a fully virulent *Y. pestis* strain. I demonstrate the importance of YopM for neutrophil survival *in vitro* as well as for neutrophil integrity and reduction of apoptosis *in vivo*, as demonstrated by lesion histopathology and TUNEL staining. Linking the *in vitro* phenotype of increased neutrophil survival to apoptosis *in vivo* further validates the LCM-RNAseq conclusion that the apoptosis pathway is inhibited in the center of lung lesions compared to the periphery. The decrease in disseminated bacteria is intriguing, as it implies that YopM prevents *Y. pestis* killing by neutrophils. The function of neutrophils is typically to attack invading bacteria, degranulate, and undergo apoptosis, necrosis, or the formation of neutrophil extracellular traps (NETs). Along with observing cells that lacked a discernable nucleus, we detected increased, diffuse TUNEL staining after infection with the Δ*yopM* mutant strain. This physiology and diffuse damaged DNA staining could suggest the formation of neutrophil extracellular traps (NETs) within the lung lesions. Further investigating the formation of NETs after infection with a Δ*yopM* mutant strain of *Y. pestis* could elucidate the specific function that YopM is having on neutrophils. However, the continuing hypothesis for the line of questioning leading into Chapter 4 is that the increase in neutrophil survival may result from the failure to

degranulate, suggesting that YopM is inhibiting degranulation of neutrophils and buildup of granule contents is aiding in lung lesion formation.

In summary, I introduced a unique application of LCM technology to examine directly the spatially distinct microenvironments resulting from host-pathogen interactions during primary pneumonic plague. As a result, I was able to show that *Y. pestis* modulates neutrophil survival *in vivo* in a YopM-dependent manner. Further defining and characterizing mediators of the dramatic pulmonary inflammation that occurs during pneumonic plague will help in understanding the lethality of this disease and may contribute to our understanding of severe pulmonary infection with other respiratory pathogens.

3.6 Figures

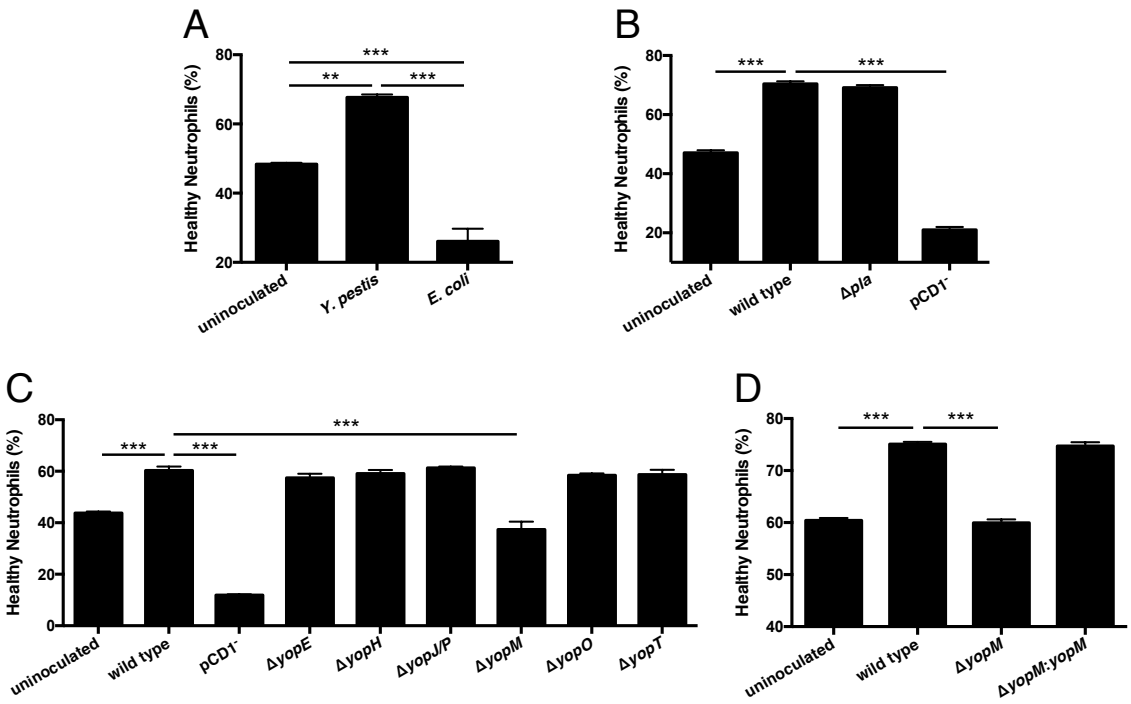

Figure 3.1: The type III secretion system effector YopM is necessary for enhanced neutrophil survival

Primary human neutrophils were incubated in buffered RPMI at 37°C and 5% CO_2, with or without bacterial inoculation. After 24 hours, remaining "healthy neutrophils" were assayed by flow cytometry ($CD16^+$, $CD66b^+$, $AnnexinV^-$, 7-AAD/PI^-). (**A**) After incubation with wild type *Y. pestis,* there were significantly more healthy neutrophils compared to both uninoculated cells and non-pathogenic *E. coli*-inoculated cells. (**B**) After incubation with a Δ*pla* mutant, there was no difference in healthy neutrophils compared to inoculation with wild type *Y. pestis*. However, inoculation with a $pCD1^-$ (T3SS negative) mutant caused a significant decrease in healthy neutrophils. (**C**) Comparing inoculations with six individual T3SS effector mutants, only the Δ*yopM* mutant significantly decreased the percentage of healthy neutrophils compared to

inoculation with wild type *Y. pestis*. (**D**) Complementation of the Δ*yopM* strain restored neutrophil survival to the level seen with wild type *Y. pestis*. Results are from representative experiments performed in triplicate. Data are represented as mean ± SEM; asterisks represent statistical significance based on Tukey's multiple comparison tests from an ordinary one-way ANOVA, $^{**}p < 0.01$, $^{***}p < 0.001$.

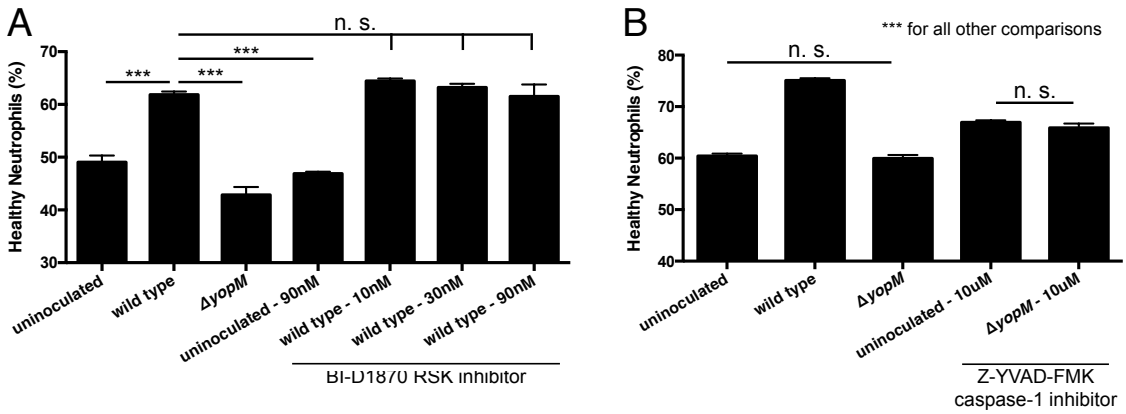

Figure 3.2: Inhibiting known functions of YopM does not alter neutrophil survival

Primary human neutrophils were incubated with or without bacterial inoculation and drug treatment. After 24 hours, remaining "healthy neutrophils" were assayed by flow cytometry ($CD16^+$, $CD66b^+$, $AnnexinV^-$, $7\text{-}AAD/PI^-$). (**A**) Treatment with the RSK inhibitor BI-D1870 had no effect on the percentage of healthy neutrophils in culture for either uninoculated or wild type *Y. pestis*-inoculated samples. (**B**) Treatment with the caspase-1 inhibitor Z-YVAD-FMK showed a significant increase in the percentage of healthy neutrophils compared to untreated samples. However, there was also still a significant difference in the percentage of healthy neutrophils remaining in uninoculated and Δ*yopM* mutant-inoculated samples compared to wild type *Y. pestis*-inoculated samples. Results are from representative experiments performed in triplicate. Data are represented as mean ± SEM; asterisks represent statistical significance based on Tukey's multiple comparison tests from an ordinary one-way ANOVA, ***$p < 0.001$.

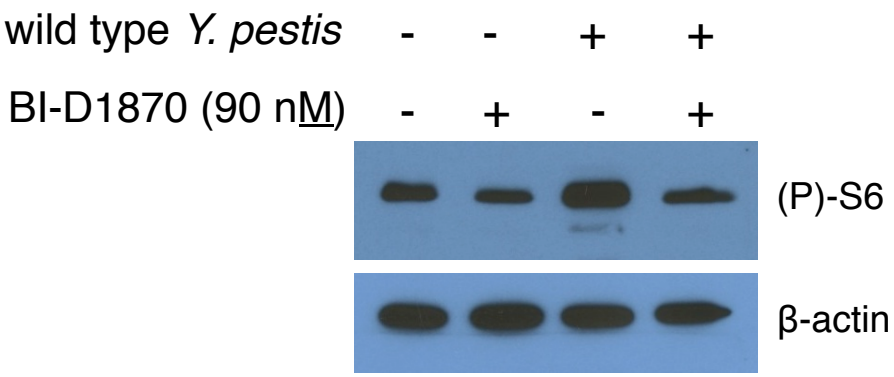

Figure 3.3: BI-D1870 continues to inhibit RSK activity after 24 hours in isolated human neutrophils

Primary human neutrophils were incubated with or without bacterial inoculation and RSK inhibitor (BI-D1870). After 24 hours, neutrophils were harvested and lysed for Western blot analysis. Treatment with the BI-D1870 caused a decrease in the phosphorylation of S6 in both uninoculated and wild type *Y. pestis*-inoculated samples, even after 24 hours.

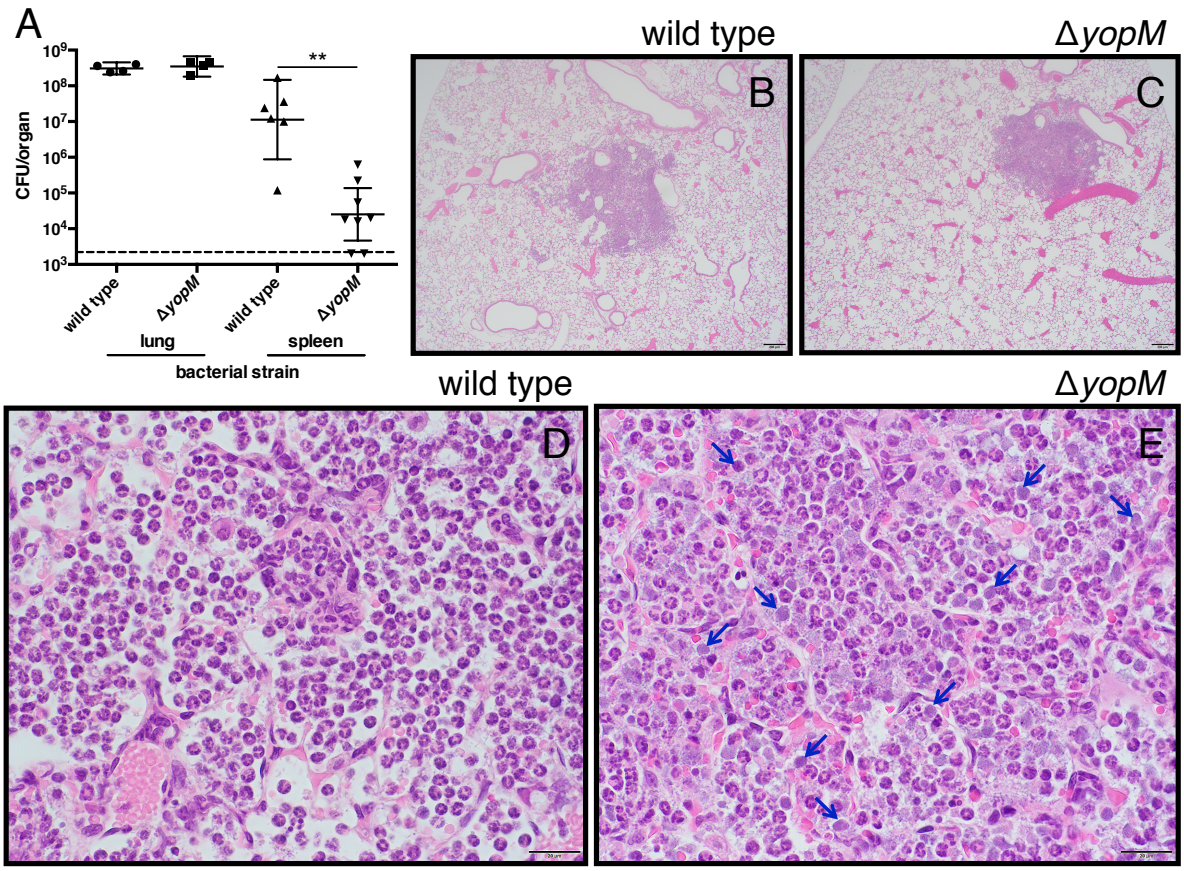

Figure 3.4: YopM-dependent effects on bacterial burden and histopathology during pulmonary infection with *Y. pestis*

(**A**) At 48 hpi, there is no difference in lung bacterial burden but there is a significant difference in spleen bacterial burden between mice infected with wild type and Δ*yopM* mutant *Y. pestis*. (**B, C**) At low magnification there is no distinct difference in size or number of lung lesions in mice infected with wild type or Δ*yopM* mutant *Y. pestis*. (**D, E**) At higher magnification, however, large numbers of necrotic cells can be seen throughout the lung lesions in mice infected with the Δ*yopM* mutant (representative cells marked with blue arrows) that are not present during an infection with wild type *Y. pestis*. Scale bar in images represents (**B, C**) 200 µm or (**D, E**) 20 µm. Data are compiled from two separate experiments and represented as

geometric mean ± 95% CI; asterisks represent statistical significance based on Mann-Whitney tests, **$p < 0.005$.

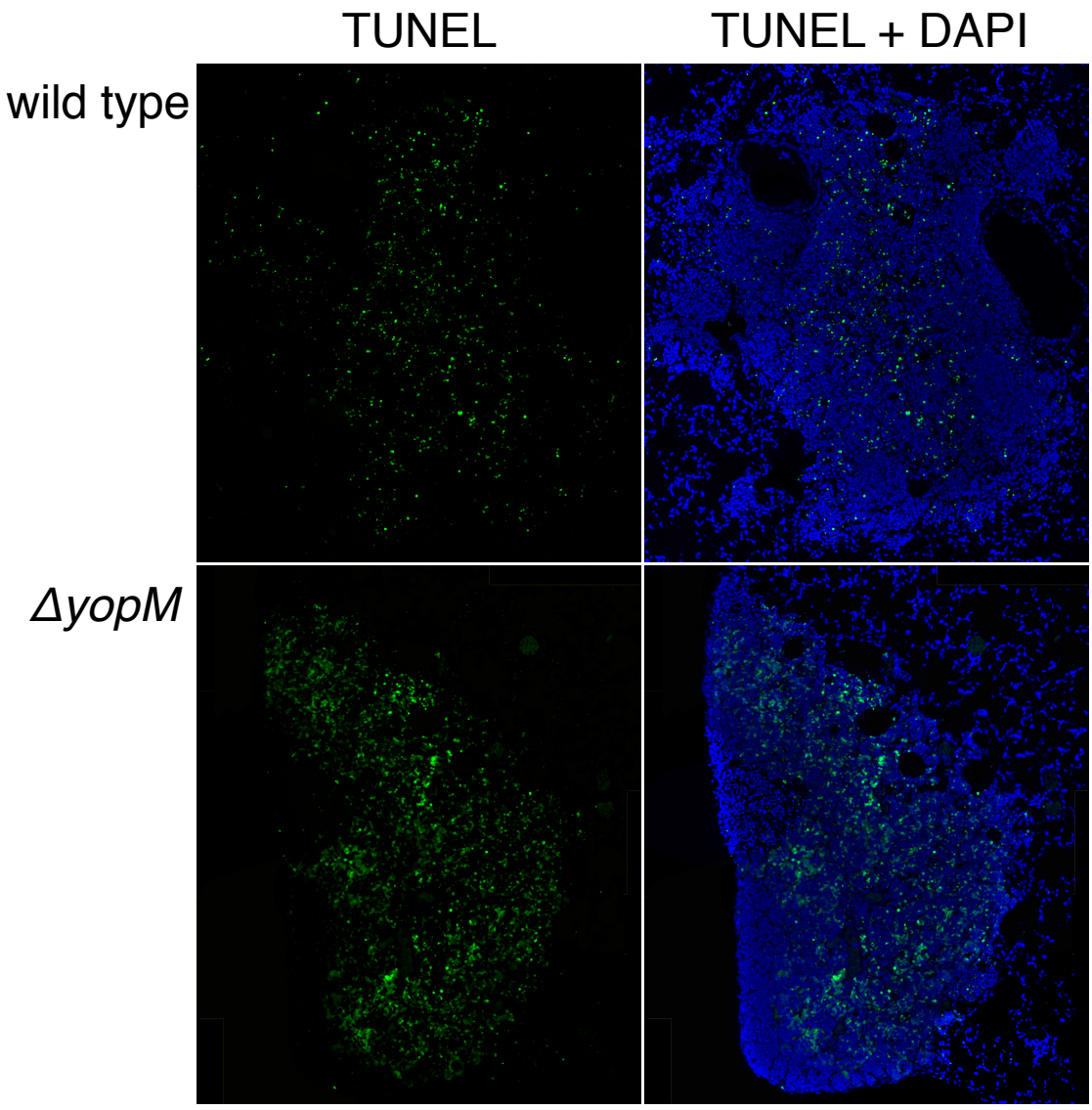

Figure 3.5: TUNEL staining of infected mouse lung sections

Representative composite images of lung lesions (48 hpi) stained for damaged DNA using TUNEL (green) and total DNA using DAPI (blue). TUNEL staining, generally indicative of apoptosis, was primarily restricted to lung lesions during *Y. pestis* infection. More apoptosis was evident in the lung lesions of mice infected with the Δ*yopM* mutant compared to those infected with wild type *Y. pestis*.

REFERENCES

Aepfelbacher, M., Trasak, C., and Ruckdeschel, K. (2007). Effector functions of pathogenic *Yersinia* species. Thrombosis and Haemostasis *98*, 521–529.

Bearden, S.W., Fetherston, J.D., and Perry, R.D. (1997). Genetic organization of the yersiniabactin biosynthetic region and construction of avirulent mutants in *Yersinia pestis*. Infection and Immunity *65*, 1659.

Ben-Gurion, R., and Shafferman, A. (1981). Essential virulence determinants of different *Yersinia* species are carried on a common plasmid. Plasmid *5*, 183–187.

Buchrieser, C., Rusniok, C., Frangeul, L., Couve, E., Billault, A., Kunst, F., Carniel, E., and Glaser, P. (1999). The 102-kilobase *pgm* locus of *Yersinia pestis*: Sequence analysis and comparison of selected regions among different *Yersinia pestis* and *Yersinia pseudotuberculosis* strains. Infection and Immunity *67*, 4851–4861.

Cathelyn, J.S., Crosby, S.D., Lathem, W.W., Goldman, W.E., and Miller, V.L. (2006). RovA, a global regulator of *Yersinia pestis*, specifically required for bubonic plague. Proceedings of the National Academy of Sciences of the USA *103*, 13514–13519.

Caulfield, A.J., and Lathem, W.W. (2012). Substrates of the plasminogen activator protease of *Yersinia pestis*. In Advances in Experimental Medicine and Biology, (New York, NY: Springer New York), pp. 253–260.

Caulfield, A.J., Walker, M.E., Gielda, L.M., and Lathem, W.W. (2014). The Pla protease of *Yersinia pestis* degrades Fas ligand to manipulate host cell death and inflammation. Cell Host Microbe *15*, 424–434.

Chung, L.K., Philip, N.H., Schmidt, V.A., Koller, A., Strowig, T., Flavell, R.A., Brodsky, I.E., and Bliska, J.B. (2014). IQGAP1 is important for activation of caspase-1 in macrophages and is targeted by *Yersinia pestis* type III effector YopM. mBio *5*, 01402–01414.

Cornelis, G.R., Boland, A., Boyd, A.P., Geuijen, C., Iriarte, M., Neyt, C., Sory, M.P., and Stainier, I. (1998). The virulence plasmid of *Yersinia*, an antihost genome. Microbiology and Molecular Biology Reviews *62*, 1315–1352.

Fetherston, J.D., Kirillina, O., Bobrov, A.G., Paulley, J.T., and Perry, R.D. (2010). The yersiniabactin transport system is critical for the pathogenesis of bubonic and pneumonic plague. Infection and Immunity *78*, 2045–2052.

Hentschke, M., Berneking, L., Campos, C.B., Buck, F., Ruckdeschel, K., and Aepfelbacher, M. (2010). *Yersinia* virulence factor YopM induces sustained RSK activation by interfering with dephosphorylation. PLoS One *5*, 13165.

Heusipp, G., Spekker, K., Brast, S., Fälker, S., and Schmidt, M.A. (2006). YopM of *Yersinia enterocolitica* specifically interacts with alpha1-antitrypsin without affecting the anti-protease activity. Microbiology *152*, 1327–1335.

Hinnebusch, B.J., Perry, R.D., and Schwan, T.G. (1996). Role of the *Yersinia pestis* hemin storage (hms) locus in the transmission of plague by fleas. Science *273*, 367–370.

Jackson, S., and Burrows, T.W. (1956). The pigmentation of *Pasteurella pestis* on a defined medium containing haemin. British Journal of Experimental Pathology *37*, 570–576.

Kerschen, E.J., Cohen, D.A., Kaplan, A.M., and Straley, S.C. (2004). The plague virulence protein YopM targets the innate immune response by causing a global depletion of NK cells. Infection and Immunity *72*, 4589–4602.

LaRock, C.N., and Cookson, B.T. (2012). The *Yersinia* virulence effector YopM binds caspase-1 to arrest inflammasome assembly and processing. Cell Host Microbe *12*, 799–805.

Lathem, W.W., Price, P.A., Miller, V.L., and Goldman, W.E. (2007). A plasminogen-activating protease specifically controls the development of primary pneumonic plague. Science *315*, 509–513.

Lathem, W.W., Crosby, S.D., Miller, V.L., and Goldman, W.E. (2005). Progression of primary pneumonic plague: A mouse model of infection, pathology, and bacterial transcriptional activity. Proceedings of the National Academy of Sciences *102*, 17786–17791.

Leung, K.Y., Reisner, B.S., and Straley, S.C. (1990). YopM inhibits platelet aggregation and is necessary for virulence of *Yersinia pestis* in mice. Infection and Immunity *58*, 3262–3271.

Marketon, M.M., DePaolo, R.W., DeBord, K.L., Jabri, B., and Schneewind, O. (2005). Plague bacteria target immune cells during infection. Science *309*, 1739–1741.

McCoy, M.W., Marre, M.L., Lesser, C.F., and Mecsas, J. (2010). The C-terminal tail of *Yersinia pseudotuberculosis* YopM is critical for interacting with RSK1 and for virulence. Infection and Immunity *78*, 2584–2598.

McDonald, C., Vacratsis, P.O., Bliska, J.B., and Dixon, J.E. (2003). The *Yersinia* virulence factor YopM forms a novel protein complex with two cellular kinases. Journal of Biological Chemistry *278*, 18514–18523.

McPhee, J.B., Mena, P., and Bliska, J.B. (2010). Delineation of regions of the *Yersinia* YopM protein required for interaction with the RSK1 and PRK2 host kinases and their requirement for interleukin-10 production and virulence. Infection and Immunity *78*, 3529–3539.

McPhee, J.B., Mena, P., Zhang, Y., and Bliska, J.B. (2012). Interleukin-10 induction is an important virulence function of the *Yersinia pseudotuberculosis* type III effector YopM. Infection and Immunity *80*, 2519–2527.

Navarro, L., Koller, A., Nordfelth, R., Wolf-Watz, H., Taylor, S., and Dixon, J.E. (2007). Identification of a molecular target for the *Yersinia* protein kinase A. Molecular Cell *26*, 465–477.

Park, H., Teja, K., O'Shea, J.J., and Siegel, R.M. (2007). The *Yersinia* effector protein YpkA induces apoptosis independently of actin depolymerization. The Journal of Immunology *178*, 6426–6434.

Pechous, R.D., Sivaraman, V., Price, P.A., Stasulli, N.M., and Goldman, W.E. (2013). Early host cell targets of *Yersinia pestis* during primary pneumonic plague. PLoS Pathogens *9*, e1003679.

Perry, R.D., and Fetherston, J.D. (1997). *Yersinia pestis* - Etiologic agent of plague. Clinical Microbiology Reviews *10*, 35–66.

Price, P.A., Jin, J., and Goldman, W.E. (2012). Pulmonary infection by *Yersinia pestis* rapidly establishes a permissive environment for microbial proliferation. Proceedings of the National Academy of Sciences *109*, 3083–3088.

Quenee, L.E., Hermanas, T.M., Ciletti, N., Louvel, H., Miller, N.C., Elli, D., Blaylock, B., Mitchell, A., Schroeder, J., Krausz, T., et al. (2012). Hereditary hemochromatosis restores the virulence of plague vaccine strains. Journal of Infectious Diseases *206*, 1050–1058.

Roux, P.P., Shahbazian, D., Vu, H., Holz, M.K., Cohen, M.S., Taunton, J., Sonenberg, N., and Blenis, J. (2007). RAS/ERK Signaling Promotes Site-specific Ribosomal Protein S6 Phosphorylation via RSK and Stimulates Cap-dependent Translation. Journal of Biological Chemistry *282*, 14056–14064.

Ruckdeschel, K., Roggenkamp, A., Schubert, S., and Heesemann, J. (1996). Differential contribution of Yersinia enterocolitica virulence factors to evasion of microbicidal action of neutrophils. Infection and Immunity *64*, 724–733.

Sodeinde, O.A., Sample, A.K., Brubaker, R.R., and Goguen, J.D. (1988). Plasminogen activator/coagulase gene of *Yersinia pestis* is responsible for degradation of plasmid-encoded outer membrane proteins. Infection and Immunity *56*, 2749.

Spinner, J.L., Seo, K.S., O'Loughlin, J.L., Cundiff, J.A., Minnich, S.A., Bohach, G.A., and Kobayashi, S.D. (2010). Neutrophils are resistant to *Yersinia* YopJ/P-induced apoptosis and are protected from ROS-mediated cell death by the type III secretion system. PLoS One *5*, e9279–e9279.

Trosky, J.E., Liverman, A.D.B., and Orth, K. (2008). *Yersinia* outer proteins: Yops. Cellular Microbiology *10*, 557–565.

Walker, K.A., and Miller, V.L. (2004). Regulation of the Ysa type III secretion system of *Yersinia enterocolitica* by YsaE/SycB and YsrS/YsrR. Journal of Bacteriology *186*, 4056–4066.

Wren, B.W. (2003). The *Yersiniae* - a model genus to study the rapid evolution of bacterial pathogens. Nature Reviews: Microbiology *1*, 55–64.

Ye, Z., Gorman, A.A., Uittenbogaard, A.M., Myers-Morales, T., Kaplan, A.M., Cohen, D.A., and Straley, S.C. (2014). Caspase-3 mediates the pathogenic effect of *Yersinia pestis* YopM in liver of C57BL/6 mice and contributes to YopM's function in spleen. PLoS One *9*, 110956.

Ye, Z., Kerschen, E.J., Cohen, D.A., Kaplan, A.M., van Rooijen, N., and Straley, S.C. (2009). Gr1+ cells control growth of YopM-negative *Yersinia pestis* during systemic plague. Infection and Immunity *77*, 3791–3806.

Ye, Z., Uittenbogaard, A.M., Cohen, D.A., Kaplan, A.M., Ambati, J., and Straley, S.C. (2011). Distinct CCR2(+) Gr1(+) cells control growth of the *Yersinia pestis* delta *yopM* mutant in liver and spleen during systemic plague. Infection and Immunity *79*, 674–687.

CHAPTER 4: CHARACTERIZING THE IMPACT OF REACTIVE OXYGEN/NITROGEN SPECIES *IN VIVO* DURING PNEUMONIC PLAGUE

4.1 Overview

This chapter describes the *in vivo* characterization of small reactive molecule stresses that *Y. pestis* experiences within the lung during pneumonic plague. Activated neutrophils release both reactive oxygen and nitrogen species (ROS and RNS) that can kill bacteria, but may also injure host cells. I initially hypothesized that the inflammatory lung lesions that develop during pneumonic plague are a result of host-mediated injury via ROS and RNS. In the work described in this chapter, however, I provide evidence to the contrary that indicates ROS and RNS play a significant role in hindering early establishment of *Y. pestis* during pneumonic plague. Both the extent of lung injury and bacterial burdens in the lungs were increased when these stresses were negated in a murine intranasal infection. This work is the first to evaluate *in vivo* how these small host defense molecules affect the tissue damage and lesion composition in lungs during pneumonic plague. Characterizing innate immune stresses, and how *Y. pestis* is affected by them, will lead to a better understanding of *Y. pestis* - host interactions during pneumonic plague, and may help to identify new therapeutics that can prolong the treatment window for *Y. pestis* infection.

4.2 Introduction

The studies presented in this chapter focus on the small molecules, termed reactive oxygen species (ROS) and reactive nitrogen species (RNS), that are generated by neutrophils and other innate immune cells in response to infection. These small molecules act during host defense to kill invading microbes by disrupting normal cell function, but can also incidentally injure the host. Therefore, a delicate balance must be kept to prevent extensive host damage while maintaining the antimicrobial activity of ROS/RNS. Consequently, many bacteria have evolved mechanisms to counteract oxidative and nitrosative bursts. If an immune response is prolonged due to bacterial resistance, ROS and RNS can cause damage to host tissue, particularly in a location like the alveolar spaces, which are lined by a single layer of epithelial cells (Folkerts et al., 2001). Based on the rapid neutrophil response and hyper-inflammatory state in the lungs late during pneumonic plague, the lung lesions that form may be the result of the over-production of ROS and RNS due to the uncontrolled burden of *Y. pestis* that replicates unchecked in the lungs early during infection (Lathem et al., 2005).

In response to infection, most antimicrobial ROS are generated from the initial reaction of O_2 and NADPH with the NADPH oxidase complex. This reaction generates superoxide (O_2^-) that can be converted to hydrogen peroxide (H_2O_2) and then to hydroxyl radicals. O_2^- can also react with nitric oxide (NO) to generate peroxynitrite ($ONOO^-$), another potent reactive molecule (Bogdan et al., 2000; Fang, 1997; Segal, 2005; Thomas et al., 1988). Additionally, conversion of H_2O_2 by neutrophil myeloperoxidase (MPO) can generate antimicrobial hypochlorous acid

(HOCl) and chloramines (Bogdan et al., 2000; Thomas et al., 1988). It is important for immune cells to control and target the ROS they produce due to their generalized pleiotropic and harmful effects. Proteins, lipids, DNA, and RNA can all be targets of oxygen radicals, and if ROS are overproduced they can damage the host through their interactions with these cellular components. Both the sugar moieties and the base structures of DNA and RNA can be targeted, resulting in strand breaks. Membrane lipids are attacked at polyunsaturated fatty acids to disrupt membrane fluidity and membrane-protein structures. Proteins can likewise be targeted, causing the modification of sulfur bonds, oxidation of amino acids around metal binding sites, and peptide fragmentation, among other effects (Cabiscol et al., 2000).

Most RNS generated in response to bacterial infection result from the metabolism of L-arginine by the inducible nitric oxide synthase (iNOS) protein, which utilizes O_2 and NADPH to form citrulline and NO. NO can be further converted into other antimicrobial RNS including $ONOO^-$, S-nitrosothiols (RSNO), various nitrogen oxides, and dinitrosyl-iron complexes (Fang, 1997). NO can be an inflammatory mediator, up-regulating the production of over 20 cytokines within numerous cell types. Both NO and RSNOs can also affect the apoptotic potential of cells (Bogdan et al., 2000). Specifically within neutrophils, NO is important for recruitment and adhesion through cytokine regulation and integrin expression. RNS can work by altering transcription through signaling pathways, or can directly affect activity through tyrosine nitration of proteins (Bogdan, 2001). These RNS can hinder bacterial growth in many ways. For example, RSNOs can be generated through NO

reacting with SH-groups on free amino acids, which are able to disrupt metal-sulfur clusters to kill bacteria (Bogdan et al., 2000; Fang, 1997; Marcinkiewicz, 1997; Pacelli et al., 1995). Interestingly, there is some evidence that host-NO can react with bacterial-derived O_2^- and generate $ONOO^-$ within a bacterium to cause tyrosine nitration of bacterial proteins to affect their functions (Bogdan, 2001).

The NADPH oxidase complex and iNOS have been studied in the context of many bacterial infections. Both ROS (Brennan et al., 2004; Cha et al., 2010; Jann et al., 2009; Mendez-Samperio et al., 2009; Pacelli et al., 1995) and RNS (Bogdan, 2001; Brennan et al., 2004; Fang, 1997; Marcinkiewicz, 1997; Pacelli et al., 1995; Richardson et al., 2006) have been shown to be important to varying degrees in controlling a number of bacterial infections. *In vitro* studies of *Y. pestis* have described a role for these reactive small molecules in regulating bacterial gene expression and how the bacterium attempts to control host generation of these molecules (Paauw et al., 2009; Pradel et al., 2014; Sebbane et al., 2006). It is necessary, however, to define the role of ROS and RNS *in vivo* during pneumonic plague. If these mechanisms contribute to the progression of pneumonic plague, they could be manipulated to prolong the timeframe during which treatment is effective. The work described in this chapter examines the affects of both ROS and RNS on pneumonic plague using intranasal infection with a fully virulent strain of *Y. pestis*. The use of mouse strains that lack production of leukocyte based ROS (gp91phox$^{-/-}$) and RNS (iNOS$^{-/-}$) allow us to determine how these reactive species influence pneumonic plague disease progression and lesion development.

4.3 Methods

All reagents were obtained form Sigma-Aldrich™ unless otherwise noted.

4.3.1 Ethics statement

The use of live vertebrate animals was performed in accordance with the Public Health Service (PHS) policy on Humane Care and Use of Laboratory Animals, the Amended Animal Welfare Act of 1985, and the regulations of the United States Department of Agriculture (USDA). All animal studies were approved by the University of North Carolina at Chapel Hill Office of Animal Care and Use, protocols #12-028.0 and #15-022.0.

4.3.2 Bacterial strains and culture conditions

The fully virulent *Yersinia pestis* strain CO92 was obtained from the U.S. Army, Ft. Detrick, MD. *Y. pestis* was grown on brain-heart infusion (BHI) agar (Difco Laboratories) at 26°C for two days. For infections, liquid cultures of *Y. pestis* CO92 were grown in BHI broth for 6–12 h at 26°C. The cultures were then diluted to an OD_{620} of 0.05–0.1 in BHI supplemented with 2.5 mM $CaCl_2$ and grown 12–16h at 37°C with constant shaking.

4.3.3 Animals and infections

Six- to eight-week old female C57BL/6J mice were obtained from Jackson Laboratories. Knockout mouse strains, gp91phox$^{-/-}$ and iNOS$^{-/-}$, were originally

obtained from Jackson Laboratories and bred at the University of North Carolina at Chapel Hill according to the Division of Laboratory Animal Medicine regulations. Mice were provided with food and water ad libitum and maintained at 25°C and 15% humidity with alternating 12 h periods of light and dark. For animal infections, groups of three to ten mice were lightly anesthetized with ketamine/xylazine and inoculated intranasally with a lethal dose of 10^3-10^4 colony-forming units (CFUs) suspended in 20µL PBS. Actual CFUs inoculated was determined by plating serial dilutions of the inoculum on BHI. Mice were continuously monitored at 12-hour intervals and scored for disease severity. If mice were moribund at any time point they were humanely euthanized as per the Animal Care and Use protocol.

4.3.4 Bacterial organ burden determination

After humanely euthanizing infected mice, both lungs and spleens are removed and separately placed into conical tubes containing PBS. Organs were homogenized in the PBS using a Dremel® tissue homogenizer. Dilutions of tissue homogenate were prepared samples were spotted onto BHI agar. Agar was incubated at 26°C for 2 days to allow for growth of the bacterial colony forming units (CFUs). The CFUs were enumerated and back-calculating the dilutions revealed the bacterial burden per organ.

4.3.5 Lung histopathology staining

Groups of three mice were inoculated intranasally as described above. At the defined time point mice were humanely euthanized and lungs were inflated with 10% neutral buffered formalin via tracheal cannulation, then removed and incubated in 10% formalin for a minimum of 2 h. Lungs were placed in phosphate buffered saline (pH 7.4) with 30% Sucrose and 20% O.C.T. compound (Tissue-Tek®) for 3 h with intermittent inverting. Lungs were removed, covered in O.C.T. for 10 min, frozen on dry ice, and stored at -80°C. Ten-µm lung sections were adhered to glass slides, stained with hematoxylin/eosin for examination, and a coverslip was added.

4.4 Results

Chapters 2 and 3 of this Dissertation have shown that during pneumonic plague, neutrophils aggregate outward from small initiating foci and suffer from a lack of turnover and cell clearance, which results in alveolar destruction late during pneumonic plague. This damage likely results from neutrophil defense mechanisms such as degranulation and the release of granule contents as new neutrophils begin infiltrating into the lungs. These neutrophil granules include proteins and protein complexes that generate ROS and RNS that can lead to damaging effects on host tissue. Determining the effects of ROS and RNS on lung lesion development will give insight into how components of the innate immune response cause alveolar damage during pneumonic plague.

4.4.1 Histological comparison of the effects of reactive oxygen and nitrogen species on pneumonic plague lung lesions

To determine the effects of small ROS and RNS molecules on the development of lung lesions during pneumonic plague, I obtained gp91phox$^{-/-}$ mice lacking the ability to produce ROS from the leukocyte NADPH oxidase complex, and iNOS$^{-/-}$ mice lacking the ability to produce RNS. Mice were infected via intranasal inoculation with 10^4 fully virulent *Y. pestis,* and lungs were harvested at various time points and sectioned for gross histopathological analysis by hematoxylin and eosin staining. At 36 hpi, C57BL/6J (wild type) mice showed very little lung damage with only a few small foci beginning to form (Figure 4.1A). Alternatively, infected iNOS$^{-/-}$ and gp91phox$^{-/-}$ mice both had significant lung lesion development by 36 hpi. Lungs of iNOS$^{-/-}$ mice displayed levels of inflammatory damage similar to what is seen in the lungs of wild type mice later at 48 hpi (Figure 4.1C, 4.1B respectively). Similarly, lungs of gp91phox$^{-/-}$ mice had more consolidated lesions by 36 hpi, and also appeared similar to wild type lungs at 48 hpi (Figure 4.1E, 4.1B respectively). This difference was less defined at later time points during infection, where by 48 hpi the lungs of iNOS$^{-/-}$ mice had a similar amount of lung area covered by lesions as wild type mice. However, the distribution of lesions appeared unique: there tended to be *fewer* but *larger* lesions that likely cause more severe alveolar damage at this later time point in the lungs of iNOS$^{-/-}$ mice (Figures 4.1D). In contrast, lung lesion development in gp91phox$^{-/-}$ mice displayed more coverage of lung surface area, and lungs contained visibly more lesions compared to wild type mice (Figure 4.1F).

4.4.2 Determining the effects of ROS/RNS on bacterial burden after intranasal infection with *Y. pestis*

The more advanced lesion development in the lungs of both iNOS$^{-/-}$ and gp91phox$^{-/-}$ mice at 36 hpi led me to question whether there were differences in bacterial burden within the organs of these mice. To this end, both lung and spleen burdens were assessed at 36 and 48 hpi in all three strains of mice after intranasal inoculation with 10^4 *Y. pestis* CFUs. Spleen burden is a representative assessment of bacterial dissemination from the lungs (Lathem et al., 2005). The *Y. pestis* burden in the lungs of all three strains of mice remained equivalent at both 36 and 48 hpi (Figure 4.2). Bacterial burden in the spleen, however, was altered between the three mouse strains. While at 36 hpi there was no significant difference in spleen burdens between the three strains of mice, there was a clear trend that the iNOS$^{-/-}$ and gp91phox$^{-/-}$ mice had higher spleen burdens at this time point (Figure 4.2). The difference in spleen bacterial burden became more apparent by 48 hpi, where both the iNOS$^{-/-}$ and gp91phox$^{-/-}$ mice had significantly higher bacterial burdens compared to those seen in wild type mice (Figure 4.2). These findings imply that dissemination is occurring earlier in the iNOS$^{-/-}$ and gp91phox$^{-/-}$ mice, suggesting that establishment of *Y. pestis* in the lungs is unhindered in these mice compared to wild type mice.

4.4.3 Survival of mice lacking the ability to produce small reactive species

Based on differences in both lung lesion area and *Y. pestis* burdens in the spleen, I sought to determine if the absence of ROS and RNS effected the survival of mice during pneumonic plague. An intranasal dose of 10^3 *Y. pestis* was administered to wild type, iNOS$^{-/-}$, and gp91phox$^{-/-}$ mice. Due to the extremely rapid progression of pneumonic plague this lower dose was used to attempt to compensate for the overwhelming burden normally experienced in wild type mice. I could then better determine survival differences specifically do to earlier development of disease. The health of all mice was assessed every 12 hours, and when the mice became moribund they were euthanized and the span of their survival was recorded. While iNOS$^{-/-}$ mice had a moderately extended time to death compared to wild type mice, this difference was not statistically significantly. Likewise, gp91phox$^{-/-}$ mice had a similar survival time as wild type mice (Figure 4.3). This data suggests that, while small reactive molecules may have effects on lung lesion development and composition, they are dispensable in relation to survival during our mouse model of infection.

4.5 Discussion

While several laboratories have demonstrated relevance of innate immune cells (including neutrophils) during plague infection (Grabenstein et al., 2006; Kerschen et al., 2004; Laws et al., 2010; Lukaszewski et al., 2005; Marketon et al., 2005; O'Loughlin et al., 2010; Pechous et al., 2013; Pujol and Bliska, 2005; Welkos

et al., 1998; Zauberman et al., 2006), there is a lack of information regarding whether neutrophils use small reactive species such at ROS and RNS to control *Y. pestis* within lung lesions during pneumonic plague. Neutrophils are able to confer several different stresses on bacteria while attempting to control infection (Kobayashi et al., 2003; Segal, 2005; Tsai and Grayson, 2008). We predicted that ROS/RNS likely contribute to lung damage in pneumonic plague due to the densely packed, neutrophil-rich nature of the inflammatory lung lesions (Bogdan, 2001; Bogdan et al., 2000; Brennan et al., 2004; Fang, 1997; Pacelli et al., 1995; Roos et al., 2003; Segal, 2005). While ROS (Gao et al., 2011; Sebbane et al., 2006), RNS (Sebbane et al., 2006), and neutrophils (Laws et al., 2010; O'Loughlin et al., 2010) have each proven effective in combating *Y. pestis in vitro*, no comprehensive study has observed these effects during pneumonic plague, a disease characterized largely as the destruction of lung tissue by a hyper-activated innate immune response (Lathem et al., 2005).

In this chapter, I sought to determine the *in vivo* affects of small reactive molecules on disease progression and development of lung lesions during pneumonic plague. To perform these studies I utilized two strains of knockout mice: iNOS$^{-/-}$ and gp91phox$^{-/-}$. In generating ROS, neutrophils utilize a specific phagocytic/leukocyte version of NADPH oxidase that contains the gp91phox (NOX2) subunit (Brandes and Kreuzer, 2005). The specificity of this gp91phox subunit can be taken advantage of, and gp91phox$^{-/-}$ mice can be used to study the depletion of leukocyte ROS (Gao et al., 2002). Inhibiting the NADPH oxidase complex in this

manner can also affect the generation of ROS by MPO since H_2O_2, a downstream product generated by the NADPH oxidase complex, is necessary for the activity of MPO (Bogdan et al., 2000). In generating RNS, there are three forms of NOS: inducible, endothelial, and neuronal. The eNOS protein is necessary for vasodilation, nNOS is necessary for neuronal cell communication, and both aid in the regulation of blood pressure (Folkerts et al., 2001; Forstermann and Sessa, 2012). The iNOS protein is found expressed in cells as a defense response to invading pathogens, and is therefore primarily found in innate immune cells or cells such as airway epithelial cells that act as sentinels to detect and combat invading pathogens (Bogdan et al., 2000; Folkerts et al., 2001). The specificity of iNOS during infection can be taken advantage of, and $iNOS^{-/-}$ mice can be used to study the depletion of RNS *in vivo* (MacMicking et al., 1995; Wei et al., 1995).

The observation that small lung lesions begin to develop at 36 h after intranasal infection of wild type mice with *Y. pestis* is consistent with previous findings in the Goldman lab (Lathem et al., 2005). It was therefore surprising to observe that larger lesions had developed by 36 h in the lungs of both the $iNOS^{-/-}$, and $gp91phox^{-/-}$ mice after intranasal infection. This was contrary to my initial hypothesis that ROS and RNS were responsible for a large amount of damage in the lungs after infection, and that their depletion would mitigate much of this damage. On the contrary, this data suggests that both ROS and RNS play a role in preventing initial establishment of *Y. pestis* in the lungs.

Along with early lesion development, the increased dissemination of *Y. pestis* from the lungs of both iNOS$^{-/-}$ and gp91phox$^{-/-}$ mice may indicate that there is an initial stalling of *Y. pestis* by these reactive species that prevents earlier systemic spread. There is a potential correlation between the increase in bacterial dissemination, as determined by bacterial burden in the spleen, and the earlier development of larger lung lesions. An increase in the spleen burden of both the iNOS$^{-/-}$ and gp91phox$^{-/-}$ mice suggests that dissemination from the lungs begins earlier during these infections. This earlier infiltration could lead to lesions developing earlier in the iNOS$^{-/-}$ and gp91phox$^{-/-}$ mice after intranasal infection with *Y. pestis*. This could imply that there is a threshold of bacterial burden or host damage in the lungs that triggers dissemination, and without these reactive species *Y. pestis* is less adept at disseminating from the lungs into distal tissues.

The initial hypothesis that ROS and RNS were responsible for extensive damage within lung lesions also predicted that there would be an increase in the survival of the iNOS$^{-/-}$ and gp91phox$^{-/-}$ mice once that damage was mitigated. Upon observing that there was earlier lesion development and increased dissemination in knockout mice, it was not surprising that there was no change in iNOS$^{-/-}$ or gp91phox$^{-/-}$ mouse survival compared to wild type mice after intranasal challenge. On the contrary, my current model suggests that the iNOS$^{-/-}$ and gp91phox$^{-/-}$ mice would succumb to disease more quickly due to the advanced progression of lesion formation and increased septicemia. It is possible that using an inoculum above the LD50 for *Y. pestis* overwhelms the mouse and masks any significant change in

survival. Use of a lower inoculum, at which not all wild type mice succumb to infection, may be necessary to observe a change in survival in the iNOS$^{-/-}$ and gp91phox$^{-/-}$ mice.

A great deal of work has focused specifically on *Y. pestis* itself, or the direct interaction of bacteria with specific host innate immune cells. However, as *Y. pestis* represents a potential bio-weapon threat, more research should focus on a whole-host view of disease. Observing *in vivo* immune responses during disease progression allows for the identification of new pathways that could not be identified with *in vitro* assays alone. *Y. pestis* vaccine research is primarily focused on proteins known to directly interact with host cells. In addition to these, *Y. pestis* proteins affecting and responding to the environment may be equally important. This unique look at the effect of ROS and RNS in lung lesions gives insight into how individual molecules can affect disease symptoms. It also offers a peek into the potential information that may be revealed when the RNAseq data from Chapter 2 are evaluated to identify patterns in genes affected by the generation of ROS and RNS.

4.6 Figures

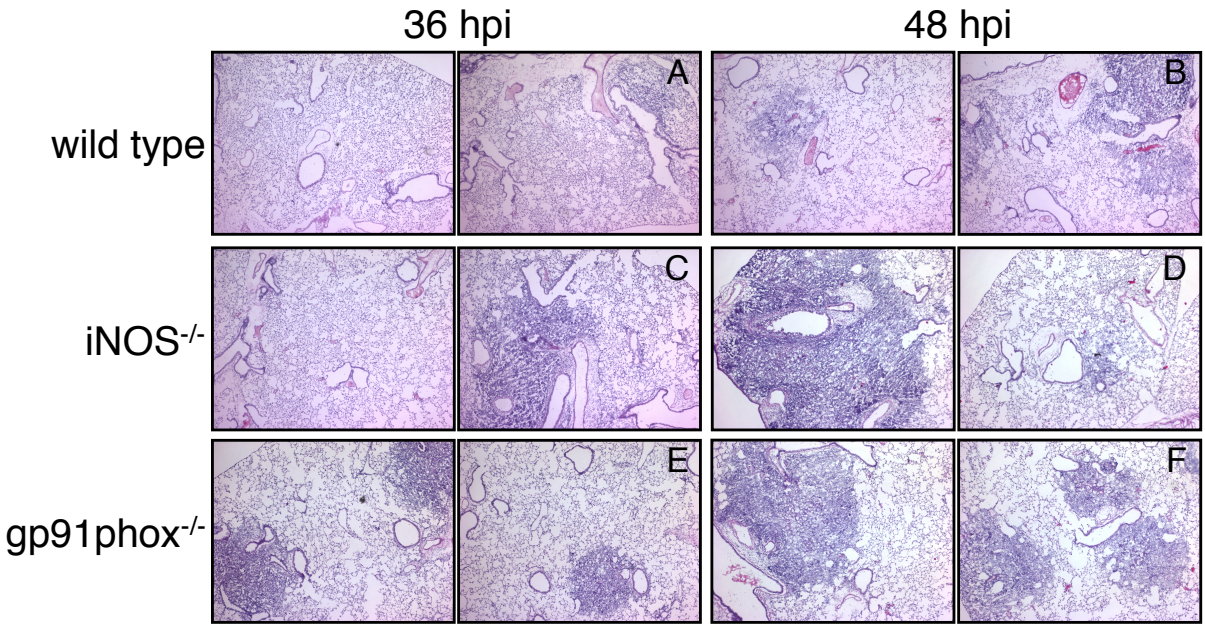

Figure 4.1: Comparative histopathology of wild type, iNOS$^{-/-}$, and gp91phox$^{-/-}$ mice during intranasal *Y. pestis* infection

At 36 hpi lung sections of (**A**) wild type mice infected with 10^4 *Y. pestis* had very little apparent inflammation. At this same time point, lungs sections of both (**C**) iNOS$^{-/-}$ and (**E**) gp19phox$^{-/-}$ mice had much more progressed inflammation with the development of sizeable lesions. At 48 hpi (**B**) lung sections of wild type showed the typical progressive development of lung lesions. At this same time point lung sections of (**D**) iNOS$^{-/-}$ mice had a few expansive lung lesions taking up a majority of individual lung lobes. Lung sections of (**F**) gp91phox$^{-/-}$ mice had an abundant number of lesions throughout all lobes of the lung consuming a large expanse of the lung. All representative images are captured at 40x magnification.

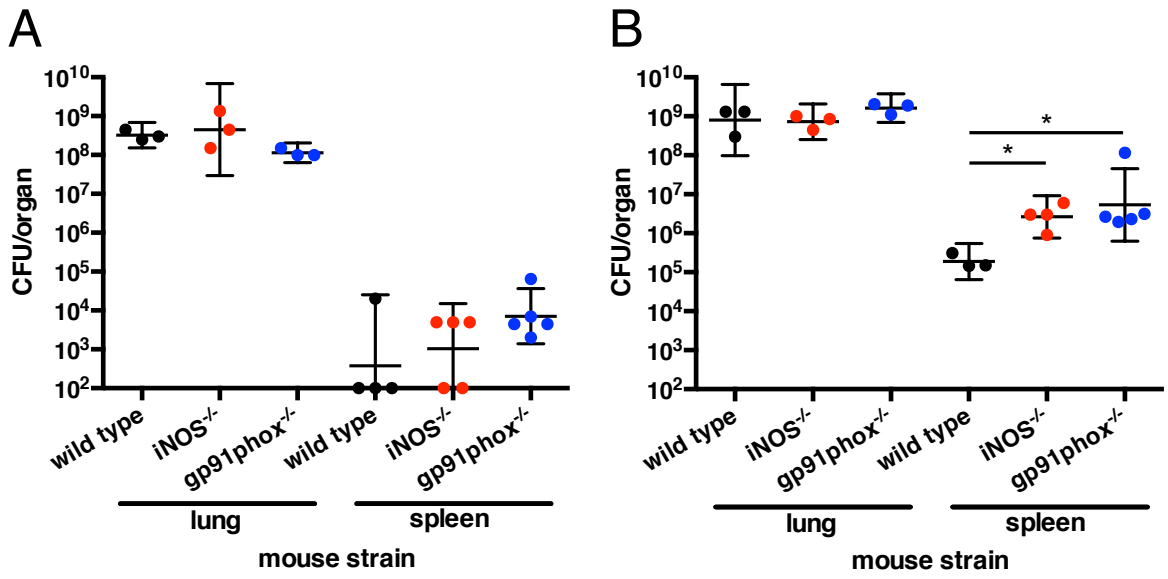

Figure 4.2: Bacterial burden of both the lung and spleen of wild type, iNOS$^{-/-}$, and gp91phox$^{-/-}$ mice during intranasal *Y. pestis* infection

After intranasal infection with 10^4 *Y. pestis*, wild type, iNOS$^{-/-}$, and gp91phox$^{-/-}$ mice were euthanized at various time points to obtain a measurement of bacterial burden. (**A**) After 36 hpi the lung burden of all 3 mouse strains were equivalent. Spleen burden also did not show a significant change, but there was a trend of higher burden in iNOS$^{-/-}$ and gp91phox$^{-/-}$ mice. (**B**) After 48 hpi the lung burden of all 3 mouse strains was still equivalent. Spleen burden differences had become more apparent and there was a significant increase in burden for both iNOS$^{-/-}$ and gp91phox$^{-/-}$ mice compared to wild type mice. Data are from representative experiments and represented as geometric mean ± 95% CI; asterisks represent statistical significance based on Mann-Whitney tests, *$p < 0.05$.

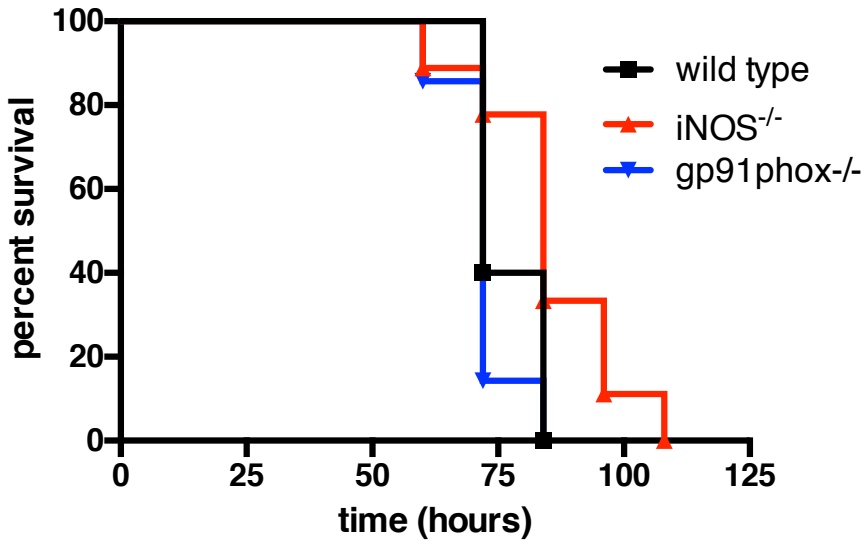

Figure 4.3: Survival graph of wild type, iNOS$^{-/-}$, and gp91phox$^{-/-}$ mice during intranasal *Y. pestis* infection

All mice were inoculated with 10^3 *Y. pestis* and were observed for disease symptoms. Wild type, iNOS$^{-/-}$, and gp91phox$^{-/-}$ had median survival times of 72 h, 84 h, and 72 h respectively. Data is represented as percent survival of mice and there was no significant difference in survival by log-rank Mantel-Cox tests.

REFERENCES

Bogdan, C. (2001). Nitric oxide and the immune response. Nature Immunology *2*, 907–916.

Bogdan, C., Röllinghoff, M., and Diefenbach, A. (2000). Reactive oxygen and reactive nitrogen intermediates in innate and specific immunity. Current Opinion in Immunology *12*, 64–76.

Brandes, R.P., and Kreuzer, J. (2005). Vascular NADPH oxidases: molecular mechanisms of activation. Cardiovasc Res *65*, 16–27.

Brennan, R.E., Russell, K., Zhang, G.Q., and Samuel, J.E. (2004). Both inducible nitric oxide synthase and NADPH oxidase contribute to the control of virulent phase I *Coxiella bumetii* infections. Infection and Immunity *72*, 6666–6675.

Cabiscol, E., Tamarit, J., and Ros, J. (2000). Oxidative stress in bacteria and protein damage by reactive oxygen species. International Microbiology *3*, 3–8.

Cha, B., Lim, J.W., Kim, K.H., and Kim, H. (2010). HSP90 beta interacts with Rac1 to activate NADPH oxidase in *Helicobacter pylori*-infected gastric epithelial cells. International Journal of Biochemistry & Cell Biology *42*, 1455–1461.

Fang, F.C. (1997). Perspectives series: host/pathogen interactions. Mechanisms of nitric oxide-related antimicrobial activity. Journal of Clinical Investigation *99*, 2818–2825.

Folkerts, G., Kloek, J., Muijsers, R., and Nijkamp, F.P. (2001). Reactive nitrogen and oxygen species in airway inflammation. European Journal of Pharmacology *429*, 251–262.

Forstermann, U., and Sessa, W.C. (2012). Nitric oxide synthases: regulation and function. European Heart Journal *33*, 829–837.

Gao, H., Zhang, Y., Han, Y., Yang, L., Liu, X., Guo, Z., Tan, Y., Huang, X., Zhou, D., and Yang, R. (2011). Phenotypic and transcriptional analysis of the osmotic regulator OmpR in *Yersinia pestis.* BMC Microbiology *11*, 39–39.

Gao, X.-P., Standiford, T.J., Rahman, A., Newstead, M., Holland, S.M., Dinauer, M.C., Liu, Q.-H., and Malik, A.B. (2002). Role of NADPH oxidase in the mechanism of lung neutrophil sequestration and microvessel injury induced by Gram-negative sepsis: studies in p47phox$^{-/-}$ and gp91phox$^{-/-}$ mice. Journal of Immunology (Baltimore, Md. : 1950) *168*, 3974–3982.

Grabenstein, J.P., Fukuto, H.S., Palmer, L.E., and Bliska, J.B. (2006). Characterization of phagosome trafficking and identification of PhoP-regulated

genes important for survival of *Yersinia pestis* in macrophages. Infection and Immunity *74*, 3727–3741.

Jann, N.J., Schmaler, M., Kristian, S.A., Radek, K.A., Gallo, R.L., Nizet, V., Peschel, A., and Landmann, R. (2009). Neutrophil antimicrobial defense against *Staphylococcus aureus* is mediated by phagolysosomal but not extracellular trap-associated cathelicidin. Journal of Leukocyte Biology *86*, 1159–1169.

Kerschen, E.J., Cohen, D.A., Kaplan, A.M., and Straley, S.C. (2004). The plague virulence protein YopM targets the innate immune response by causing a global depletion of NK cells. Infection and Immunity *72*, 4589–4602.

Kobayashi, S.D., Voyich, J.M., and DeLeo, F.R. (2003). Regulation of the neutrophil-mediated inflammatory response to infection. Microbes and Infection *5*, 1337–1344.

Lathem, W.W., Crosby, S.D., Miller, V.L., and Goldman, W.E. (2005). Progression of primary pneumonic plague: A mouse model of infection, pathology, and bacterial transcriptional activity. Proceedings of the National Academy of Sciences *102*, 17786–17791.

Laws, T.R., Davey, M.S., Titball, R.W., and Lukaszewski, R. (2010). Neutrophils are important in early control of lung infection by *Yersinia pestis*. Microbes and Infection *12*, 331–335.

Lukaszewski, R.A., Kenny, D.J., Taylor, R., Rees, D.G.C., Hartley, M.G., and Oyston, P.C.F. (2005). Pathogenesis of *Yersinia pestis* infection in BALB/c mice: effects on host macrophages and neutrophils. Infection and Immunity *73*, 7142–7150.

MacMicking, J.D., Nathan, C., Hom, G., Chartrain, N., Fletcher, D.S., Trumbauer, M., Stevens, K., Xie, Q.W., Sokol, K., and Hutchinson, N. (1995). Altered responses to bacterial infection and endotoxic shock in mice lacking inducible nitric oxide synthase. Cell *81*, 641–650.

Marcinkiewicz, J. (1997). Nitric oxide and antimicrobial activity of reactive oxygen intermediates. Immunopharmacology *37*, 35–41.

Marketon, M.M., DePaolo, R.W., DeBord, K.L., Jabri, B., and Schneewind, O. (2005). Plague bacteria target immune cells during infection. Science *309*, 1739–1741.

Mendez-Samperio, P., Perez, A., and Torres, L. (2009). Role of reactive oxygen species (ROS) in *Mycobacterium bovis* bacillus Calmette Guerin-mediated up-regulation of the human cathelicidin LL-37 in A549 cells. Microbial Pathogenesis *47*, 252–257.

O'Loughlin, J.L., Spinner, J.L., Minnich, S.A., and Kobayashi, S.D. (2010). *Yersinia pestis* two-component gene regulatory systems promote survival in human neutrophils. Infection and Immunity *78*, 773–782.

Paauw, A., Leverstein-van Hall, M.A., van Kessel, K.P.M., Verhoef, J., and Fluit, A.C. (2009). Yersiniabactin reduces the respiratory oxidative stress response of innate immune cells. PLoS One *4*, –e8240.

Pacelli, R., Wink, D.A., Cook, J.A., KRISHNA, M.C., Degraff, W., Friedman, N., Tsokos, M., Samuni, A., and Mitchell, J.B. (1995). Nitric-oxide potentiates hydrogen peroxide-induced killing of *Escherichia coli*. The Journal of Experimental Medicine *182*, 1469–1479.

Pechous, R.D., Sivaraman, V., Price, P.A., Stasulli, N.M., and Goldman, W.E. (2013). Early host cell targets of *Yersinia pestis* during primary pneumonic plague. PLoS Pathogens *9*, e1003679.

Pradel, E., Lemaitre, N., Merchez, M., Ricard, I., Reboul, A., Dewitte, A., and Sebbane, F. (2014). New insights into how *Yersinia pestis* adapts to its mammalian host during bubonic plague. PLoS Pathogens *10*, e1004029.

Pujol, C., and Bliska, J.B. (2005). Turning *Yersinia* pathogenesis outside in: subversion of macrophage function by intracellular yersiniae. Clinical Immunology *114*, 216–226.

Richardson, A.R., Dunman, P.M., and Fang, F.C. (2006). The nitrosative stress response of *Staphylococcus aureus* is required for resistance to innate immunity. Molecular Microbiology *61*, 927–939.

Roos, D., van Bruggen, R., and Meischl, C. (2003). Oxidative killing of microbes by neutrophils. Microbes and Infection *5*, 1307–1315.

Sebbane, F., Lemaitre, N., Sturdevant, D.E., Rebeil, R., Virtaneva, K., Porcella, S.F., and Hinnebusch, B.J. (2006). Adaptive response of *Yersinia pestis* to extracellular effectors of innate immunity during bubonic plague. Proceedings of the National Academy of Sciences *103*, 11766–11771.

Segal, A.W. (2005). How neutrophils kill microbes. Immunology *23*, 197–223.

Thomas, E.L., Lehrer, R.I., and Rest, R.F. (1988). Human neutrophil antimicrobial activity. Reviews of Infectious Diseases *10*, S450–S456.

Tsai, K.S., and Grayson, M.H. (2008). Pulmonary defense mechanisms against pneumonia and sepsis. Current Opinion in Pulmonary Medicine *14*, 260–265.

Wei, X.Q., Charles, I.G., Smith, A., Ure, J., Feng, C.J., Huang, F.P., XU, D.M.,

Muller, W., Moncada, S., and Liew, F.Y. (1995). Altered immune responses in mice lacking inducible nitric oxide synthase. Nature *375*, 408–411.

Welkos, S., Friedlander, A., McDowell, D., Weeks, J., and Tobery, S. (1998). V antigen of *Yersinia pestis* inhibits neutrophil chemotaxis. Microbial Pathogenesis *24*, 185–196.

Zauberman, A., Cohen, S., Mamroud, E., Flashner, Y., Tidhar, A., Ber, R., Elhanany, E., Shafferman, A., and Velan, B. (2006). Interaction of *Yersinia pestis* with macrophages: limitations in YopJ-dependent apoptosis. Infection and Immunity *74*, 3239–3250.

CHAPTER 5: DISCUSSION AND FUTURE EXPERIMENTS

5.1 Summary of results

Chapter 1 of this dissertation gives a brief overview of the intriguing past of *Yersinia pestis* and how plague disease has altered human history. It also focuses on pneumonic plague and discusses the lung and the innate immune system that attempts to control infection but instead leads to lung damage and pneumonia.

While *in vitro* work is certainly critical to advancing our understanding of pathogenesis, certain information can only be obtained through *in vivo* analysis during infection. Chapter 2 tackles this *in vivo* research using a novel method to evaluate infection in the lung, using LCM and RNAseq to investigate spatial differences in transcription within inflammatory sites after intranasal inoculation with fully virulent *Y. pestis*. We isolated RNA from the center and periphery of the inflammatory lung lesions that form during the later stages of pneumonic plague in order to define, by generating a transcriptome using RNAseq, how *Y. pestis* was affecting the cells present in these two regions. In addition, we isolated and sequenced RNA from bone marrow isolated neutrophils (BM-PMNs) of infected and uninfected mice as a distal match to our lung samples, providing us with a gene repertoire that was known to be neutrophil-specific. By performing statistical comparisons between the lesion center and periphery, and separately between the

uninfected and infected BM-PMNs, we uncovered 976 and 3,198 genes that were significantly different between these comparisons, respectively. Comparing these two gene sets resulted in a list of 224 genes with an enrichment value of p=0.02 that represented genes in the lung lesion comparison that were neutrophil specific. The transcriptional profiles for the 224 genes were then clustered to identify patterns between the four tested groups based on the differential regulation between the two comparisons (e.g. A gene is up-regulated in the infected BM-PMNs compared to the uninfected BM-PMNs and then down-regulated in the lesion center compared to the lesion periphery). Interestingly, we observed that the profiles of the uninfected BM-PMN and lesion center regulation clustered together, while the infected BM-PMN and lesion periphery regulation profiles clustered together, indicating that neutrophil transcription profiles in the center of the lesions are more similar to “unstimulated” neutrophils (The above example would represent this profile phenotype). This apparent down-regulation of neutrophil transcription was supported through density curve analysis of defined gene sets using a ratio of genes in the lesion periphery compared to the lesion center. We found that gene sets involved in leukocyte (neutrophil) migration and apoptotic pathways were overall more down-regulated in the center of lung lesions compared to the periphery, indicating that these pathway functions were being down-regulated in the center of lesions. For example, more genes in the apoptosis pathways were being down regulated than expected by chance, indicating that neutrophils in the center of lesions are hindered in going through apoptosis.

Chapter 3 validates the RNAseq analysis that indicated genes involved in neutrophil apoptosis are down-regulated in the lesion centers. *In vitro* infection assays using isolated human neutrophils were subsequently employed to evaluate the survival of neutrophils after challenge with various bacterial strains. We concluded that, compared to neutrophils that were uninfected or infected with non-pathogenic *Escherichia coli*, fully virulent *Y. pestis* infection caused an increase in neutrophil survival after 24 h. We went on to identify the T3SS effector YopM as being important in causing this prolonged survival of neutrophils. Despite identifying a role for YopM, the mechanism of YopM function in this system remains unknown. We tested the two known intracellular binding functions of YopM using the appropriate inhibitors, but preventing either of the known functions had no effect on neutrophil survival. Moving to our *in vivo* mouse model of infection, we determined that YopM is important for the composition of lung lesions during pneumonic plague. We observed a significant population of cells, presumably neutrophils, which appear to be degranulated in the lungs of mice infected with a Δ*yopM* strain of *Y. pestis*. This observation also correlates with increase TUNEL staining within lung lesions after a Δ*yopM* infection, indicative of increased apoptosis. This supports the *in vitro* data and indicates that *Y. pestis* prolongs neutrophil survival *in vivo* in a YopM-dependent manner.

Chapter 4 focuses on the role of reactive small molecules released by neutrophils that should kill invading bacteria, but can end up harming host tissue in the process. Interestingly, these *in vivo* studies involving intranasal infection of wild

type, iNOS$^{-/-}$, and gp91phox$^{-/-}$ mouse strains with *Y. pestis,* indicated that both ROS and RNS may be important for hindering early establishment of *Y. pestis* in the lungs. The lung histopathology of both the iNOS$^{-/-}$, and gp91phox$^{-/-}$ mice showed increased lung damage compared to wild type mice after infection. Both iNOS$^{-/-}$, and gp91phox$^{-/-}$ mice also had increased dissemination of bacteria from their lungs as observed by bacterial burden in spleens. These differences did not significantly affect the survival of infected iNOS$^{-/-}$, and gp91phox$^{-/-}$ mice at the doses tested. Together, these three chapters unite to better define the cause of lung lesion development during pneumonic plague by looking directly at interactions of *Y. pestis* with relevant cell types in an *in vivo* intranasal infection model.

5.2 Filling gaps in plague research

Several laboratories have demonstrated the relevance of innate immune cells during plague pathogenesis (Laws et al., 2010; Marketon et al., 2005; Pechous et al., 2013), and the effects on macrophages (Grabenstein et al., 2006; Pujol and Bliska, 2005; Zauberman et al., 2006) and neutrophils (O'Loughlin et al., 2010; Spinner et al., 2013; 2008; 2010; Welkos et al., 1998) after interacting with various virulence determinants of *Y. pestis*. Despite this work, there remains a large gap in the field regarding the inability of neutrophils, the most abundant cell type interacting with *Y. pestis* in the lungs during pneumonic plague (Pechous et al., 2013), to control *Y. pestis* infection leading to the lesions seen in this disease. Prior to the research presented in this dissertation, no in-depth analysis has been performed to determine how *Y. pestis* may be altering neutrophil function within the lungs to facilitate lesion

expansion in the absence of noticeable immune cell or bacterial clearance. Isolating the most relevant cell type in lung lesions and using assay conditions that most closely mimic the extracellular nature of *Y. pestis* during pneumonic plague (Price, 2011) enhanced the study of this common theme throughout this dissertation. A unique tissue level approach is described in Chapter 2 that investigated the effects of *Y. pestis* on neutrophils *in vivo*. Evaluation of the spatial differences in gene regulation within lung lesions not only allows for the isolation for relevant cell types, but also highlights the idea that there are some questions that cannot be tackled using *in vitro* assays and attenuated *Y. pestis* strains. Through the use of LCM and RNAseq, we specifically evaluated neutrophil transcript regulation within lung lesions that developed during pneumonic plague. In Chapter 2, we evaluated three sets of genes for their spatial regulation within lesions, and found that two of these sets were significantly altered between the two regions. The RNAseq approach offers the opportunity to look for host pathways that are differentially regulated within these sites of tissue damage to identify how neutrophils are altered after interaction with *Y. petsis*. Additionally, chapter 3 addresses the issue of *Y. pestis* altering neutrophil function during pneumonic plague, and identifies that the T3SS effector protein YopM alters neutrophil survival both *in vitro* and *in vivo*.

Chapter 3 also investigates the unique nature of lung lesions that continue to expand throughout disease. We are the first group to focus on the composition of these lesions and how they establish within the lung. Very few of the neutrophils within these lesions appear to be undergoing apoptosis despite the highly

inflammatory microenvironment and significant bacterial numbers in the lungs. The characterization of a role for YopM in Chapter 3 begins to elucidate these observations, and shows how the unique composition of these lung lesions is partly dependent on the ability of YopM to inhibit the progression of neutrophils through the apoptotic pathway. The reason why there is not a more drastic reduction in lesion size during infection with a Δ*yopM Y. pestis* mutant is likely due to the pleiotropic effects of other Yops, which will be investigated in detail in future studies.

It is unknown what aspects of the immune response are responsible for the alveolar damage that occurs during pneumonic plague. It is possible that the lack of neutrophil turnover is a primary cause of alveolar destruction. As a result of this lack of turnover more activated neutrophils infiltrate and aggregate to form the lesions. These infiltrating neutrophils may be causing a heightened level of damage through releasing ROS and RNS while attempting to control the infection and continuously calling more neutrophils to the site of infection. While some research suggests that neutrophils can kill *Y. pestis in vitro* (Laws et al., 2010; O'Loughlin et al., 2010), these bacteria are able to persist in infected lungs despite massive neutrophilic influx. Current research has not addressed this *in vitro*/*in vivo* difference or defined the immune stresses present in the lung lesion microenvironment that may be the cause of host damage. Chapter 4 begins to reveal the impact of neutrophil defense mechanisms, and whether their granule contents contribute to lung lesion development and damage. This chapter suggests that ROS and RNS contribute to the control of *Y. pestis* in the lung, but not enough to contain infection, which soon

runs rampant in the lungs and disseminates to other organs in the body. Further investigations of the neutrophil granule contents will help to address which of these components can be manipulated to aid in treating pneumonic plague.

Many studies focus specifically on individual *Y. pestis* virulence factors and how they alone interact with host immune cells. *Y. pestis* vaccine research is also based mainly on specific *Y. pestis* surface proteins known to directly interact with host cells. However, the work presented in this dissertation has taken a different approach by focusing on how the host and *Y. pestis* respond in the context of an actual infection and not as individual components of cells or bacteria. This research is innovative in how it accounts for the host - *Y. pestis* interactions leading to lung lesion formation and identifies genes that are altered within the lesion microenvironments. No other group has looked specifically at lung lesions to determine how *Y. pestis* is able to survive and persist within this hyper-inflammatory host microenvironment. Continued research in these unexplored areas of *Y. pestis* infection may not only affect pneumonic plague treatment, but may also reveal factors involved in acute lung infection with other pathogens.

5.3 Implications for the study of plague and pathogen-associated tissue damage

Much of the research in the *Y. pestis* field is performed *in vitro* and with attenuated strains of the bacterium. In the past, these approaches have been important for studying individual virulence factors and their functions, but lack in the ability to wholly translate to fully virulent disease. While the necessity of a BSL 3

laboratory has slowed research on this historically important pathogen, The Goldman lab has consistently used fully virulent *Y. pestis*, and virulence factor mutants, to gain a greater appreciation for virulence *in vivo* (Lathem et al., 2007; 2005; Pechous et al., 2013; 2015; Price et al., 2012; Sivaraman et al., 2015) and the work in this dissertation continues in this vein. This more biologically relevant model allows us to ask questions that could not be tackled using *in vitro* assays or attenuated *Y. pestis* strains.

Combining the use of fully virulent organisms with the applications of LCM and RNAseq has allowed us to dissect regions of lung lesions that form during the late stage of pneumonic plague disease. Isolating RNA from separate regions of the center and periphery of these lesions allowed assessment of unique microenvironments within the lungs. The ultimate goal of this work was to observe how *Y. pestis* interactions with the host affected the transcription of infiltrating neutrophils, eventually causing the development of histopathologically distinct lung lesions. This technique, however, may have much broader appeal to the bacterial pathogenesis community. I have hypothesized, and observed, that even between relatively small regions of damaged tissue, there are observable spatial differences in how host cells are responding. This approach could be used in similar systems where pathogen-induced host damage leads to severe disease complications or death of the host. Investigating host pathways that could be manipulated to alter the mechanisms by which damage is occurring may bring about approaches for

specifically targeting the immune system to allow for more efficient treatment of infections.

For *in vitro* assays, we also used relevant cell types and assay conditions for the questions we were asking. This has become more important recently, as it has been observed that at least one of the Yop effector proteins has different effects on different cell types (Spinner et al., 2010). We have recently shown that neutrophils seem to be selectively targeted for injection by the *Y. pestis* T3SS and are the cell type most important for lung lesion development (Pechous et al., 2013). We therefore wanted to use neutrophils in the *in vitro* assays presented in this dissertation. Our findings that YopM has a novel undefined function in prolonging neutrophil survival only emphasizes the importance of using relevant cells types during research. Neutrophils are a notoriously difficult cell type to assay, but we emphasize with this work that, while immortalized and derived cell lines can be extremely useful, primary cells of the relevant lineages are necessary to more deeply understand the pathogenesis of diseases. Likewise, we ensure that we are using the most relevant assay conditions for our study. While several labs pre-grow *Y. pestis* at room temperature and pre-opsonize the bacteria prior to functional infection assays, we utilized conditions most relevant to pneumonic plague. We mimic primary pneumonic plague by pre-growing *Y. pestis* at 37°C to mimic the lung temperature prior to person-to-person transmission, and we do not pre-opsonize our bacteria since we observe very little intracellular *Y. pestis* during pneumonic plague. Varying conditions in other neutrophil studies could very well explain some of the conflicting

data on their ability to kill *Y. pestis* and how they are affected by various virulence factors (Laws et al., 2010; Lukaszewski et al., 2005; O'Loughlin et al., 2010; Spinner et al., 2010). Better defining the interactions between the host and *Y. pestis* that are responsible for the formation of lung lesions and pneumonia will lead to a better understanding of *Y. pestis* infection and identification of potential treatments to improve survival during a *Y. pestis* infection.

In conclusion, my work has advanced the field by introducing a new method for analyzing the transcription of cells within areas of tissue damage caused by bacterial infection. I have also characterized the effects of both bacterial and host factors on the lung lesions that develop during pneumonic plague, including the *Y. pestis* T3SS effector YopM and host ROS and RNS.

5.4 Future Experiments

Future work on the studies performed within this dissertation will continue to lead to a better understanding of *Y. pestis* disease development. This new information can be utilized to prolong the time window during which treatment can be effectively delivered against pneumonic plague and other inflammatory respiratory pathogens. Below are suggestions for continuing the work in this dissertation to define the lung damage caused by the interaction of *Y. pestis* and neutrophils:

1. Continue generating gene lists of interest and testing them on the density curve model to find pathways that are altered between the lesion periphery and center.

2. Perform LCM to isolate *Y. pestis* RNA from the periphery and center of lesions to transcript profiles after RNAseq.
3. Perform qRT-PCR on lung lesion-obtained RNA for genes in the pathways identified as being altered in the density curve model to identify genes which are truly regulated by the interactions of *Y. pestis*.
4. Perform qRT-PCR analyses on lung lesion-obtained RNA from mice infected with Δ*yopM* and wild type *Y. pestis* to compare apoptosis pathway genes and determine how YopM is inhibiting cell turnover and increasing the survival of neutrophils.
5. Explore how the degranulation of neutrophils alters infection and the survival of *Y. pestis*. Particularly investigate a Δ*yopM* mutant and the effect YopM may have on neutrophil degranulation based on histology of lungs from Δ*yopM*-infected mice.
6. Investigate the formation of NETs by neutrophils after infection with a Δ*yopM* mutant based on histology of lungs from Δ*yopM*-infected mice. Also explore the effect of NET formation on *Y. pestis* survival.
7. Test a Δ*lcrV Y. pestis* mutant (The component of the T3SS that encodes the tip of the needle necessary for injecting the effectors) or double-Δ*yop* mutants, in the neutrophil assay. This will help determine if the Δ*yopM* mutant-infected neutrophil phenotype (in

between wild type and pCD1^{-} infections) is due to compensation from other Yops or is due to some other factor on the pCD1 plasmid.

8. Generate lists of host genes that are regulated by the presence of ROS and RNS and plot them on a density curve model using the RNAseq data to identify regulation of these genes in lung lesions.

9. Infect iNOS$^{-/-}$ and gp91phox$^{-/-}$ mice with Δ*yopM Y. pestis* to observe how the lack of ROS or RNS response affects lesion formation when neutrophils are more readily going through apoptosis (and presumably degranulating).

10. Monitor survival of wild type, iNOS$^{-/-}$, and gp91phox$^{-/-}$ mice at the *Y. pestis* LD50 of wild type mice to determine of the more advanced lung lesions in iNOS$^{-/-}$ and gp91phox$^{-/-}$ mice cause increased mortality.

11. Test strains of knockout mice which are deficient for components of neutrophils granules such as myeloperoxidase, neutrophil elastase, or various proteases (Eyles et al., 2006; Faurschou and Borregaard, 2003) to determine components of neutrophil defense important for lesion formation.

REFERENCES

Eyles, J.L., Roberts, A.W., Metcalf, D., and Wicks, I.P. (2006). Granulocyte colony-stimulating factor and neutrophils--forgotten mediators of inflammatory disease. Nature Clinical Practice Rheumatology *2*, 500–510.

Faurschou, M., and Borregaard, N. (2003). Neutrophil granules and secretory vesicles in inflammation. Microbes and Infection *5*, 1317–1327.

Grabenstein, J.P., Fukuto, H.S., Palmer, L.E., and Bliska, J.B. (2006). Characterization of phagosome trafficking and identification of PhoP-regulated genes important for survival of *Yersinia pestis* in macrophages. Infection and Immunity *74*, 3727–3741.

Lathem, W.W., Price, P.A., Miller, V.L., and Goldman, W.E. (2007). A plasminogen-activating protease specifically controls the development of primary pneumonic plague. Science *315*, 509–513.

Lathem, W.W., Crosby, S.D., Miller, V.L., and Goldman, W.E. (2005). Progression of primary pneumonic plague: A mouse model of infection, pathology, and bacterial transcriptional activity. Proceedings of the National Academy of Sciences *102*, 17786–17791.

Laws, T.R., Davey, M.S., Titball, R.W., and Lukaszewski, R. (2010). Neutrophils are important in early control of lung infection by *Yersinia pestis*. Microbes and Infection *12*, 331–335.

Lukaszewski, R.A., Kenny, D.J., Taylor, R., Rees, D.G.C., Hartley, M.G., and Oyston, P.C.F. (2005). Pathogenesis of *Yersinia pestis* infection in BALB/c mice: effects on host macrophages and neutrophils. Infection and Immunity *73*, 7142–7150.

Marketon, M.M., DePaolo, R.W., DeBord, K.L., Jabri, B., and Schneewind, O. (2005). Plague bacteria target immune cells during infection. Science *309*, 1739–1741.

O'Loughlin, J.L., Spinner, J.L., Minnich, S.A., and Kobayashi, S.D. (2010). *Yersinia pestis* two-component gene regulatory systems promote survival in human neutrophils. Infection and Immunity *78*, 773–782.

Pechous, R.D., Broberg, C.A., Stasulli, N.M., Miller, V.L., and Goldman, W.E. (2015). *In vivo* transcriptional profiling of *Yersinia pestis* reveals a novel bacterial mediator of pulmonary inflammation. mBio *6*, e02302–e02314.

Pechous, R.D., Sivaraman, V., Price, P.A., Stasulli, N.M., and Goldman, W.E. (2013). Early host cell targets of *Yersinia pestis* during primary pneumonic plague. PLoS Pathogens *9*, e1003679.

Price, P.A. (2011). Dominant suppression of early innate immune mechanisms by *Yersinia pestis*. All Theses and Dissertations (ETDs). Paper 633.

Price, P.A., Jin, J., and Goldman, W.E. (2012). Pulmonary infection by *Yersinia pestis* rapidly establishes a permissive environment for microbial proliferation. Proceedings of the National Academy of Sciences *109*, 3083–3088.

Pujol, C., and Bliska, J.B. (2005). Turning *Yersinia* pathogenesis outside in: subversion of macrophage function by intracellular yersiniae. Clinical Immunology *114*, 216–226.

Sivaraman, V., Pechous, R.D., Stasulli, N.M., Miao, E.A., and Goldman, W.E. (2015). *Yersinia pestis* activates both IL-1β and IL-1 receptor antagonist to modulate lung inflammation during pneumonic plague. PLoS Pathogens *11*, e1004688.

Spinner, J.L., Carmody, A.B., Jarrett, C.O., and Hinnebusch, B.J. (2013). Role of *Yersinia pestis* toxin complex family proteins in resistance to phagocytosis by polymorphonuclear leukocytes. Infection and Immunity *1*, 4041–4052.

Spinner, J.L., Cundiff, J.A., and Kobayashi, S.D. (2008). *Yersinia pestis* type III secretion system-dependent inhibition of human polymorphonuclear leukocyte function. Infection and Immunity *76*, 3754–3760.

Spinner, J.L., Seo, K.S., O'Loughlin, J.L., Cundiff, J.A., Minnich, S.A., Bohach, G.A., and Kobayashi, S.D. (2010). Neutrophils are resistant to *Yersinia* YopJ/P-induced apoptosis and are protected from ROS-mediated cell death by the type III secretion system. PLoS One *5*, e9279–e9279.

Welkos, S., Friedlander, A., McDowell, D., Weeks, J., and Tobery, S. (1998). V antigen of *Yersinia pestis* inhibits neutrophil chemotaxis. Microbial Pathogenesis *24*, 185–196.

Zauberman, A., Cohen, S., Mamroud, E., Flashner, Y., Tidhar, A., Ber, R., Elhanany, E., Shafferman, A., and Velan, B. (2006). Interaction of *Yersinia pestis* with macrophages: limitations in YopJ-dependent apoptosis. Infection and Immunity *74*, 3239–3250.